

CRANFIELD UNIVERSITY

Xiaowei Hu

**Analysis and Experiment of an Ultra-light
Flapping Wing Aircraft**

CENTRE OF AERONAUTICS
SCHOOL OF ENGINEERING

MSc by research

MSc THESIS
Academic Year: 2012 - 2013

Supervisor: Dr S. Guo

21st August 2013

CRANFIELD UNIVERSITY

SCHOOL OF ENGINEERING

MSc by research

MSc THESIS

Academic Year 2012 - 2013

Xiaowei Hu

**Analysis and Experiment of an Ultra-light
Flapping Wing Aircraft**

Supervisor: Dr S. Guo
21st August 2013

This thesis is submitted in partial fulfilment of the requirements for the
degree of Master of Science

© Cranfield University 2013. All rights reserved. No part of this
publication may be reproduced without the written permission of the
copyright owner.

ABSTRACT

Inspired by flying animals in nature especially birds, human has designed and attempted to achieve man-powered flapping wing aircraft in very early aviation history. Limited by the understanding of the aerodynamic theory and materials in practise, the bird-like aircraft remains as a dream and ambition for over a contrary. As the relevant knowledge and technology are fast developing in the last decade, the research topic becomes attractive again with encouraging results from a few full scale aircraft flight tests. Although it is suspected that a manned scale flapping wing may not be as efficient as fixed wing, the unique advantages of high manoeuvrability and short take-off and landing capability will keep flapping wing as one of the most potential type of personal and aerobatic aircraft in the future market.

The aim of this project is to investigate into the feasibility and development of a bio-inspired bird-like man-powered ultra-light flapping wing aircraft (ULFWA). The project is based on analytical and experimental study of a scaled model taking an existing hang glider as the baseline airframe. Based on the characteristics of flying animals in nature and manmade hang glider properties, this thesis focuses its study on evaluating the feasibility and analysis of primarily a human powered aircraft. For this purpose, there are four main features as guidance in the ULFWA design. Firstly the flapping frequency was limited to below 2Hz. Secondly the hang glider airframe was adapted with a simple flapping mechanism design. Thirdly the flapping wing stroke and kinematics has been kept with the simplest and resonant movement to achieve high mechanical efficiency. Finally the wing structure has flexible rib of chord wise unsymmetrical bending stiffness to offset the aerodynamic lift loss in upstroke. An engine powered mechanism design was also studied as additional option of the ULFWA.

The initial design and aerodynamic calculation of the ULFWA was based on the hang glider data including dimensions, MTOW (226 kg) and cruising speed. The unsteady aerodynamic lift and thrust forces were calculated based on Theodorsen's theory and unsteady panel method in 2D and extended to 3D using strip theory. A set of optimal flapping kinematic parameters such as amplitude and combination of the heaving and pitching motion of the 2D wing section were determined by calculation and comparison in the limited range. Considering the maximum power and lag motion that human could achieve, the flapping frequency in the ULFWA design is limited to 1Hz. This slow motion leads to a much lower propulsive efficiency in terms of the optimum Strouhal Number ($St=0.2-0.4$), which was used as the design reference. Mechanism and structure design

with inertia force calculation was then completed based on the kinematics. This led to the evaluation of power requirement, which was divided into two components, drag and inertia forces. The results show that the ULFWA needs minimum 2452.25W (equals to 3.29Bhp) to maintain sustainable cruise flight.

In order to demonstrate the ULFWA flapping mechanism and structure design, a 1:10 scaled model with two pairs of wings of different stiffness were built for testing and measurement. Two servomotors were used as to simulate human power actuation. With this model, simplified structure and one of mechanism designs was shown. Four experiments were carried out to measure the model's lift and thrust force. Because of the limited response of the servo motors, the maximum flapping frequency achieved is only 0.75 Hz in the specified flapping amplitude which is close to reality and has improvement margin. By reducing the flapping amplitude, the frequency can be increased to gain higher thrust. Although it is found that the result from scaled model test is a little lower than theoretical result, it has demonstrated the feasibility and potential of human powered flapping wings aircraft.

ACKNOWLEDGEMENTS

Firstly, I would like especially thanks to Dr Guo, who is my supervisor, for giving me so much supervision and helps. He is a genius but he never stingy his encourages on me to make everything be advance. With his kindly supervise and helpful ideas, I could achieve this project. That was much appreciated.

Thanks to my family for giving me this chance to study with Dr Guo in Cranfield University. This is a fantastic experience in my life. And thank you for your care oversea.

Thanks Alasdair Macbean for giving me such a chance to help you in previous model. This experience gave me many ideas on model; it was very helpful for my later works. And there is a time you drove us to visit a human powered aircraft test show in early morning. I feel very grateful.

Thanks to Jingyi Cui for helping me book a private study room for my thesis writing. So I could concentrate on the thesis. Additionally, we encouraged each other about writing thesis.

Thanks to Xueyuan Wang, Ying Liu and your family for kindly advice and helps. And helped me used high-speed camera and helps in experiments.

And thanks to everyone who involved; from Sebastian who very like discuss and went to model shop with me, Baoying Yang drove us testing Alex's model to everyone else.

Table of Content

ABSTRACT.....	2
ACKNOWLEDGEMENTS.....	4
Table of Content	5
List of Figures	8
List of Tables	12
Symbols.....	13
1. Introduction	1
1.1 The Project Aim.....	2
1.2 Thesis outline	2
1.3 General understanding of ornithopter	3
1.4 Flapping wing micro air vehicles.....	3
1.5 Gliders and Hang Gliders.....	4
1.6 The state of the art manned flapping wing aircraft.....	5
2. Literature Review	7
2.1 Theodorsen Theory.....	7
2.2 Aerodynamics of Flapping aircraft.....	7
2.3 Wings.....	8
2.4 Leading-edge suction coefficient	9
2.5 Investigation on flapping wing aircraft in forward flight.....	10
2.6 Motion analysis during take-off from butterfly	11
2.7 A nonlinear aeroelastic model for the study of flapping wing aircraft	13
2.8 Structures and mechanism system.....	15
2.8.1 Powered mechanism design	15

2.8.2 Electromagnet.....	18
2.8.3 Servo motor	19
2.8.4 Material.....	20
3. Methodology study and Conceptual Design.....	21
3.1 Methodology study.....	21
3.2 Flow chart of methodology.....	22
3.3 Conceptual Design	23
3.3.1 Lift force by using Theodorsen Theory	24
3.3.2 Analysis an aerofoil of hang glider	25
3.3.3 Leading-edge suction efficiency.....	26
3.3.4 Strouhal number study and force analysis	27
4. Initial design - aerodynamic analysis and power evaluation.....	32
4.1 Initial aerodynamic analysis.....	32
4.1.1 Lift force	32
4.1.2 Thrust force.....	35
4.2 Analysing and comparing some typical motion.....	36
4.2.1 Lift force analysis	36
4.2.2 Thrust analysis	44
4.2.3 Mixed motion analysis	47
4.3 Power estimating	52
5. Detailed Design	55
5.1 Landing gear design	55
5.1.1 Tricycle-Type Landing Gear.....	55
5.1.2 Tail Wheel-Type Landing Gear	56
5.1.3 Bicycle type	56

5.1.4 Car type	56
5.2 Mechanism design	57
5.2.1 Man powered mechanism design.....	57
5.2.2 Engine powered mechanism detailed design.....	59
5.3 Structure design	62
5.4 Wing structure	63
6. Manufacture, Experiment and Measurement of a Scaled Model	65
6.1 Manufacture of a scaled model	65
6.1.1 Wing model manufacture	65
6.1.2 Actuation and flapping mechanism	69
6.2 Test and measurement	70
6.2.1 The first experiment	70
6.2.2 The Second experiment	73
6.2.3 The third experiment	76
6.2.4 The forth experiment.....	79
6.3 Structure model and analysis of the wing	81
7. Conclusions	85
Reference	88
APPENDICES	91
Appendix A: Relevant Theodorsen Theory	91
Appendix B: Fortran code	96

List of Figures

Figure 1.1 Image of the Pterosaur	1
Figure 1.2(a) A flapping wing rotor MAV; (b) a nano flapping wing - Mosquito	4
Figure 1.3 Motorized gliders	4
Figure 1.4 Hang gliders	5
Figure 1.5 The Snowbird (University of Toronto)	6
Figure 2.1 An analysis of bird fly	8
Figure 2.2 Leading-edge flow conditions	9
Figure 2.3 The experimental flapping wing model	10
Figure 2.4 The average lift versus flapping frequency at different speed and AoA [15]...	11
Figure 2.5 flapping wing motion of butterfly in take-off	11
Figure 2.6 An example of relationship among flapping angle, abdomen angle, and pitch angle of a butterfly during takeoff [16]	12
Figure 2.7 Pressure contours in the plan including leading edge during downstroke	12
Figure 2.8 Project Ornithopter (University of Toronto) [18]	13
Figure 2.9 Quarter-scale lift performance. $U = 45 \text{ ft/s}$; $\theta_a = 6 \text{ deg}$	14
Figure 2.10 Quarter-scale thrust performance. $U = 45 \text{ ft/s}$; $\theta_a = 6 \text{ deg}$	14
Figure 2.11 Illustration of a free-piston gas generator [21]	16
Figure 3.1 The design procedure for an ULFWA	22
Figure 3.2 Parameters of Falcon 3 [26]	23
Figure 3.3 Details of the wing	24
Figure 3.4 Frame and structure of Falcon3	24
Figure 3.5 The aerodynamic result from xflr5	26
Figure 3.6 Lift force in 1s	28
Figure 3.7 Thrust force in 1s	29
Figure 3.8 Lift force in 1s	29
Figure 3.9 Thrust force in 1s	29
Figure 3.10 Lift force in 1s	30

Figure 3.11 Thrust force in 1s	30
Figure 4.1 Lift Force Result from Different Methods.....	33
Figure 4.2 Lift Force Result from Different Methods.....	33
Figure 4.3 Lift Force Result from Different Methods.....	34
Figure 4.4 Lift Force Result from Different Methods.....	34
Figure 4.5 thrust Force Result From Different Methods	35
Figure 4.6 thrust Force Result From Different Methods	35
Figure 4.7 The lift force and components from the wing tip 2D section (case 5)	37
Figure 4.8 Total lift force for single wing	37
Figure 4.9 The lift force and components from the wing tip 2D section (case 6)	38
Figure 4.10 Total lift force for single wing	39
Figure 4.11 The lift force and components from the wing tip 2D section (case 7)	40
Figure 4.12 Total lift force for single wing (case 7).....	40
Figure 4.13 The lift force and components from the wing tip 2D section (case 8)	41
Figure 4.14 Total lift force for single wing	42
Figure 4.15 The lift force and components from the wing tip 2D section (case 9)	43
Figure 4.16 Thrust force with wingtip section (case 5).....	44
Figure 4.17 Thrust force with wingtip section (case 6).....	45
Figure 4.18 Thrust force with wingtip section (case 7).....	45
Figure 4.19 Thrust force with wingtip section (case 9).....	46
Figure 4.20 Thrust force with wingtip section (case 10).....	46
Figure 4.21 Total Lift force with single wing.....	47
Figure 4.22 Total Lift force with single wing.....	48
Figure 4.23 Total Lift force with single wing.....	48
Figure 4.24 Total Lift force with single wing.....	49
Figure 4.25 Total Thrust force with single wing.....	49
Figure 4.26 Total Thrust force with single wing.....	50
Figure 4.27 Total Thrust force with single wing.....	50
Figure 4.28 Total Lift force with single wing.....	51
Figure 4.29 Total Thrust force with single wing.....	51

Figure 4.30 The drag result from xflr5	53
Figure 5.1 Landing gear arrangement.....	57
Figure 5.2 Air Rowing machine	58
Figure 5.3 Human powered mechanism design	58
Figure 5.4 Single piston engine	59
Figure 5.5 Mechanism design – two piston engine	60
Figure 5.6 Out-swing door cylinder	60
Figure 5.7 Mechanism design – electromagnet engine.....	61
Figure 5.8 Mechanism design – two electromagnet engines.....	62
Figure 5.9 Structure design	63
Figure 5.10 Wing structure design.....	64
Figure 6.1 Scaled model.....	65
Figure 6.2 A flapping wing made of CFRP beams	66
Figure 6.3 Single glass fibre reinforce plastic wing.....	66
Figure 6.4 Joints of rib to wing spar.....	67
Figure 6.5 Glass fibre reinforced plastic ribs	68
Figure 6.6 Glass fibre reinforce plastic rib	69
Figure 6.7 Actuation mechanism and supporting frame	70
Figure 6.8 Model set up for experiment 1	71
Figure 6.9 Model Test Setup for Measurement	71
Figure 6.10 Model Test Set on Table with large AoA	72
Figure 6.11 Model Test Set on Table with reduced AoA	72
Figure 6.12 Model suspended in Experiment 2	73
Figure 6.13 Model Test Setup in Experiment 2	74
Figure 6.14 Model Test Setup on Table for Thrust Measurement	74
Figure 6.15 Model Test for Thrust Measurement	75
Figure 6.16 Force diagram for experiment 2	75
Figure 6.17 Model Test setup in the 3 rd Test.....	76
Figure 6.18 Force diagram for experiment 3	77
Figure 6.19 Measurement by high-speed camera (case-1).....	79

Figure 6.20 Measurement by high-speed camera (case-2)	80
Figure 6.21 Measurement by high-speed camera (case-3)	80
Figure 6.22 FE model of the flapping wing	83
Figure 6.23 Rigid mode of the flapping wing	83
Figure 6.24 First elastic mode of the flapping wing.....	84
Figure 6.25 Second elastic mode of the flapping wing.....	84
Figure 6.26 Third elastic mode of the flapping wing (torsional)	84

List of Tables

Table 6.1 The original measurement results from experiment 3.....	77
Table 6.2 The processed experiment results.....	78
Table 6.3 The wing spar-rib joint mass	81
Table 6.4 The wing spar and rib mass.....	82
Table 6.5 The wing spar and rib dimensions and equivalent E values	82

Symbols

C_s	Leading-edge suction coefficient
Λ	Sweep angle
L	Lift force
ρ	Density of the air
b	half Chord
U	Speed
a	Aerodynamic centre
$C(k)$	Theodorsen Function
α	Angle of attack
h	Paths of the wing
W	Work
E_k	Kinetic energy
C_L	Lift coefficient
K_i	Induced-drag parameter
K_p	Constant of proportionality in potential-flow lift equation
C_T	Leading-edge thrust coefficient
C_{Di}	Theoretical induce-drag coefficient
V	Speed
L	Lenth
r	Radius
ω	Palstance
E_p	Potential energy

1. Introduction

As known to us, flying animals in nature exist on earth since 250 million years ago (e.g. Triassic), and there are thousands different kind of flying animals and insects around us in human daily live. Though they look similar in the manner of flapping wing, they have different flapping kinematics which can be divided into two types. One is the flapping wing in up and down stroke to fly in the air as demonstrated typically by Birds, which have the heaviest bodies, but are able of flying highest and furthest. The hummingbird in hovering flight is an exceptional. Another type has the wings flapping in for and back stroke in a nearly horizontal plane which is also called eight-figure flapping demonstrated by most flying insects such as flies. The dragonfly wings in hovering are exceptional and belong to the first type. They have complicated airfoil and the flapping kinematics that allow them to achieve such incredible flying agility and high performance in multi flying modes. The most magnificent and attractive example to us is the Pterosaur as illustrated in Fig. 1.1 who has an extremely huge body and 16 meters wingspan. Research shows that their wings are different from any birds which could speed reach 120 kilometres per hour. But when they taking off they need to run or dap very hard. [1] Unfortunately, they have died out, but at the same time their lives made a hard evidence of flying with such huge thing.

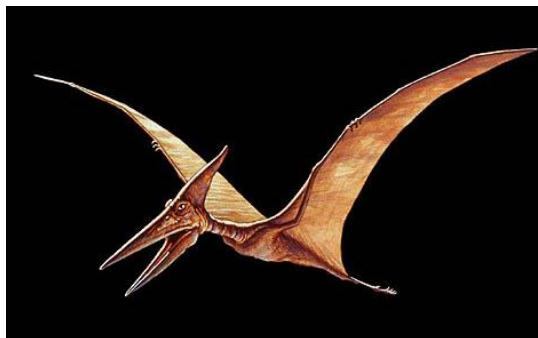


Figure 1.1 Image of the Pterosaur

Human beings have a dream to fly in the sky by their own power for thousands of years. Unfortunately, the man powered flapping wing aircraft has not yet successful from practical point of view so far. This is mainly limited by the human power of cause and also by the materials and techniques in mechanical and structural design. Instead of that, people pay more attention to developing fixed wing and rotorcraft air vehicles at the moment. However, flapping wing aircraft has several advantages than fixed wing aircraft and rotorcraft in specially missions. For example, flapping wing aircraft has better

manoeuvrability and very low stall speed, which leads to the capability of short take-off and landing and flight safety. It is also power efficient according to flying animals. For safety aspect, it is obviously safer than rotorcraft because of the wing motion velocity and gliding capability. The most exciting and attractive point to motivate the research is its potential market for future personal aircraft.

1.1 The Project Aim

The overall aim of this project is to evaluate the feasibility and develop a human powered bird-like ultra-light flapping wing aircraft (ULFWA) through design and analysis. This project focuses on the practical design and analysis of a simple flapping mechanism and wing structure for the flapping wing aircraft. Experiment and measurement were carried out based on a scaled model to demonstrate the design and performance.

For practical design purpose, an existing hang glider (Falcon 3) airframe and performance was adapted as the baseline of the bird-like ULFWA. To achieve the aim, number of objectives is set in this project.

- Designing a simple and practical flapping mechanism from linear actuation motion to flapping wing stroke
- Determine optimal flapping parameters based on a simple up and down stroke kinematics under the limited human power and motion
- Theoretical and numerical analysis of aerodynamics and structures of the ULFWA
- Design a flexible wing structure to achieve a desirable and practical mixture of rigid body heaving motion from stroke and pitching angle from elastic twist
- Estimate the flapping power requirement.
- Build a 1:10 scaled model and carry out experiment to demonstrate the design and analysis.

1.2 Thesis outline

This thesis is divided into eight chapters. Chapter 1 gives a general understanding of flapping wings and motivation of developing the ultra-light flapping wing aircraft. Chapter 2 contains literature review of the research. In chapter 3, the methodology of design is given to guide the whole project.

The conceptual design of the full scale ULFWA is given in chapter 4, in which some useful theory and important parameters that could affect the design were considered. Following this, the initial design has been presented in Chapter 5. This chapter includes initial analysis and comparison of typical kinematics to determine the best possible flapping motion for the ULFWA and power requirement based on the practical human powered motion. The detail design is given in chapter 6 with different design options.

In chapter 7, a 1:10 scaled test model was designed and built for experiment and measurement. Four experiments were carried out to demonstrate the design, test the mechanism and measure the motion, inertia and aerodynamic forces. Finally conclusions are presented in Chapter 8.

1.3 General understanding of ornithopter

The ancient concept of human aircraft was built on the observation of flying animals existing in nature, especially birds, and the early design of flapping wing machine was called ornithopter. Although various ornithopter to mimic bird wing motion was designed and built, no successful sustainable flapping aircraft has been made at that time. Instead, engine powered fixed wing aircraft using propeller was successfully take-off since 1903. Afterwards, fixed wing aircraft has been fast developed and improved during World War I and II by military, and further extended in civil air transport in post war. It has played a very important role in human life for air transport.

1.4 Flapping wing micro air vehicles

The micro air vehicle is defined by size of less than 6 inches, and performance of maximum speed 25 mile per hour.[2] Flapping wing micro aerial vehicles (MAVs) having vertical take-off and landing (VTOL) and hovering capabilities are ideally suited to carry out intelligence, surveillance, target acquisition and reconnaissance (ISTAR) missions especially in highly complex and risky environments such as inside buildings, deep urban canyons and hostile fields. Therefore flapping wing MAV has attracted many research attentions in this country.

One of the flapping wing MAV model is the novel flapping wing rotor as shown in Fig.1.2(a) developed by Dr Guo at Cranfield University [4]. Another example of nano flapping wing model produced by American military is a so-called insect spy as shown in Fig.1.2(b). The dimension of this model is the same as a mosquito. It has biomimetic

wings and flaps like real mosquito. This aircraft is able to equip camera, voice recorder and even weapon, which could attack terrorist. Besides, this aircraft could live in a crowd of mosquito disguise the real mosquito.

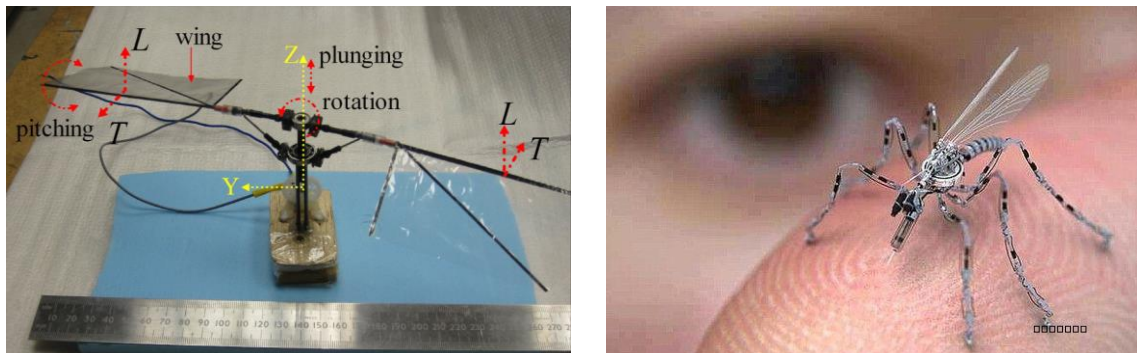


Figure 1.2(a) A flapping wing rotor MAV; (b) a nano flapping wing - Mosquito

Most of the micro flapping wings are made by mimicking the flying insects, which have quite different flapping kinematics and frequency from birds. However there are similarities in unsteady aerodynamics for better understanding the mechanism of the aircraft.

1.5 Gliders and Hang Gliders

Gliding is a popular sport in the UK. It easily satisfies people who want to fly themselves. There are 2 kinds of glider, one is engine powered gliding which can produce thrust force to gain speed and keep sufficient lift force. When they reach enough height they drop the engine - a safer and efficient way to glide. The other is unpowered which takes different ways to take off and gain the aircraft speed. Some big gliders as shown in Fig.1.3 need to be towed to take-off by other vehicles. Small gliders such as hang gliders as shown in Fig.1.4 normally take off from higher places to gain speed and lift.



Figure 1.3 Motorized gliders



Figure 1.4 Hang gliders

Different to a parachute, the aerofoil is specifically made for all gliders to have lift force to keep flying even at low speed. That is the reason all the wings of gliders are made to high aspect ratio. The shapes of the wings generally are designed in a triangle or rectangle. To decrease the effect of drag, the covers of the wings are usually polished very smoothly; some of them are even waxed. Woods, laminate, fabric, glass fibre and aluminium are the materials which are used to produce the wings to make vehicles light.

The most difficult problem with all gliders was landing. Landing without power could cause them to crash on landing. Some gliders are equipped with a reliable dive brake to increase drag force and control posture while landing. However, hang gliders could not be equipped such a complicated system, so pilots pull back the cables hard which connect the wingtips when they only have a couple meters left. That motion makes the hang glider rapidly decelerate and even rise for a short time.

Flapping could create lift force from the example of motion taken from the hang glider pilot, and this gives me great confidence that flapping wings are able to enable to fly by human power.

1.6 The state of the art manned flapping wing aircraft

With the improvement of understanding, design and technology for flapping wings, the development of a manned flapping wing aircraft becomes realistic and worth of further investigation. Compared with fixed wing aircraft, manned ornithopters should be more agile and have very low stall speed for safer cruising and landing.

The newest flapping wing aircraft that basically fly with fluttering is called Snowbird produced by the University of Toronto. The Snowbird is extremely light with a weight of only 42.6 kilograms but with a 32 meters wingspan as shown in Fig.1.5.



Figure 1.5 The Snowbird (University of Toronto)

The Snowbird took off towed by a car. After gliding in the air, the pilot started to pedal to make the wings flap. It only flapped 15 times until it landed, and most of the time in a glide but it made a point that humans are able, by their own power to maintain flying though only a few seconds.

It made a remarkable time in 2010; however, there are some problems in this aircraft. First of all, the transmission system is not efficient enough to flap by using human power. Pedalling in circular pattern like cycling, is a steady and consecutive way to export power but not similar to flapping. To flap like a bird needs a great of energy in a few tenths of a second. In this situation, the wings could gain the maximum lift force. The second problem is that the Aspect Ratio is too large to make efficient flapping and achieve the required flapping motion by human power.

The Snowbird was actually towed by another powered vehicle to take-off. This is a practical and simple way to take-off since the Snowbird is unable to take-off by human power.

2. Literature Review

2.1 Theodorsen Theory

Theodorsen [5] developed a classic unsteady aerodynamics theory base on thin airfoil in small oscillation. It provides a basic and convenient method to analyse and better understand how bird and insect fly. It provides an essential and very useful method to design a flapping wing aircraft.

This theory has assumptions for simplified analysis of the wing, flow and the wake:

1. The flow is always attached.
2. The wing is a flat plate.
3. The wake is flat.

The first simplification makes the theory valid only for small amplitude of the wing motion. Theodorsen's function makes an optimization of the influence from circulation flow to the total lift force.

Numerical method

Because of assumptions taken from the Theodorsen Theory, the result is not necessarily accurate for the large flapping wing aircraft which normally has large flapping amplitude. There are types of numerical methods developed to simulate the flapping wing aerodynamics for more accuracy. One is the double lattice method for 3-D model and unsteady Panel method for solving incompressible potential flow. The method used in this thesis is the one developed for 2D model [6]. The other one is CFD (Computational Fluid Dynamics) method which uses numerical methods and algorithms to solve and analysis unsteady fluid flow for flapping wings [7].

2.2 Aerodynamics of Flapping aircraft

Flying animals are able to produce lift force and thrust force by flapping their wings as shown in Fig.2.1. They could complete complicated movement at the same time. Observing flight patterns in nature is a good way to understand the nature of flapping wing aircraft. [8]

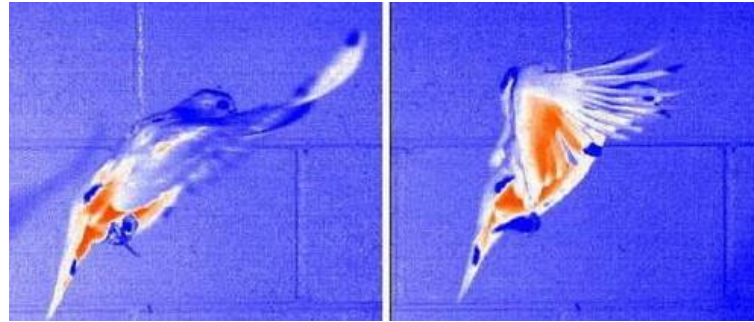


Figure 2.1 An analysis of bird fly

Basically birds flutter like rowers in the sea but they always change the shape of their wings to gain lift force and to decrease drag force, but they increase lift force and drag force at the same time for hovering. When they glide, they may lose height to gain speed or keep speed, which is similar to a glider aircraft. When they are gliding they normally change their angle of attack to adjust their speed and height similar to fixed wing aircraft, hence flights in nature all have high lift-to-drag ratio.

The flying animals flap not only up and down, but twist, bend and sweep forward and backward as well, so that they can gain enough force to fly forward and upward. The ability to hover by birds and insects [9] is mainly practiced by small species. Even if some big birds could hover in the air; they could only make it for few seconds, which means hovering uses a large amount of energy and need to have a very good control system. Thus, normally, small insects with high flapping frequency [10] could hover steady, for instance drone flies.

There are a lot of species which leap forward to produce enough speed for taking off, especially birds with a large body. Birds of this size need a special means of landing such as into water.

In addition to the bird-like flapping wings, there are other research work on insect-like flapping wings and extended novel design of micro flapping wing air vehicles. Typical recent research in this field includes the so called flapping wing rotor by Dr Guo [11] [12]

2.3 Wings

The wing is the most important part of a flapping wing aircraft and also the most difficult subject to study even through many examples exist in nature. Wings may produce

significantly different potential even with a little change in shape [13]. Thus the study on flapping wing is the key for success of the ULFWA.

As the conclusion of this reference, wing shape and aerofoil are two subjects that affect the future design and require prior consideration. Slender wing can produce larger thrust force per unit mass since the thrust is generated from every single g/Kg along the wing span. The aerofoil thickness has little effect on thrust caused by flapping motion.

The shape of the leading edge also has significant influence on wing aerodynamic performance. A sharp leading edge could keep the tendency of lift coefficient at high angle of attack, but the rounded leading edge cannot.

Almost every human powered aircraft used very light material for light weight but at the risk of too flexible to sustain the lift force. The flapping wing aircraft requires sustained flapping motion to generate adequate lift and thrust forces to maintain the flight. In this situation, a stiffer and light composite material will be chosen for the aircraft. Following an initial design of the wing structure, further optimization has been carried out.

2.4 Leading-edge suction coefficient

Leading edge suction was studied by NASA (National Aeronautics and Space Administration) [14]. The leading-edge suction as illustrated in Fig. 2.2 is caused by the potential flow about the sharp and round edge and separation condition for the sharp delta wings.

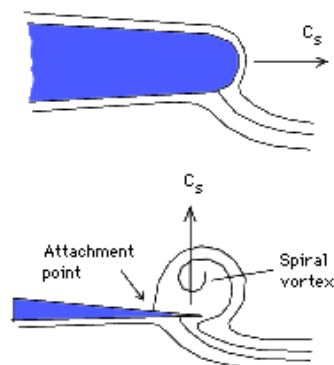


Figure 2.2 Leading-edge flow conditions

2.5 Investigation on flapping wing aircraft in forward flight

Flapping wing and motion kinematics in nature is much more complicated than fixed wing and rotorcraft. Experiment is therefore an important means in the design and research. Compared with theoretical analysis experiment results are more reliable and accurate.

For processing this experiment, an experimental flapping wing model of 80 cm long with the wing area 940 cm^2 was produced as shown in Fig.2-3 [15]. During the test, condition was changed according to the air speed, the angle of attack and flapping frequency of the wing. Average lift forces were measured and compared.

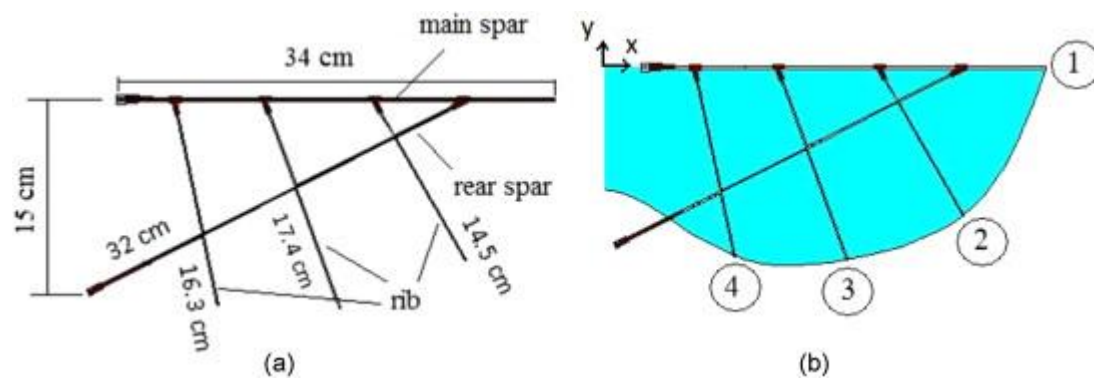


Figure 2.3 The experimental flapping wing model

The experiment results as shown in Figure 2.4 indicate that the air flow speed and built-in AOA has a significant effect on the resulting forces. Higher flapping frequency leads to increase of the lift force, but becomes less important when the built-in AOA increases. However it would not make significant influence on average lift force. Unlike a fixed wing, the flapping wing lift force in this experiment was not linearly increased with V^2 due to the aeroelastic effect of the wing.

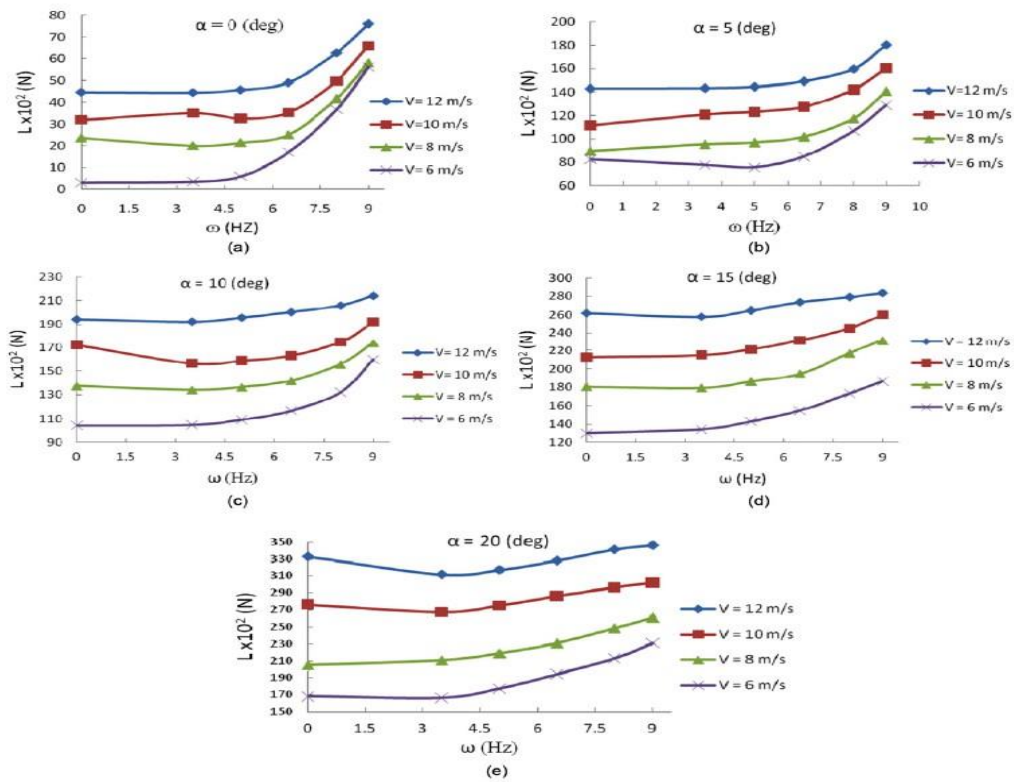


Figure 2.4 The average lift versus flapping frequency at different speed and AoA [15]

2.6 Motion analysis during take-off from butterfly

A mimic of flying animals' flapping mechanism provides an effective study of the ULFWA. Since the flapping frequency of butterflies is low, their flap mechanism is easier to follow and analyse than other species. For example, the butterfly flapping wing motion in take-off as shown in Fig. 2.5 could be used for the future of flapping aircraft. Fig. 2.6 shows the flapping angle, abdomen angle and pitch angle.

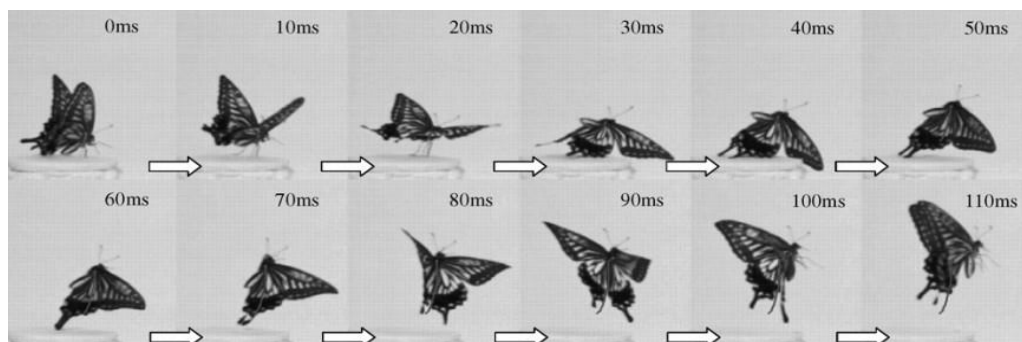


Figure 2.5 flapping wing motion of butterfly in take-off

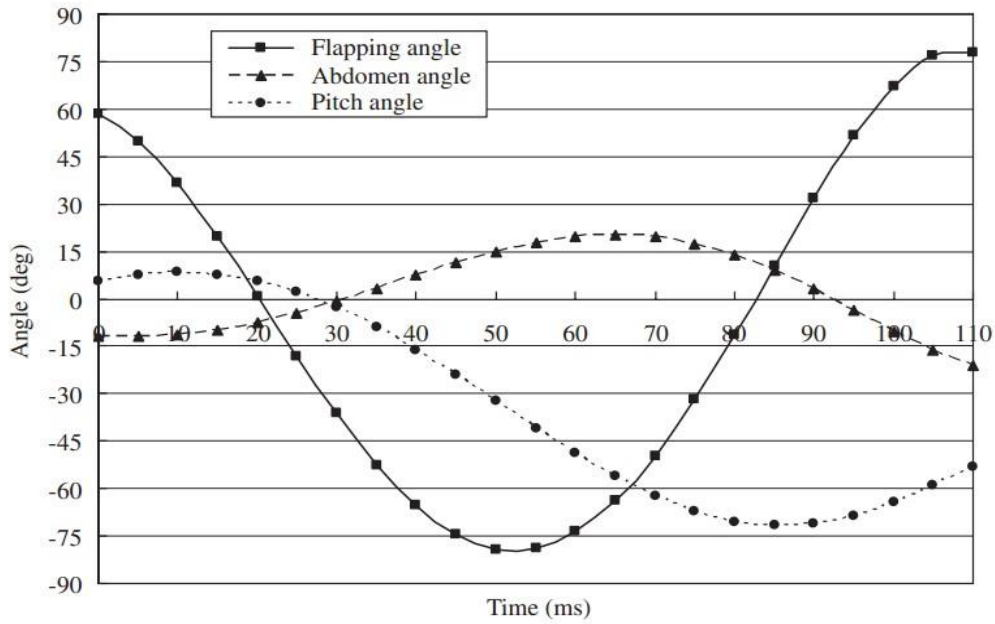


Figure 2.6 An example of relationship among flapping angle, abdomen angle, and pitch angle of a butterfly during takeoff [16]

It shows that the flapping angle and abdomen are almost antiphase but in the same frequency. That means this kind of motion could be imitated by kinematics of flapping wing aircraft. Fig.2.7 shows a CFD simulation of the aerodynamic pressure produced by the flapping wing.

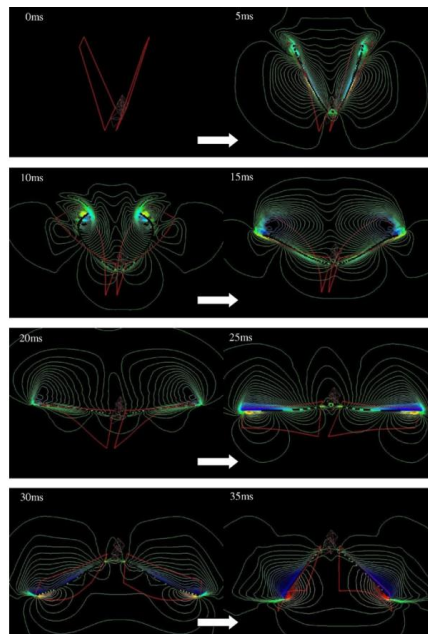


Figure 2.7 Pressure contours in the plan including leading edge during downstroke

The results show that negative vortices spread all over the wing from the tip of the leading edge. As a conclusion, butterflies produce lift force by unsteady flow and vortices. With Three-dimensional numerical simulations, it makes good understanding with vortex fluid. [17]

2.7 A nonlinear aeroelastic model for the study of flapping wing aircraft

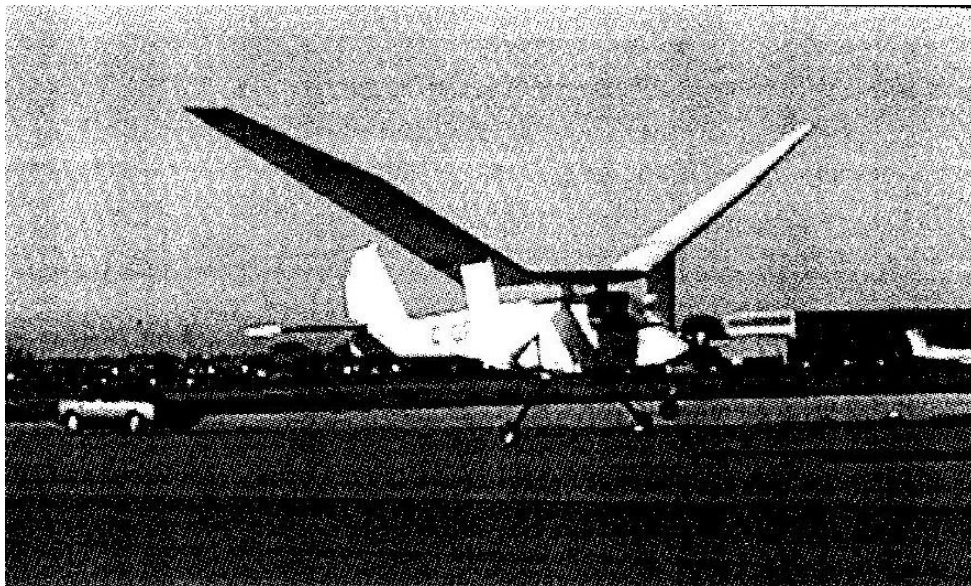


Figure 2.8 Project Ornithopter (University of Toronto) [18]

Figure 2.8 shows an example of a flapping wing aircraft with improvements in the Theodorsen Theory. It was produced by the University of Toronto in 2006. The mechanical flapping wing in this example made the aircraft take off and flew successfully for 14 seconds. However it was unable to control its level flight and crashed during the attempt of landing. It is a legend in recent years and proving it is possible to achieve flapping flying like a bird.

What they had improved of the Theodorsen Theory was the effect on the airfoil which made it to be one of the best theories at present. Thus, the result of analysis was close to the experiment result; however, the analysis result having about 15% deviation from measurement is almost the best for now but still not accurate enough [19].

Technically, the theory could be used for design because it almost considers every important element with flapping. With the equations provided by the example we could generally figure the important factors which play the significant role in flapping.

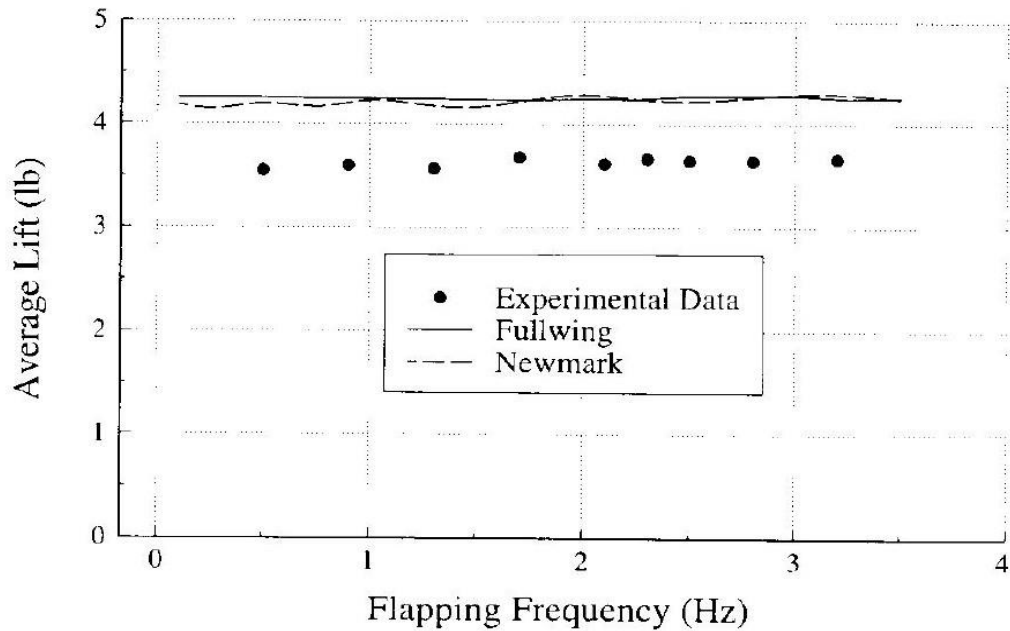


Figure 2.9 Quarter-scale lift performance. $U = 45 \text{ ft/s}$; $\theta_a = 6 \text{ deg}$ [19]

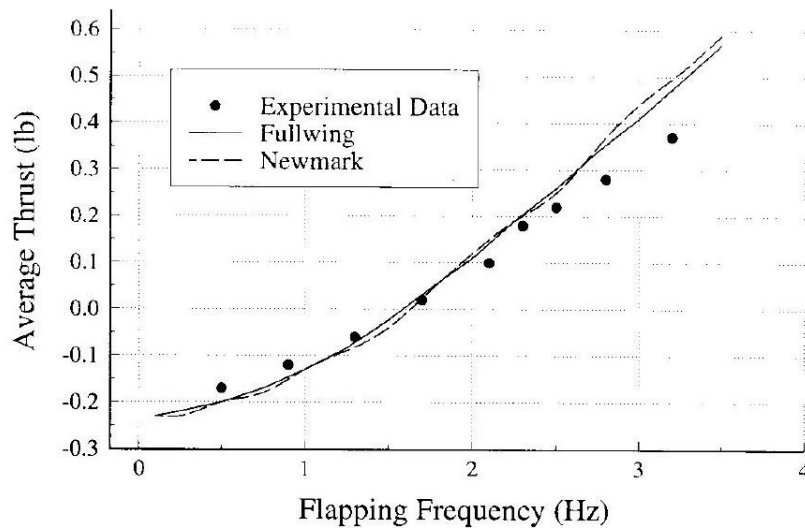


Figure 2.10 Quarter-scale thrust performance. $U = 45 \text{ ft/s}$; $\theta_a = 6 \text{ deg}$ [19]

From Figure 2.9 and Figure 2.10, the obvious differences between the calculation result and experiment data are shown. Compared with other method, the tolerance of this theory is accurate which means it is a better way to evaluate, but it is still not good enough. In this situation, panel methods and CFD will be used for the future calculation to make the result one with high accuracy.

2.8 Structures and mechanism system

Most of the light weight airframes are generally made of aluminium and composite. For man-powered aircraft, laminate, fabric, and woods are materials used to build wings. Plastic film and plastics are used for the pilot's compartment to reduce weight to a minimum, even though this does not give the pilot enough safety. However, it is not the best way to optimise the aircraft. To find another way to generate more lift force and thrust force is the way to make improvements and by decreasing weight from transmission systems and making them more powerful.

Cycling is the most popular system appearing in human powered aircraft even in flapping wing flight [20]. The power from the system and pilot are continuous and steady which means it is only suitable for propeller driven aircraft which is inefficient for human power. A flapping wing requires the maximum force which could make wings flap in high speed and attitude with frequency. So a rowing like power system will be a good solution for the flapping wing aircraft. Compared with other sports, rowing is the only sport requiring frequency and force from the whole body. And so, allows the pilot to use maximum force to make the wing flap. Besides, comparing other movement, the movement paths of rowing could be easily converted to flap. It will be an ideal layout for human powered flapping wing aircraft.

2.8.1 Powered mechanism design

The reciprocating engine that burns gasoline or diesel to generate power is widely used to power vehicles and aircraft. Normally, an engine consists of more than one piston and cylinder [21]. The fuel will be injected into a cylinder mixed with air. After injection, the fuel will be ignited to achieve heat expansion and push the piston rearward movement. This movement of the piston drives the connecting rod and crankshaft in a circular motion regarded as a linear movement, this kind of engine is often known as the internal combustion engine.

Traditionally, for four-stroke reciprocating piston engine, when the engine rotates for two cycles, it completes one progression of the cylinder intake, compression, ignition and exhaust. Whereas the rotary engine, the rotor rotating one round will have three times per cycle of the processes of intake, compression, ignition and exhaust. The gear ratio of the rotor and rotary engine output shaft is three to one. Therefore when rotary engine rotates in one round, each rotor has the process of intake, compression, ignition and exhaust once, which is equivalent to the reciprocating engine running for two rounds. Consequently, it has the advantage that a small gas displacement can accomplish high power output. However, compared with reciprocating engines under the same gas displacement, rotary engine needs more fuel. Furthermore, due to the characteristic of axial running direction of the rotor engine, it can achieve very high speed operation without requiring precise balancing crank.

2.8.1.1 Reciprocating piston engine

1. Inline

Each cylinder of the engine is located in a row, generally vertically disposed as illustrated in Fig.2.11. The structure of single row cylinder is simple and easily processed, but the length and height is large. The engines with less than six cylinders generally used by cars are single style. What is more, the engines of some automobiles are inclined at an angle in order to reduce the height of the engine.

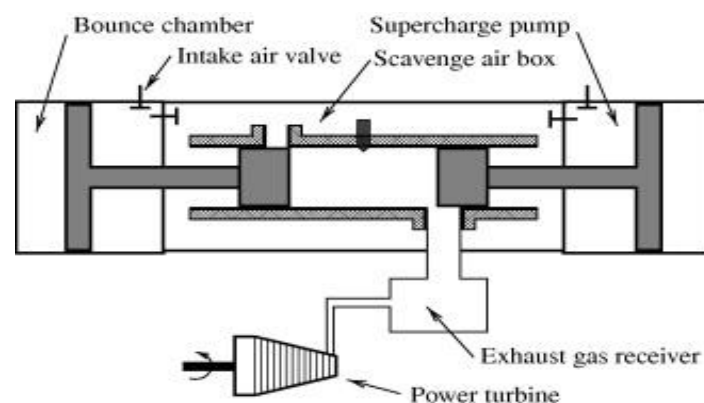


Figure 2.11 Illustration of a free-piston gas generator [21]

The illustration above is a special kind of inline piston engine. With this design, engine is able to achieve longer distance of work.

2. V-type

Cylinder of engine with the characteristic of that locates in two rows and the axis angle γ of left and right cylinders is less than 180° , is referred to as V-type engine. Compared to the structure of inline engine, V-type engine reduces the length and height of the engine body, increases stiffness of the body of the cylinder, lowers the engine weight, but enhances the width of the engine, is more complex and difficult for assembly that generally is used for more than eight-cylinder engine. Also the six-cylinder engine utilizes this style.

3. Pancake engine

The appearance of cylinder locating the same horizontal level that means the angle between axis of the left and right cylinder equals 180° is referred to as pancake engine. The advantages of it are small height, convenient for the overall layout, and cooling. But this cylinder is seldom used.

2.8.1.2 Rotary engine

The performance of rotary engine compared with that of four-stroke engine has the advantage of high horsepower capacity ratio (small volume engine can output more power), as the rotor of rotary engine works three times per rotation whereas the four-stroke rotates twice only for once output. In addition, due to the characteristic of the axial rotation direction of the rotor the engine, it can be balanced to achieve a relatively higher operation speed without precise crankshaft. The whole engine only has two moving parts, and the structure of it is more simplified as well as lower possibility of incidents occurred compared with the general four-stroke engine more than 20 structures including intake and exhaust valves. Besides the advantages mentioned previously, the rotary engine is small size, light weight and low centre of gravity. [22]

In contrast, since the three rotor engine combustion chamber is not completely isolated, so the engine is easy to have leakage, substantial increase in fuel consumption and pollution problems after a period of time because of seal material wear and tear. Its unique mechanical structure also causes this type of engine more difficult to repair.

2.8.2 Electromagnet

Electromagnet is a magnetic device to pass the electric current to generate the electromagnetic. [23]

The electromagnetic is a magnetic device by energization. Around the outside of the core of the power to match the conductive winding, this electric current through a magnetic coil like a magnet is also called solenoid (electromagnet). It is usually put into the shape of strip or plate to make the core more easily magnetized. In order to enable the electromagnet demagnetization immediately, it is actually used a fast demagnetization of soft iron or silicon steel to make material. Such a magnetic solenoid when energized has magnetic power as after power outages it disappears.

Electromagnet has many advantages: whether is with magnetic solenoid or not can be controlled by through electric current; the degree of magnetic relies on the electric current strength or the number of turns of the coil; also the magnetic poles is dependent on the directions of its pole and so on. Namely: the strength of the magnetic can be changed by controlling the presence or absence of magnetism; the magnetic pole direction can be changed, the disappearance of the magnetic because the current is vanished away.

Comparison with permanent magnets

Permanent magnets and electromagnets can produce different forms of manufactured magnetic field. In the choice of the magnetic circuit, the first consideration is that what required job is asked magnet to complete. Where under the situations of inconvenient electricity, frequent power outages, or unnecessary to adjust the magnetic force cases, permanent magnet dominants. In terms of the purposes of that force is required to change or need for remote control, the electromagnet is better than the permanent magnet. In fact magnets can only be used by the originally scheduled way, if the wrong type of magnet is applied for a special objective; it can be extremely dangerous and even fatal.

For example, in some practical fields, many machines that are operated based on the heavy block-shaped materials require permanent magnets. The majority users believe that the mechanical plant, the biggest advantage of these magnets, is not required electrical connections.

Permanent magnets have the advantages of 330 to 10,000 pounds lifting capacity, and turn on or off a magnetic circuit with only rotating the handle. A magnet equipped with safety lock, is promoted to ensure that the magnet will not be accidentally disconnected.

Magnet group can be used for relatively heavy and a single magnet without the ability of coping with long loads.

Also, in many cases, because the ready for assembled components are very fine (0.25 inch or finer), and is extracted from the pile of similar parts, the permanent magnets have the limitations on extracting one piece from a pile of parts once. Although the permanent magnet is extremely reliable under the circumstance of the right utilization method, it cannot change the magnetic force. In this regard, the electromagnet allows the operators to control the magnetic field strength by the variable voltage control means, and can select the individual piece from a stacking of parts. Self-contained units electromagnet is the most cost-effective magnets based on lifting capacity, and its lifting capacity can be extended to 10,500 pounds. The battery-powered magnets are competitive. Specifically, they use self-contained gel batteries to increase lifting capacity and can handle the products of flat, round and component shapes. Provided by the battery-powered, magnets can repeat to complete the action of upgrading, and provide a large lifting capacity in the absence of an external power supply.

2.8.3 Servo motor

Servo motor is the engine that in the servo system controls operation of the mechanical components. The servomotor can control the speed of the servo motor, and the voltage can be converted to torque and speed signals to drive the control object thanks to the position accuracy. With the help of the characteristics of that rotor speed of servo motor is controlled by the input signal, and can quickly react in the automatic control system, the servo motor is used for the implementation of components. Additionally, the servo motor has merits of small mechanical and electrical time constant, high linearity, and initiating voltage, etc. while it outputs the received signal with convert as angular displacement or angular velocity on the basis of motor shaft. Functionally, the servo motor can be classified into two categories of DC and AC. To conclude, the advantages of servo motor cover several fields: small moment of inertia, low starting voltage, low load current; when brushless servo motor operates servo control in execution, it can achieve controlling of speed, position and torque without encoder; with a long life, low noise, no electromagnetic interference and high speed.

2.8.4 Material

For flapping wing aircraft, the structural materials are required to be much lighter and stronger than fixed wing aircraft because of the dynamic load in high acceleration acting on the flap wing all the time.

2.8.4.1 Carbon fibre reinforced plastic

Carbon fibre reinforced plastic is the microcrystalline graphite material made from organic fibres by carbonization and graphitization. The microstructure of carbon fibre reinforced plastic is similar to artificial graphite - the turbostratic structure [24].

Carbon fibre reinforced plastic is a new structural material, the density of which is 1.8g/cm^3 , only a quarter compared with steel. Moreover, the tensile strength of carbon fibre reinforced plastic is over 3500Mpa, 7-9 times as steel.

2.8.4.2 Glass fibre reinforced plastic

Glass fibre reinforced plastic is a fantastic inorganic non-metallic material. It has good corrosion resistance, high mechanical strength, but it is brittle and bad wear resistance [25]. It is made from glass balls or waste glass as raw material manufactured and processed through high temperatures, The diameter of its monofilament is ranges from several microns to 20 microns so that each beam of root fibre strand consists of hundreds or even thousands of filaments and the density of glass fibre is $2.4 - 2.7\text{g/cm}^3$

Because of the advantages of tensile strength and small elongation (3%), as well as high elasticity and good rigidity, glass fibre reinforced plastic can be made for the rib of the flapping wing aircraft. The characteristic of good workability allows it to be made in almost any shape with stability. Good heat resistance also attracts the attention of the flapping wing designers. Moreover, the reasonable price and high tensile strength within the elastic limit causing impact energy absorption increases the importance of considering glass fibre to become a selected material.

2.8.4.3 Aluminium

Aluminium and aluminium alloy are remarkably widely used as the most affordable materials. Light weight and corrosion resistant are two features of Aluminium performance. The density of aluminium is about 2.7g/cm^3 , only a third density compared with iron, copper or steel.

3. Methodology study and Conceptual Design

3.1 Methodology study

The first research method for flapping wing aircraft is Concept Design which is based on the hang glider. Hang gliders are quite popular over the whole world. It is light and easy to control; the structure is simple, and used as a prototype in this project.

The second step is Initial Evaluation. There are two parts in this step; the first one is to calculate Power Requirement, which an obvious result would be given to know if it is feasible. The second part is to learn and have an understanding of unsteady Aerodynamics. The Theodorsen Theory is a classic and widely used theory, so this is the first theory to be learned for understanding unsteady aerodynamics

After Initial Evaluation, the basic and important parameter has been figured out. The next step of this project is Initial Design which is Flapping aerodynamic analysis. From this step, analysis and comparing would be given to find out the practical lift and thrust force generated by flapping or twisting motion. Results would be given for comparison and assessing the best aircraft movements.

To carry out the experimental work based on the ULFWA design and simulation, first a scaled 1:10 test model was produced by the author. The challenge of the work is to make the structure and mechanism representable to the designed ULFWA. Test and measurement of this model were made to demonstrate the concept feasibility and the design of the airframe and mechanical system.

3.2 Flow chart of methodology

Figure 3.1 shows a flow chart of the design procedure of the ULFWA.

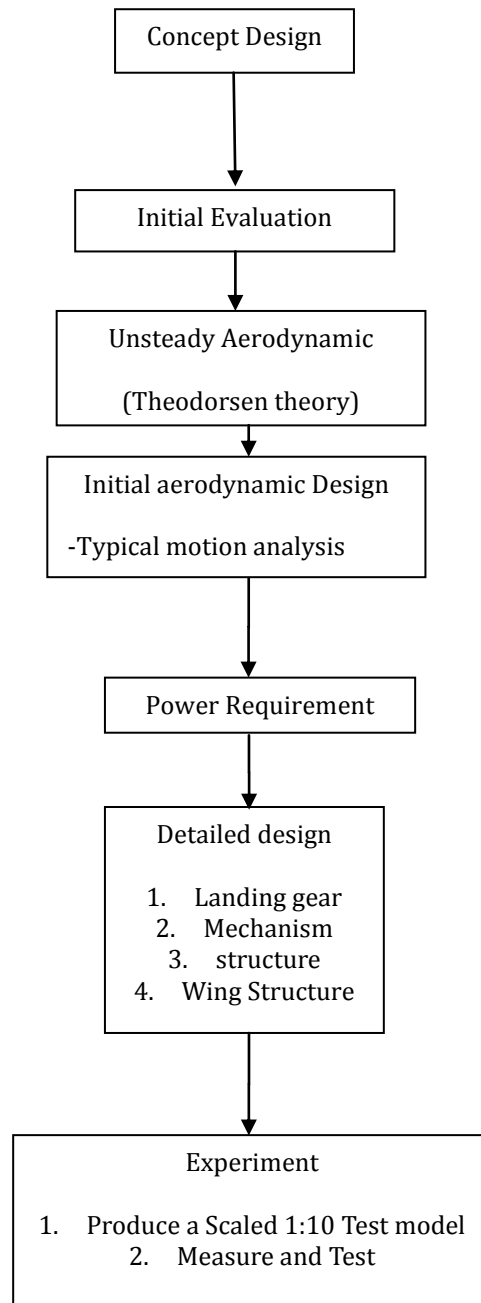


Figure 3.1 The design procedure for an ULFWA

3.3 Conceptual Design

The conceptual design of the ULFWA is based on the hang gliders and Para gliders because of their simple and light structures for high efficiency to glide. Comparing with Para gliders, hang gliders are more suitable for the ULFWA because of its manoeuvrability.

The ULFWA prototype is based on Falcon 3 [26] which is designed for novice pilots and manufactured by Wills Wing in 2006. The option was mainly because its size and the loading capacity and the speed range are appropriate for man-powered aircraft. The design data and configuration are shown in Fig.3.2, Fig.3.3 and Fig.3.4.

Hang glider model :	170
Wing area (m²) :	15.8
Wing span(m) :	9.1
Aspect ratio :	5.5
Hang glider weight (kg) :	22
Minimum pilot weight (kg) :	64
Maximum pilot weight (kg) :	77
Minimum speed (km/h) :	29
Maximum speed (km/h) :	77
Max glide ratio (L/H) :	-
Max glide ratio speed (km/h) :	-
Minimum sink rate (m/s) :	-
Packed length (m) :	5.4
Packed length short (m) :	1.8

The recommended hook in pilot weight range for the Falcon 3 is:

Falcon 3 145:	120 - 190 lbs.
Falcon 3 170:	140 - 220 lbs.
Falcon 3 195:	175 - 275 lbs.
Falcon 3 Tandem:	185 - 500 lbs.

Figure 3.2 Parameters of Falcon 3 [26]

To simplify the calculation and amend it to flapping type, the parameters will be changed slightly. The detail will be shown with graph in next page.

Wing Name	
Wing Span	= 9100.000 mm
XYProj. Span	= 9100.000 mm
Root Chord	= 2780.000 mm
M.A.C.	= 1947.203 mm
X _{CG}	= 1953.799 mm
Wing Area	= 158340.005 cm ²
XYProj. Area	= 158340.005 cm ²
Plane Mass	= 22.00 kg
Wing Load	= 0.000 kg/cm ²
Tip Twist	= 8.00
Aspect Ratio	= 5.23
Taper Ratio	= 3.97
Root-Tip Sweep	= 31.42

Figure 3.1 Details of the wing



Figure 3.2 Frame and structure of Falcon3

3.3.1 Lift force by using Theodorsen Theory

Theodorsen Theory is a classic theory for unsteady flow analysis and used to solve flutter problems. This theory provides a good base for better understanding of how flapping wing aircraft works. Further details are presented in Appendix A.

$$L = \pi\rho b^2[\ddot{h} + U\dot{\alpha} - ba\ddot{\alpha}] + 2\pi\rho UbC(\kappa)[\dot{h} + U\alpha + b(\frac{1}{2} - a)\dot{\alpha}] \quad (3.1)$$

From the formula, it is known the lift force is relevant with the changes of wingtip paths and angle of attack.

According to the analysis and test with different parameters, the acceleration of angle of attack (AoA) is the most crucial parameter for lift force especially in high flapping frequency (more than 1 Hz). For example, the term from acceleration of AoA produces 90% of the total lift force in 1 Hz. If reducing the frequency to 0.1 Hz, this particular force component becomes 40% of the total lift. As a conclusion, the flapping lift force is more sensitive to acceleration, i.e. high flapping frequency could generate high-peak positive lift force.

Unfortunately, the Theodorsen Theory is limited to predict the unsteady aerodynamics from small oscillating thin aerofoil. With the conclusion in this theory, when flapping amplitude is more than 5% of wingspan the theory will not be accurate.

3.3.2 Analysis an aerofoil of hang glider

According to the Falcon 3, the ULFWA is designed as 50 kg with wingspan 9.1 m and 5° AoA. The tip twist is 8° and the aspect ratio (AR) is 5.23 to generate the required lift force.

The analysis of the hang glider wing airfoil is a basic study for the man-powered flapping wing aircraft. This analysis will provide the basic aerodynamic data that leads to airframe especially the wing structure design. The analysis was carried out by using software XFLR based on the Vortex lattice method (VLM).

Figure 3.5 shows a simulation result of the wing including the center of lift, force under U , shape of drag force and C_p of each panel. The result indicates that the wing can lift a fully equipped pilot of 95 kg total weight at 12 m/s flight speed ($U=12\text{m/s}$).

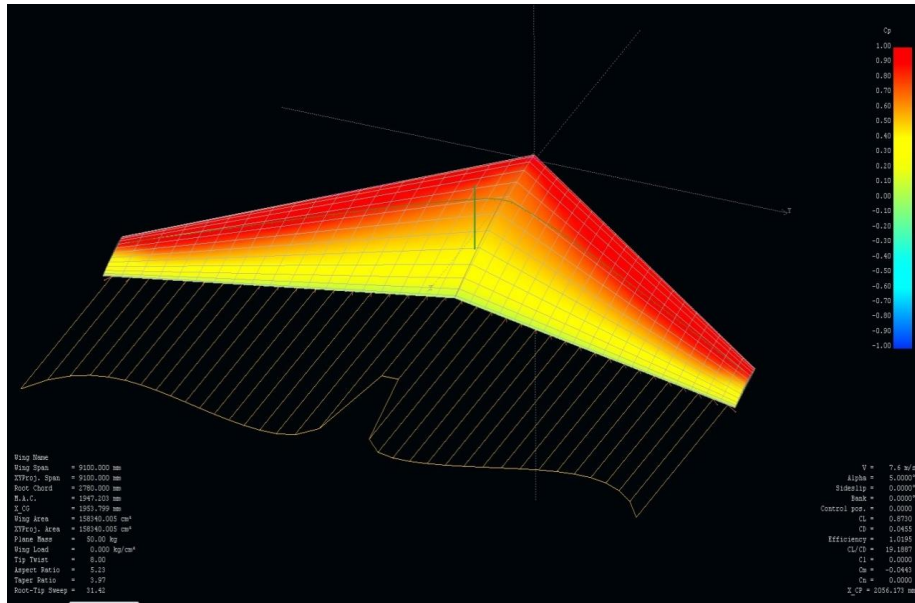


Figure 3.5 The aerodynamic result from xflr5

3.3.3 Leading-edge suction efficiency

Leading-edge suction is an important feature of the flapping wing aerodynamics especially for large AoA when vortex is generated at the leading-edge. The pressure created by vortex will have force to pull the wing, in another word, leading-edge suction will affect thrust force.

$$C_s = \frac{C_T}{\cos\Lambda} \quad (3.2)$$

$$C_T = (K_p - K_p^2 K_i) \sin^2 \alpha \quad (3.3)$$

$$K_i = \frac{\partial C_{Di}}{\partial C_L^2} \quad (3.4)$$

C_s Leading-edge suction efficiency

C_L Lift coefficient

K_i Induced-drag parameter

K_p Constant of proportionality in potential-flow lift equation

C_T Leading-edge thrust coefficient

C_{Di} Theoretical induce-drag coefficient

Depending on the shape of the wing, the efficiency is different. In this part the wing was set as the hang glider, so the result was 0.02368.

3.3.4 Strouhal number study and force analysis

Strouhal number is a dimensionless value useful for measuring the propulsive efficiency of an oscillating body in unsteady flow. In one experimental investigation [31], two experts showed the Strouhal number affects the propulsive thrust force of a flapping wing. The optimum value observed from most flying animals is in a narrow range of Strouhal numbers 0.2-0.4, which is recommended to be used by wing designers.

The Strouhal Number can be expressed as

$$St = \omega l / v \quad (3.5)$$

$St = \text{Strouhal Number}$

$\omega = \text{oscillation frequency}$

$l = \text{characteristic length}$

$v = \text{flow velocity}$

The Strouhal Number is important when analyzing unsteady oscillating flow problems. The Strouhal Number represents a measure of the ratio of inertial forces due to the unsteadiness of the flow or local acceleration to the inertial forces due to changes in velocity from one point to another in the flow field.

The vortices observed behind a stone in a river, or measured behind the obstruction in a vortex flow meter, illustrate these principles.

In animal flying or swimming, propulsive efficiency is high over a narrow range of Strouhal constants, generally peaking in the $0.2 < St < 0.4$ range. This range is used in the swimming of dolphins, sharks, and bony fish, and in the cruising flight of birds, bats and insects. However, in other forms of flight other values are found. Intuitively the ratio measures the steepness of the strokes, viewed from the side (e.g., assuming movement through a stationary fluid) – f is the stroke frequency, L is the amplitude, so the numerator fL is half the vertical speed of the wing tip, while the denominator V is the horizontal speed. Thus the graph of the wing tip forms an approximate sinusoid with aspect (maximum slope) twice the Strouhal constant.

Generally, flights in nature have very high efficiency, so the study on Strouhal number would be very useful and important for the knowledge of flapping wing aircraft.

Analysis:

To analysis and compare, the initial setting of AoA is 5° with wing geometric twist angle of 8° and cruise speed $U=15$ m/s designed for the ULFWA.

Case-1: Fig. 3.6 and Fig. 3.7 show the resulting lift and thrust with flapping amplitude (Amp) =0.8m at frequency 1Hz. With this motion, the Strouhal number is $St = \omega l / v = 1*(4*0.8)/15=0.21$ which is in the most efficient range. The average lift force 231.1N as shown in Fig. 3.6. But the thrust in one circle just like a trigonometric function curve and the average value is only 2N by integration the curve in Fig. 3.7. It means it is only able to keep the wing in 15m/s speed which is not enough for the whole aircraft. In addition, the difference between the peak and minimum lift force is only 90 N as shown in Fig. 3.7.

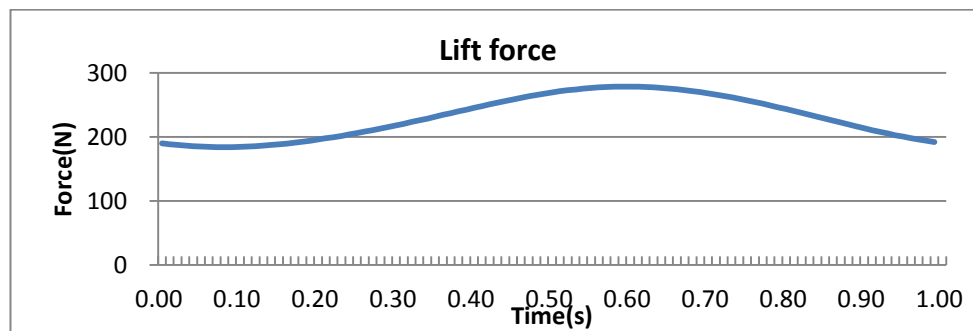


Figure 3.6 Lift force in 1s

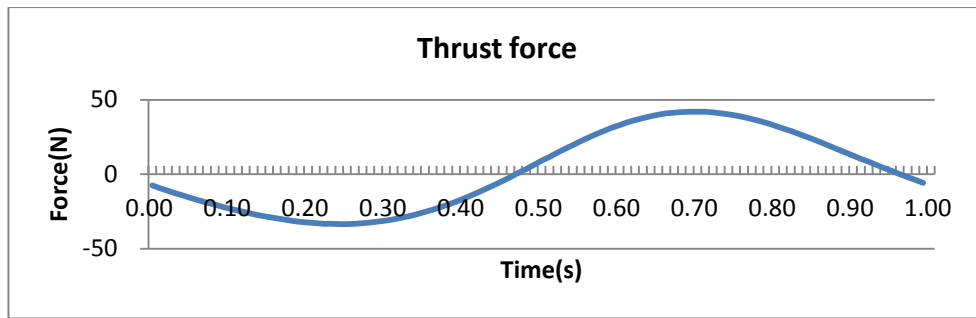


Figure 3.7 Thrust force in 1s

Case-2: Fig. 3.8 and Fig. 3.9 show the resulting lift and thrust with flapping amplitude (Amp) =1.5m at frequency 1Hz. The Strouhal number with this case is $St = \omega l / v = 1*(4*1.5)/15 = 0.40$ which is in the most thrust efficient range.

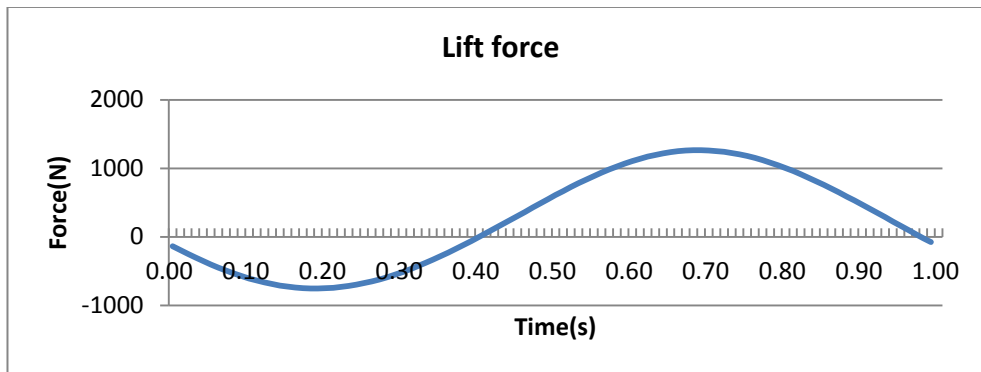


Figure 3.8 Lift force in 1s

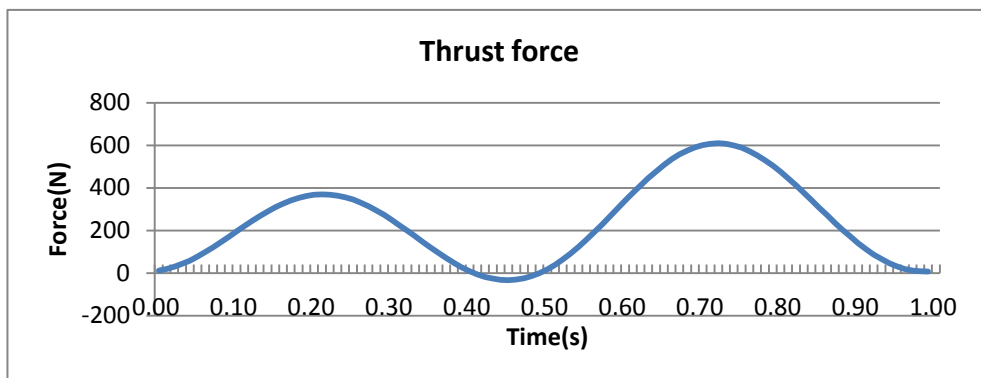


Figure 3.9 Thrust force in 1s

Although the lift force is not as steady as previous case, the average lift is much higher (244N in this case). Although the minus lift force -750N is also quite large, the average

thrust force 243.6N is also much larger than previous case. In addition, the thrust performance is much better with the negative thrust force (drag) lasting for only 0.06s. Further research on flapping wing should focus on vortex by using CFD (Computational Fluid Dynamics).

Case-3: Fig. 3.10 and Fig. 3.11 show the resulting lift and thrust with flapping amplitude (Amp) =0.75m at frequency 2Hz.

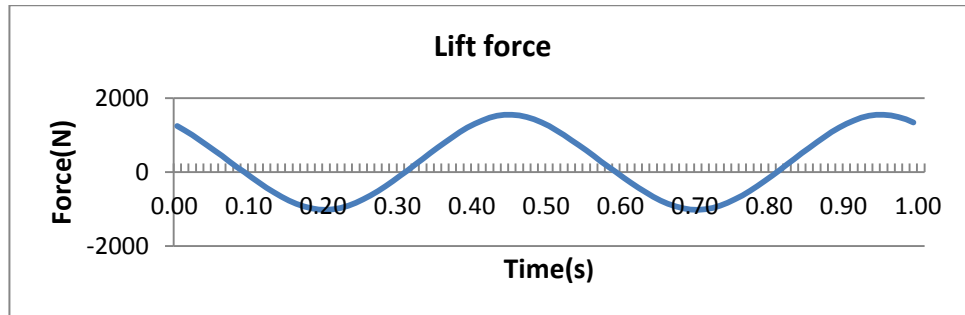


Figure 3.10 Lift force in 1s

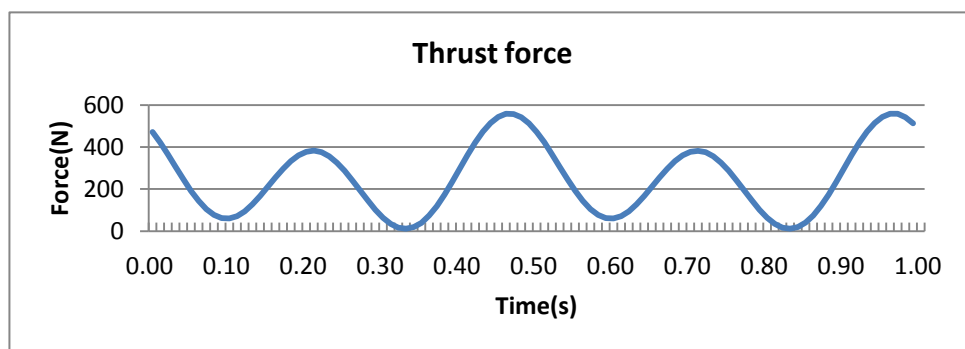


Figure 3.11 Thrust force in 1s

The Strouhal number in this case is $St = \omega l / v = 2 * (4 * 0.75) / 15 = 0.40$ as well which is same as last one. The average thrust force 255.5N is much larger than previous case although the curve of thrust is more fluctuant. The force keeps positive during the cycle.

The lift force is not as smooth as previous due to the higher frequency. However, the average lift 255N is much higher than previous case. The peak reaches more than 1500N, while the negative is -1000N. Thus, even the average lift is very high, the stability is poor. The solution is to increase frequency. However, it is extremely hard to achieve by man-powered flapping aircraft.

As a result, even if the forces are not stable in some situations, it is a better solution for flapping aircraft. Unfortunately, The St number between 0.2 and 0.4 is almost impossible to achieve by man-powered aircraft limited by the frequency and amplitude.

4. Initial design - aerodynamic analysis and power evaluation

Considering the human body movement capability in boating kinematics, the feasible flapping amplitude and frequency are limited to 0.8 m and 1 Hz. For the same Strouhal number, the higher frequency the higher lift and thrust. In this 1 Hz flapping condition, an optimal Strouhal number can be obtained. The ideal flapping motion is to generate steady lift force and positive thrust force. The steady lift force refers to the small difference between maximum and minimum lift force is less than 100N for a single wing. In this project, the minimum lift force is 700N for a single wing to achieve level flight at cruise speed.

4.1 Initial aerodynamic analysis

4.1.1 Lift force

This section presents the study on the lift force of a 2D airfoil in steady air flow to evaluate the difference by three different methods.

Case 1: The condition is $U=15$ m/s, $AOA =5^\circ$ of a fixed wing. As shown in Fig.4.1, it is found that the lift force (red) calculated by using panel method is the highest and used as a reference to compare with others. The second highest result is from the Theodorsen theory using the lift coefficient in the steady term, which is presented by Rambod F. Larijani and James D. DeLauriert (the formula is presented in appendix A and fortran program is presented in appendix B). The last on is from Theodorsen theory with the lift result 6N less than panel method.

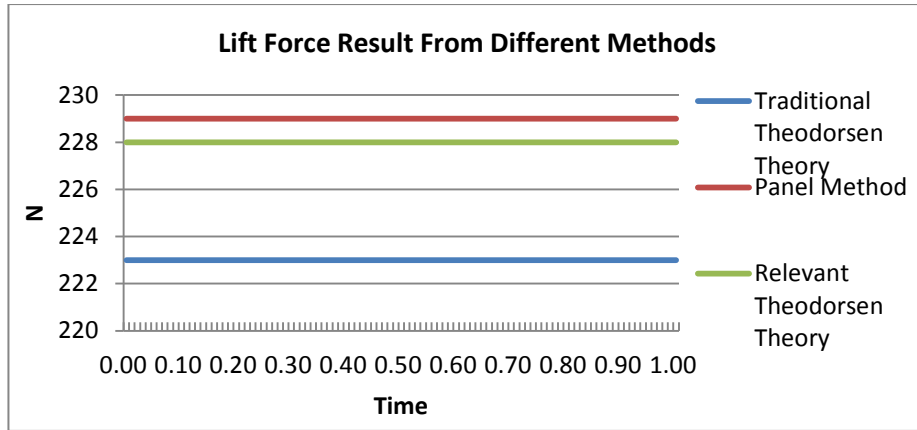


Figure 4.1 Lift Force Result from Different Methods

The Theodorsen theory assumption includes the flow always attached, the wing as a flat surface rather than airfoil. For the relevant Theodorsen theory and panel method, both take the airfoil shape into account.

Case 2: The condition in this case is set as $U=15$ m/s, $AoA=5^\circ$, twist angle= 8° and flapping amplitude 0.1 m. From the result shown in Fig.4.2, the average lift force from traditional Theodorsen theory is the smallest, only about 215N. The lift of 228N from the panel method is larger. Although the peak value from the relevant Theodorsen theory is the largest, the average lift force is about 221N. The results from traditional Theodorsen theory and relevant Theodorsen theory are almost the same as case 1. The unsteady aerodynamic force is slightly different because the airfoil effect was considered in the relevant Theodorsen theory.

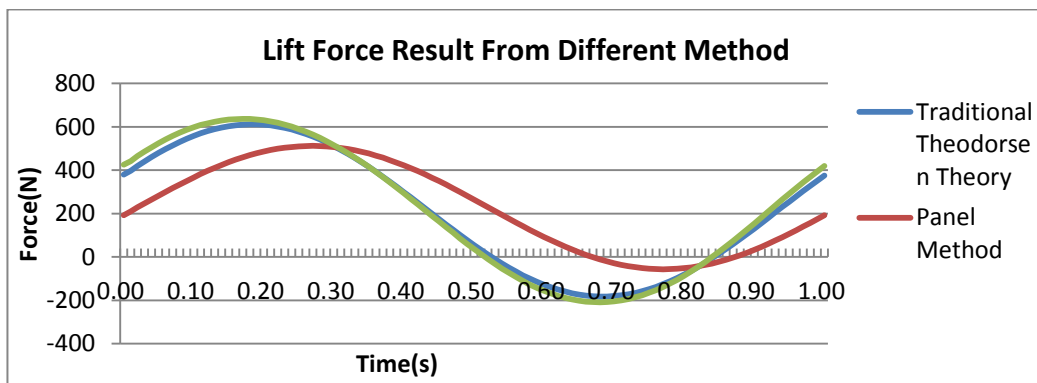


Figure 4.2 Lift Force Result from Different Methods

Kinematics in this Case seems complicated to know any detailed force generated by flapping or twisting. So in the following Case 3 and Case 4, twist and flapping would be analysis individually.

Case 3: In the case of $AOA=5^\circ$, twist angle= 8° , freq=1Hz and $U=15\text{m/s}$, it seems that there is more difference of these results as shown in Fig.4.3. The result from panel method is a bit larger than case 2. The Theodorsen's result is a little larger than last one by about 50N. There is a big difference of 120N between this result from the relative Theodorsen theory and the same one on motion 2.

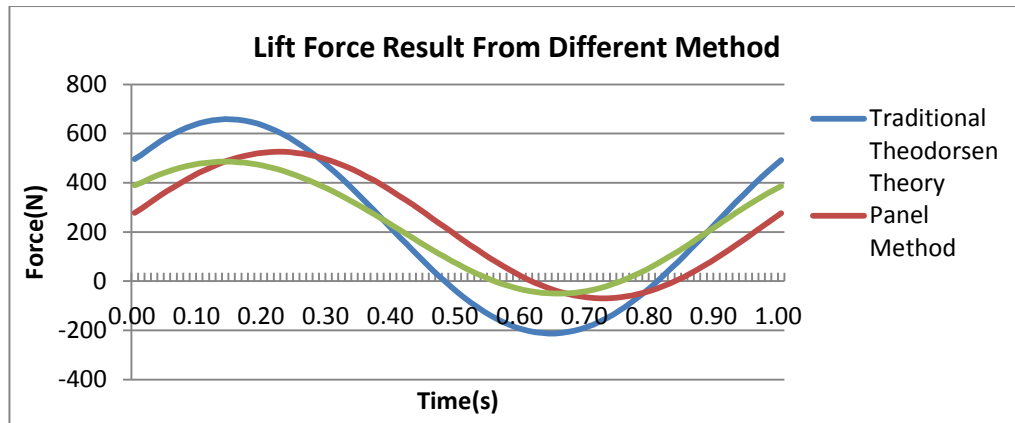


Figure 4.3 Lift Force Result from Different Methods

Case 4: In this case of $AOA=5^\circ$, AMP=0.1m, Freq=1Hz, $U=15\text{m/s}$, the results shown in Fig.4.4 shows the lift forces from three different methods. The largest amplitude is from the relevant Theodorsen theory. As usual, the average lift force from this theory is intermediate comparing with other method.

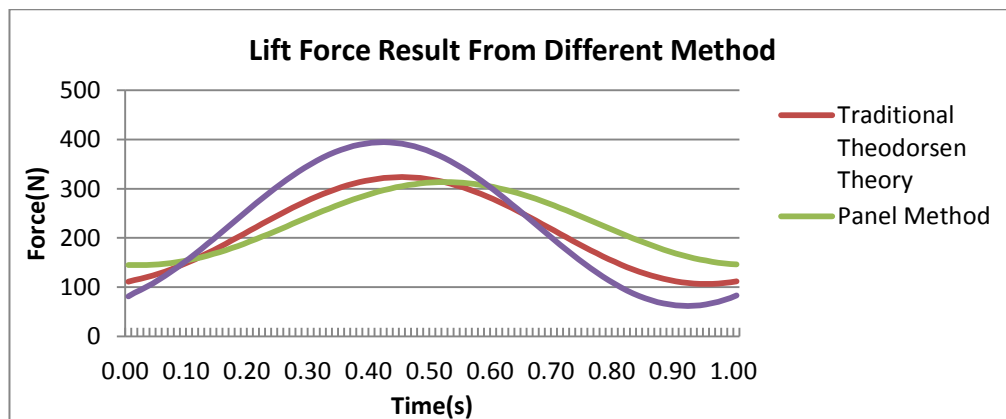


Figure 4.4 Lift Force Result from Different Methods

As a conclusion, the in-phase motion with twisting and flapping is not a best solution for flapping wing. To stabilize the lift, a solution is to find the combination of twist and flapping to figure out the best motion of kinematics.

2D panel method would be used in next step to analyse the characteristics in which airfoil and vortex effect should be considered [27].

4.1.2 Thrust force

Case 4: In this case (AOA=5°, AMP=0.1m, Freq=1Hz, U=15m/s), the thrust results are shown in Fig.4.5.

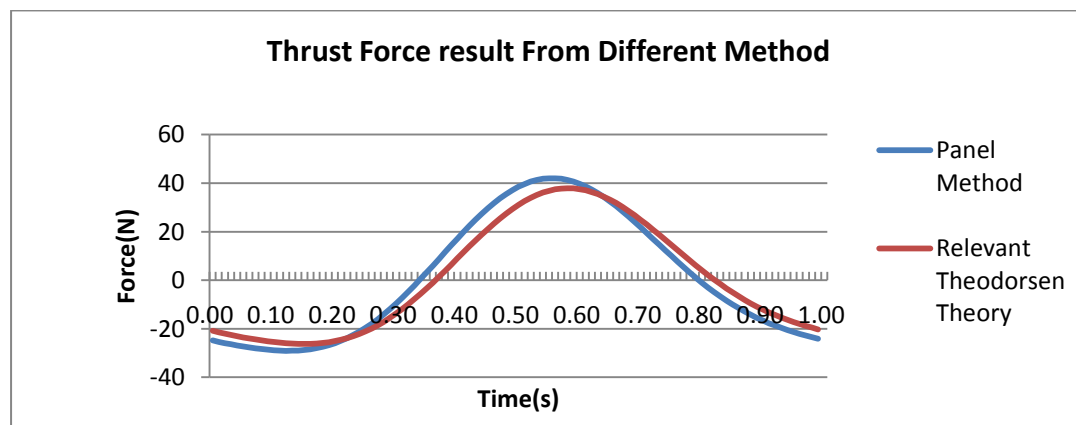


Figure 4.5 thrust Force Result From Different Methods

Case 3: In this case (AOA=5°, Twist angle=8°, AMP=0.1m, Freq=1Hz, U=15m/s), the thrust results are shown in Fig.4.6.

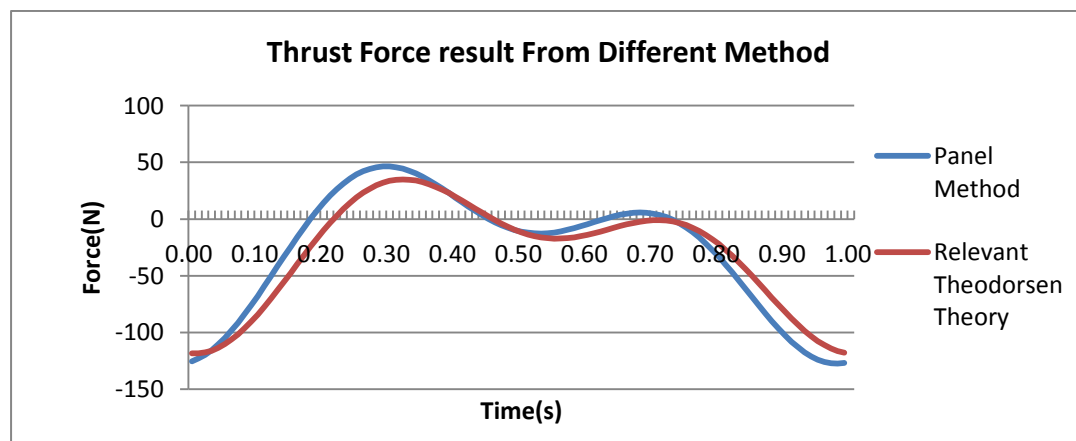


Figure 4.6 thrust Force Result From Different Methods

From the figures shown above, it shows that results from the relevant Theodorsen Theory are slightly lower than Panel Method. However, the shapes from two curves are

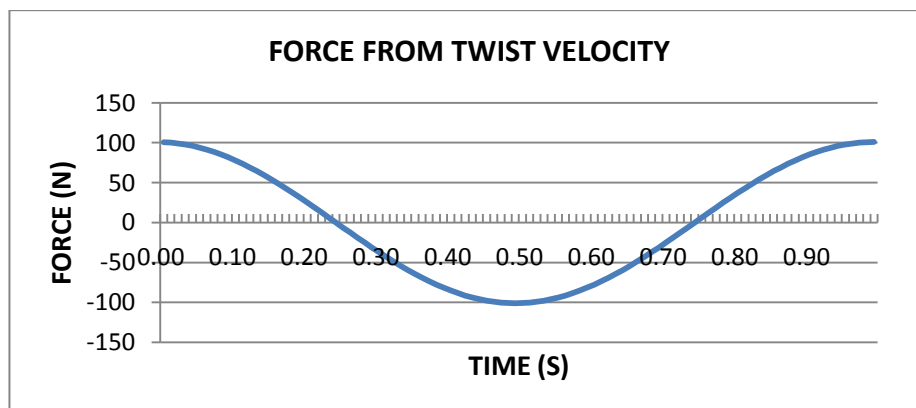
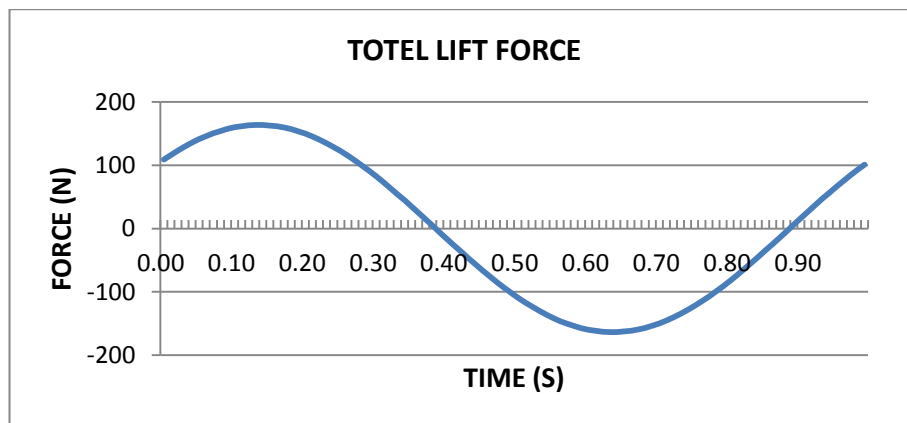
quite similar. Because of the Theodorsen theory limitation, the deviation is expected to be larger for larger flapping amplitude.

4.2 Analysing and comparing some typical motion

To figure the best motion out, for defining aircraft, we need to analyse and make comparison with some typical movement. From these databases, it is easy to be finding the most important parameters, the proportion they have, the trend via changing and how to compose the final motion. The every motion below is under the 15 meters per second airflow, which is same as the designed cruising speed.

4.2.1 Lift force analysis

Case 5 ($T_w=3^\circ$, Freq=1Hz, $U=15\text{m/s}$): Fig. 4.7 shows the lift force and each component contribution from the wing tip 2D section in sinusoidal flapping motion.



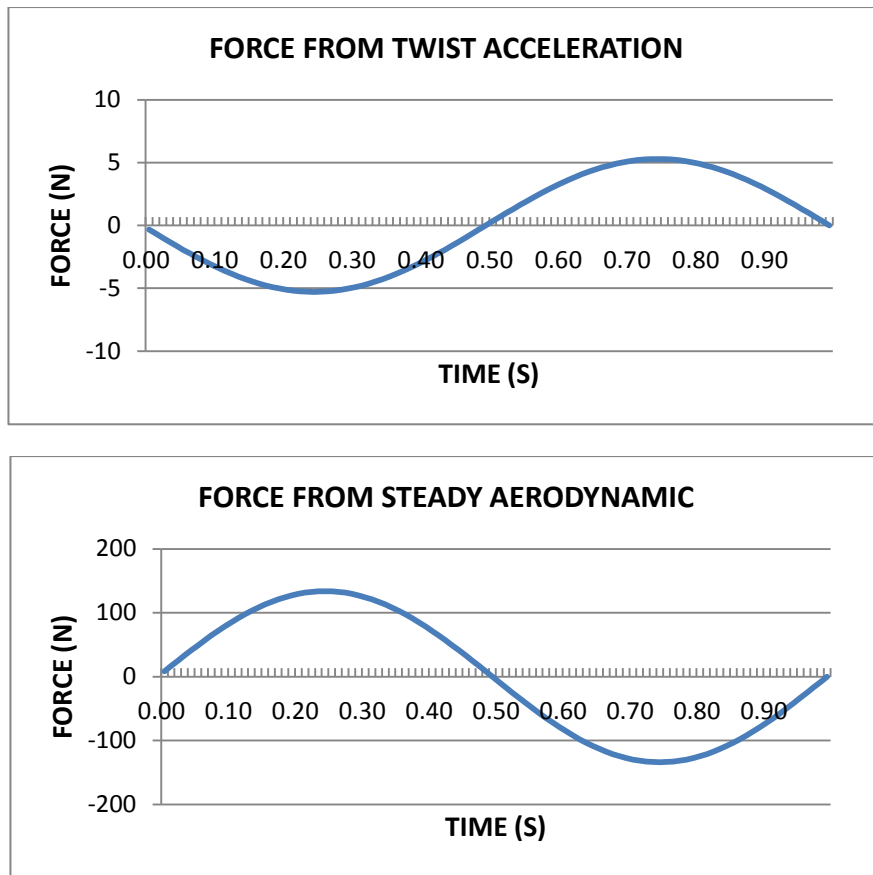


Figure 4.7 The lift force and components from the wing tip 2D section (case 5)

From these results, it is noted that the total lift force consist of force component from twist velocity, acceleration and steady aerodynamics. The force component from the steady aerodynamics and twist velocity are almost the same in magnitude, but different phase. However, the force from acceleration is quite small in this case. For this single wing of 5 m long and 30° backswept angle, the total lift of one wing is between 803N and -803N as shown in Fig.4.8 and the overall the average lift in one cycle is nearly zero.

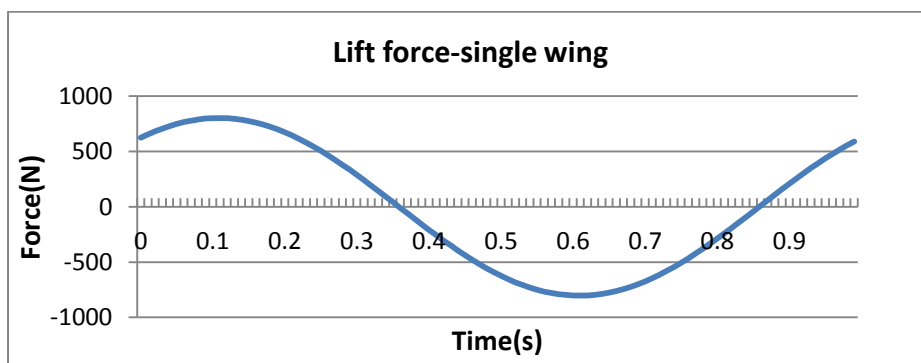


Figure 4.8 Total lift force for single wing

Case 6 ($T_w=8^\circ$, $Freq=1Hz$, $U=15m/s$): Compared with Case 5, the increased twist angle causes a significant increase of the lift force especially the components from the twist. The force components from the wing tip 2D section in sinusoidal flapping motion are shown in Fig.4.9. It is noted that the force is linearly increasing with twist angle. The result is quite similar to the previous case except the value 2.67 times greater.

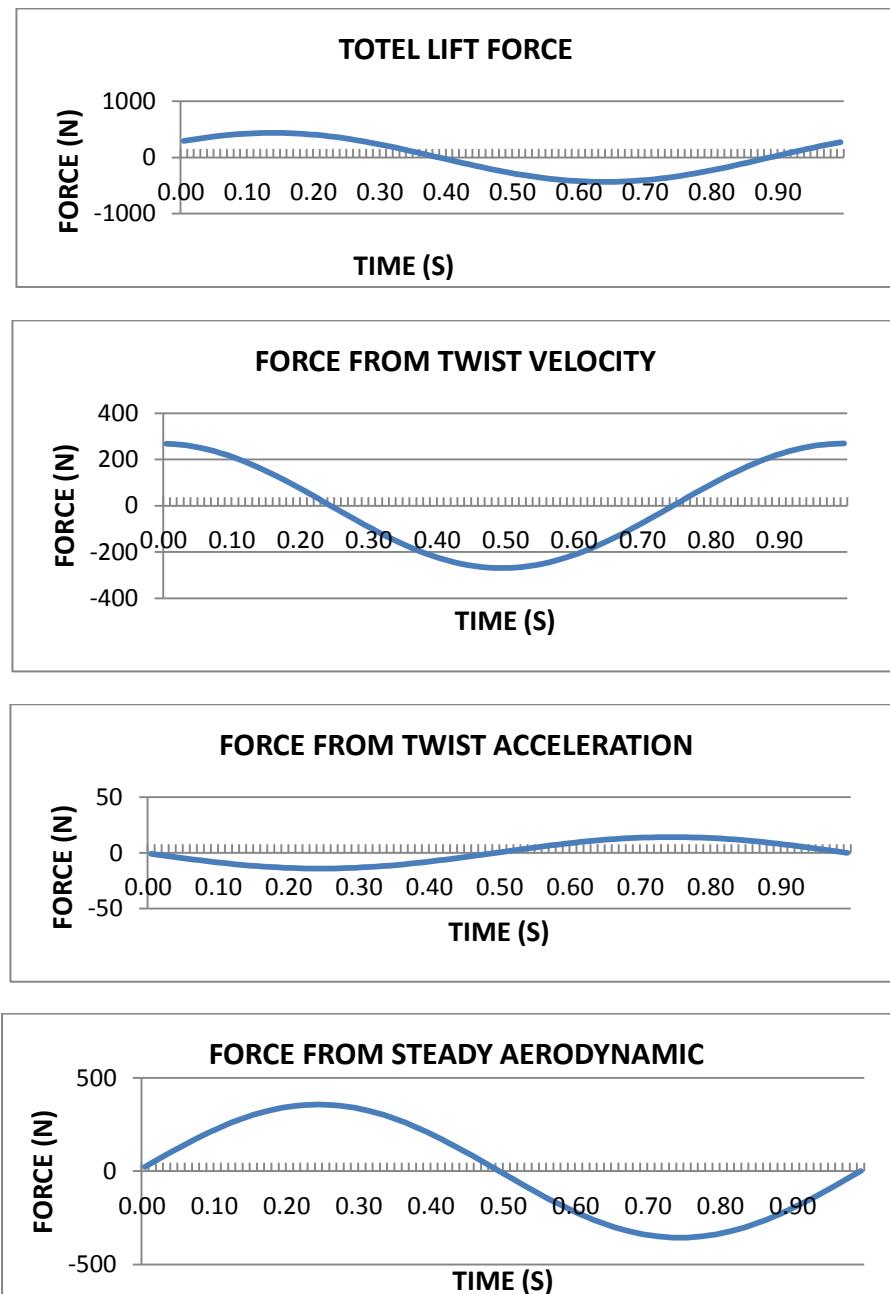


Figure 4.9 The lift force and components from the wing tip 2D section (case 6)

For one single wing, the total lift is between 2141 N and -2141 N as shown in Fig.4.10. Similar to the previous case, the force is linear variation with the twist angle and the average lift force is zero as well.

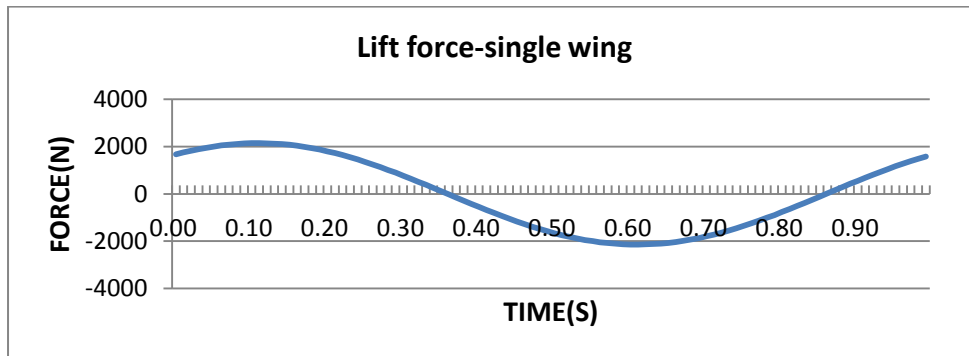
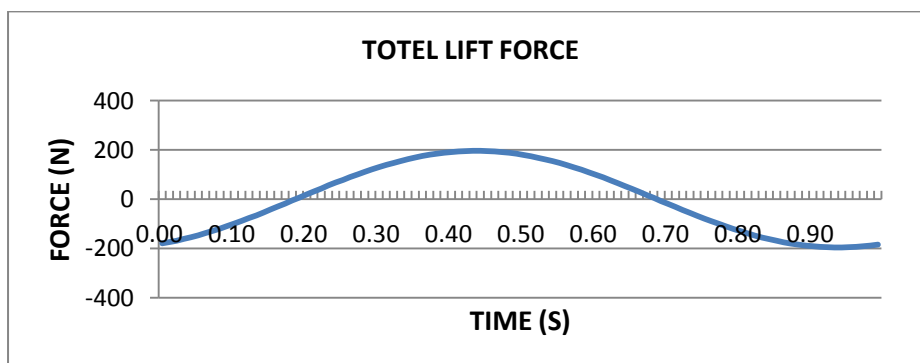


Figure 4.10 Total lift force for single wing

Case 7 (Amp=0.2m, Freq=1Hz, U=15m/s): The Fig. 4.11 shows the lift force and each component contribution from the wing tip 2D section in sinusoidal flapping motion.

Since the flapping amplitude of 0.2 m is not a big motion for 9 m span wing, it is feasible to achieve and control. The total lift force is between 196 N and -196 N and the average lift force is zero as well if the wing airfoil and AoA is not taken into account. The flapping acceleration contributes about 26.7% to the total lift force, and the rest of them belong to flapping velocity.



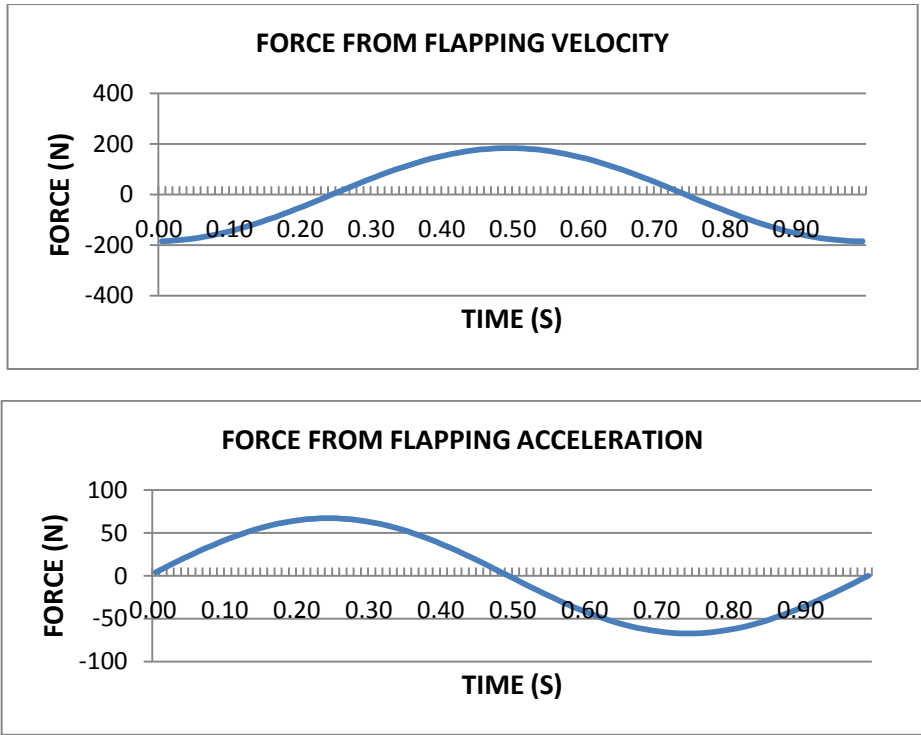


Figure 4.11 The lift force and components from the wing tip 2D section (case 7)

With the flapping motion, the single wing could generate 1034 N to -1034 N total lift with only 0.2 m flapping amplitude as shown in Fig.12.

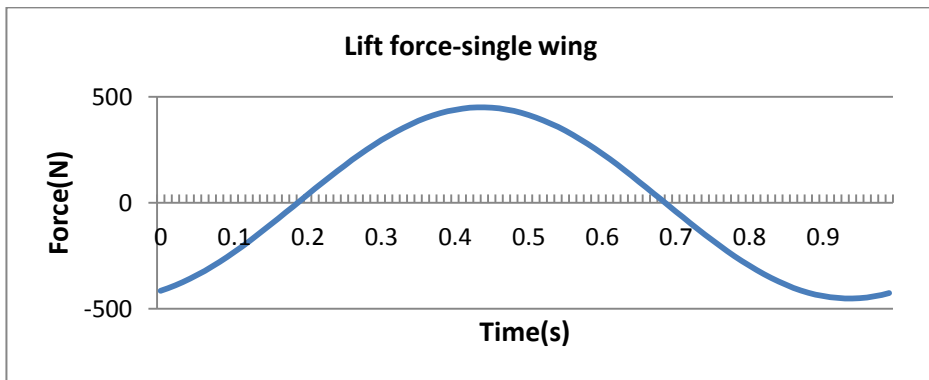


Figure 4.12 Total lift force for single wing (case 7)

Case 8 (Amp=0.4m, Freq=1Hz, U=15m/s) The Fig. 4.13 shows the lift force and each component contribution from the wing tip 2D section in sinusoidal flapping motion.

For 0.4 m amplitude flapping, the wing section lift force is around 356 N and -356 N. This value is about 1.82 times larger than Case 3, which means it is not linear, but with increasing of amplitude the force increased. In this case, the acceleration contributes about 29.0% to total lift, which is a little more than case 3.

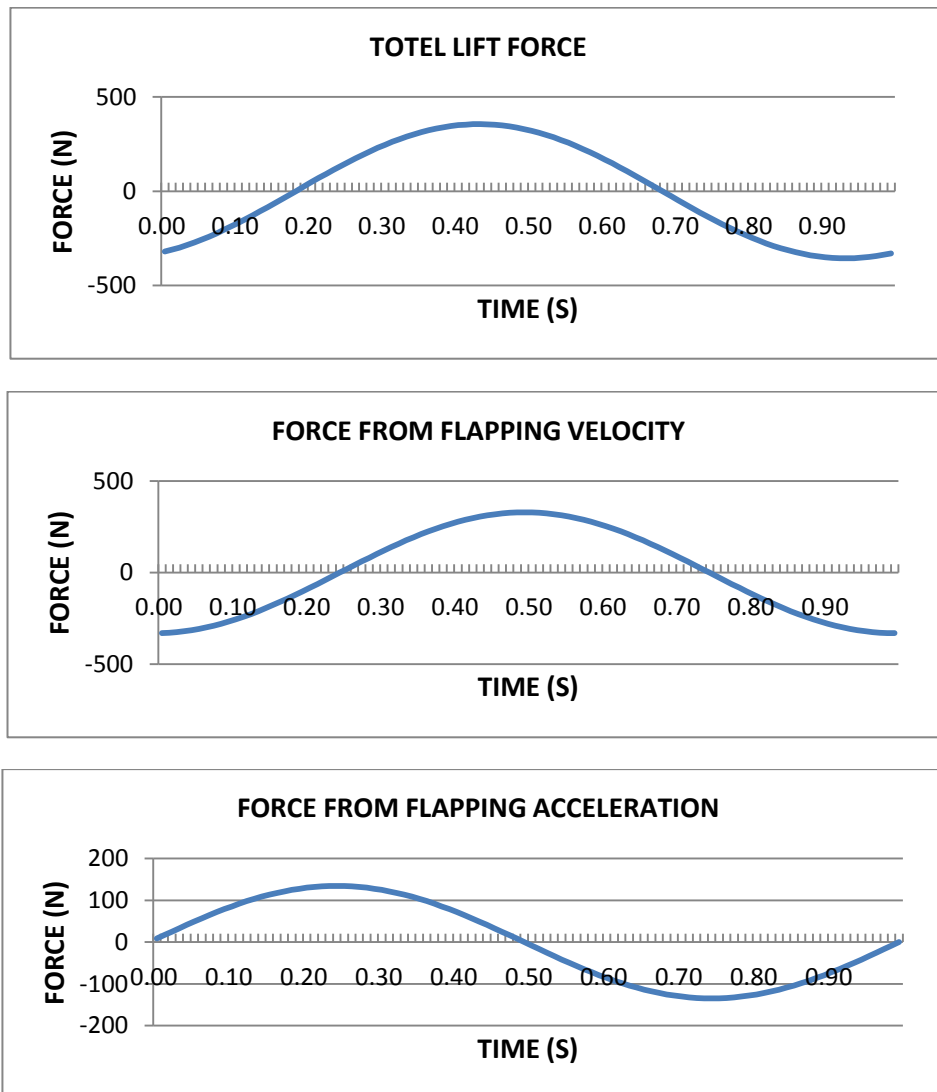


Figure 4.13 The lift force and components from the wing tip 2D section (case 8)

In this situation, the total lift force reached an extremely high peak (901 N) and extremely low bottom (-901 N). This value is two times greater than the case 3.

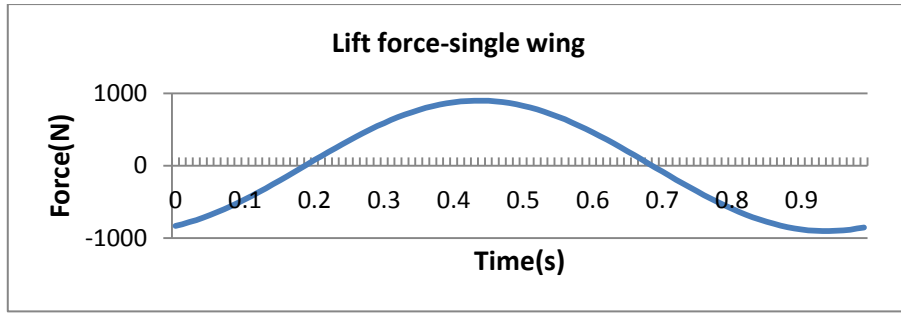
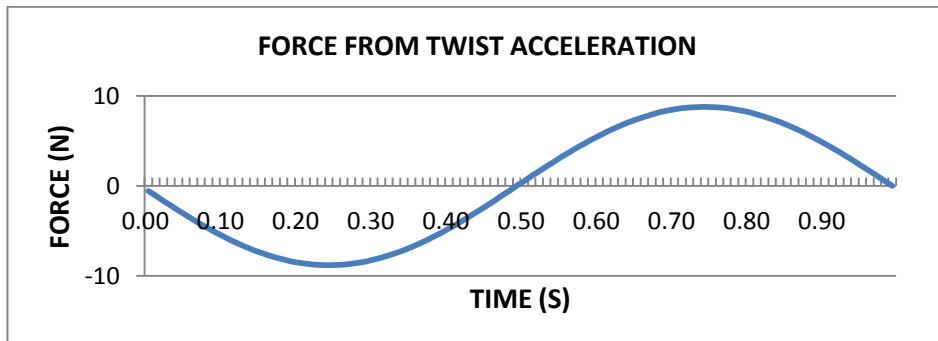
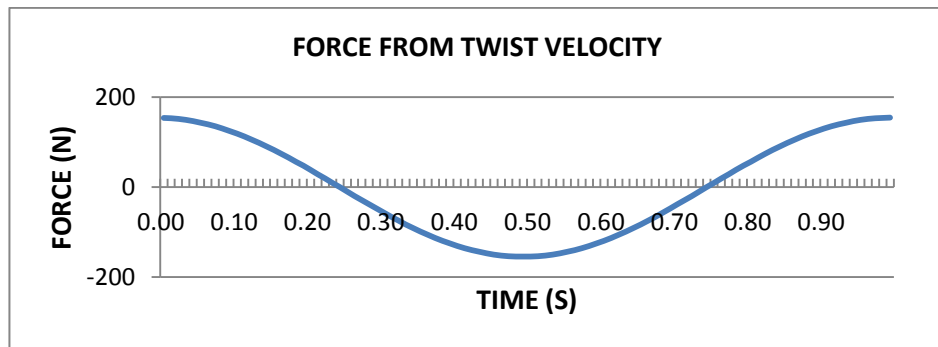
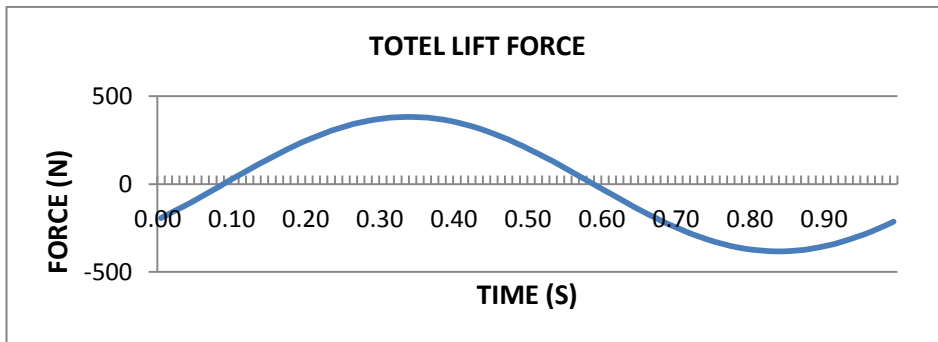


Figure 4.14 Total lift force for single wing

Case 9 ($T_w=5^\circ$, $Amp=0.4m$, $Freq=1Hz$, $U=15m/s$) The Fig. 4.15 shows the lift force and each component contribution from the wing tip 2D section in sinusoidal flapping motion.



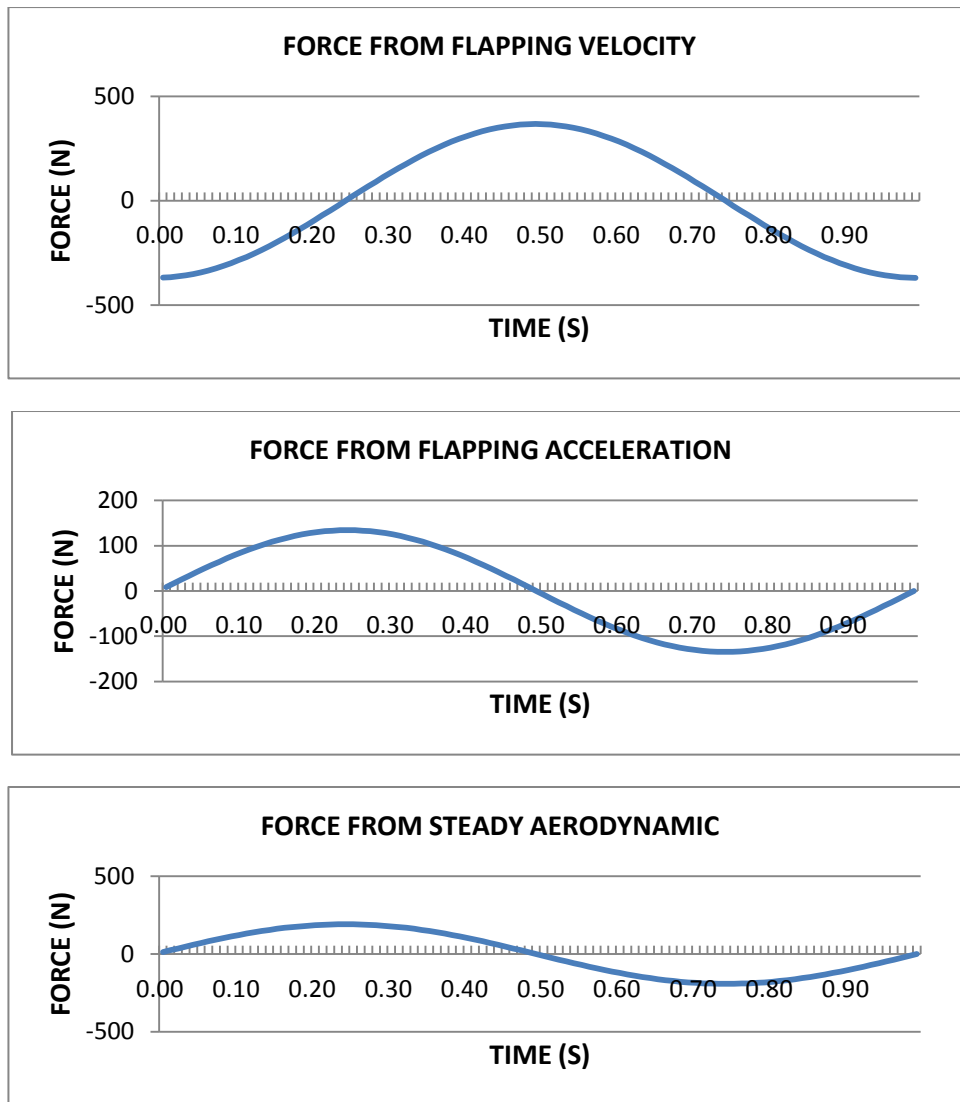


Figure 4.15 The lift force and components from the wing tip 2D section (case 9)

Summary

Twist and flapping motion could generate both positive and negative lift force. The acceleration makes significant contribution to the total lift even in such a low flapping frequency. In symmetric motion and flat surface however, the average lift force is zero.

4.2.2 Thrust analysis

Although the average lift force is zero, the thrust or drag force may not be zero. This section focuses the study on the thrust in case-5 to case-10 which is helpful to understand flapping aircraft.

Case 5 (Twist=3°, Freq=1Hz, U=15m/s): In this case, the positive thrust only appeared for 0.45s in one cycle between 0.39s and 0.83s, and only reached the peak 15.2 N as shown in Fig.4.16. The negative force indicating the drag kept so long with larger negative value 43.4 N. So the average thrust in this case is -9.75 N. In this situation, 3 degrees twist could generate positive thrust force in a short time and low value.

Unlike the lift force, this thrust curve is un-symmetric because of separate flow induced vortex especially when wing moving in down stroke.

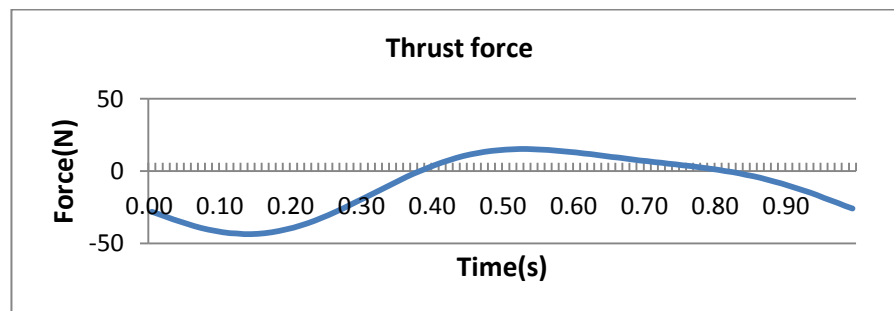


Figure 4.16 Thrust force with wingtip section (case 5)

Case 6 (Tw=8°, Freq=1Hz, U=15m/s): In this case, the thrust variation over a cycle is quite different from the previous case of 3° twist. The highest peak thrust reached 54.6 N at 0.47s, and the negative thrust dropped to -150 N at 0.15s as shown in Fig.4.17. In this case, the average thrust was -30.5 N.

From the thrust result of Case 5 and Case 6, it is clear that changing angle of twist could only generate negative thrust because of vortex. Moreover, the negative force becomes lower along with the increased changing angle of twist.

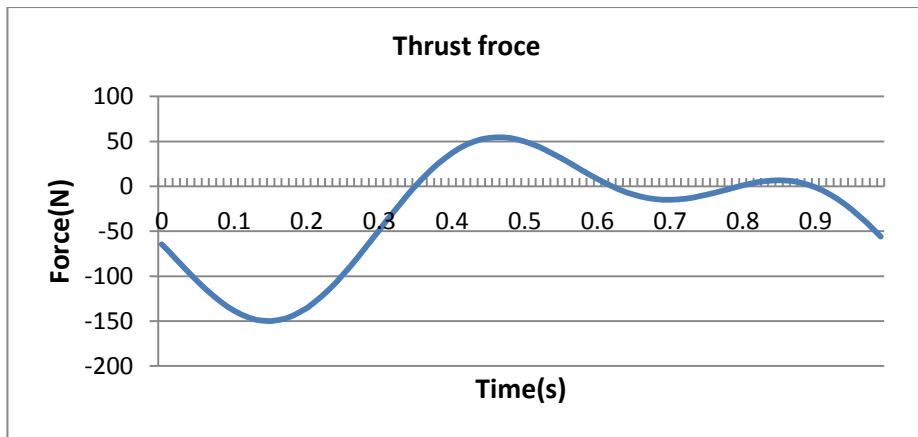


Figure 4.17 Thrust force with wingtip section (case 6)

Case 7 (Amp=0.2m, Freq=1Hz, U=15m/s): About thrust force from flapping, the curve in chart is shown above. The average thrust force is positive with a value of 23.8 N. in this time round; the peak force appeared at 0.56s reached 135N. Unfortunately, negative thrust force last 0.52s, a little more than positive force. However, the value of negative force is much smaller than positive force. Thus, in this situation, the thrust force is positive in total and it is favour of flapping aircraft.

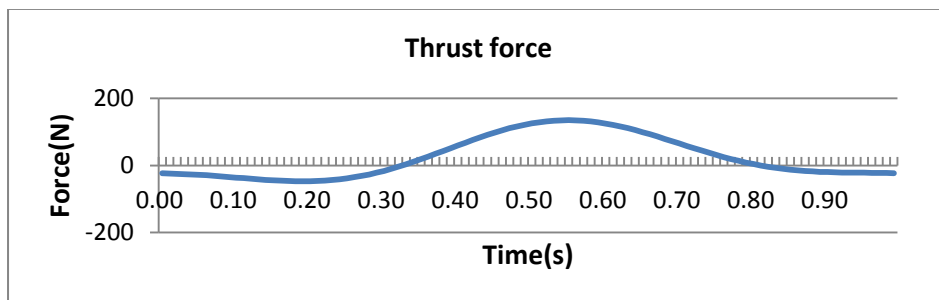


Figure 4.18 Thrust force with wingtip section (case 7)

Case 8 (Amp=0.4m, Freq=1Hz, U=15m/s): In this case, the average thrust is 115 N. This is because of the decrease of negative force time and dramatic increase of positive force in a cycle. As shown in Fig.4.19, the negative thrust only appeared for 0.85s from 0.15s to 0.32s, while at 0.85s the value almost equivalent to 0 N. the peak value appeared at 0.55s when wingtip just passed the initial position (start point) and moving downward. Compared with the previous case, the negative value became slightly higher. What's more, it last much shorter. In this situation, thrust is much better than the previous flapping because this motion has a long and constant positive thrust.

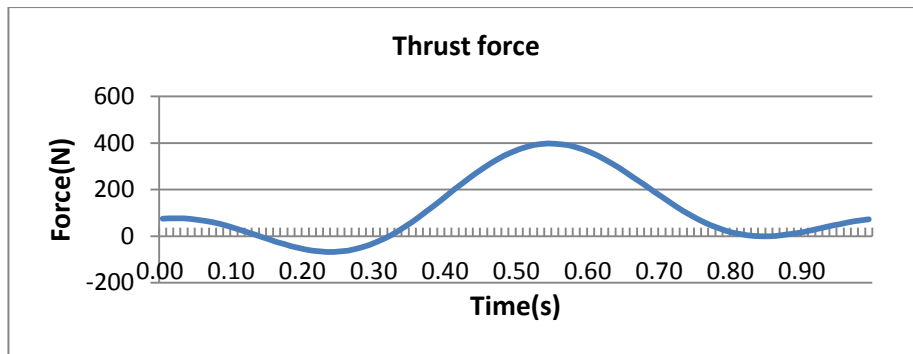


Figure 4.19 Thrust force with wingtip section (case 9)

Case 10 (Amp=0.8m, Freq=1Hz, U=15m/s): In the last two cases, it is obviously that flapping wing generates thrust which increases with the flapping amplitude. Further analysis is therefore necessary. In this case, the flapping amplitude increasing to 0.8 m seems very large for a 4.5 m single wing by man-power. In nature however almost all flying animal could flaps their wings like this or even more. In this motion, the negative thrust force occurs for only 10ms from 0.22s to 0.32s over a cycle as shown in Fig.4.20. There are 2 peaks and 2 negative points in this curve. The first peak reached 653 N at 0.04s, which is 50% greater than the last case. The second peak reached 1310 N at 0.55s, which is more than three times as large as the last one. The first negative thrust -89.9 N appeared at 0.26s. The average thrust is 483 N, which is more than 4 times larger than the last one. It is noted that the flapping could generate positive thrust and would sharply increase along with flapping amplitude increasing.

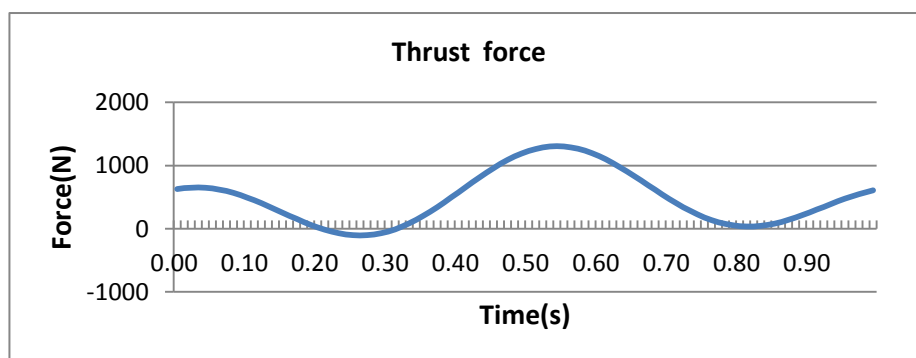


Figure 4.20 Thrust force with wingtip section (case 10)

On the other hand, increasing flapping amplitude could enlarge the difference of peak and negative lift force, which is not useful for average lift and unstable for aircraft. So it is necessary to find a best motion to make aircraft stable and generating thrust force as much as possible.

Summary

From the study, it is noted that wing twist could generate negative thrust/drag although positive thrust show up in short time. The flapping motion could generate positive thrust even if the lift is not steady enough and average lift is zero. The flapping amplitude would affect thrust force directly.

4.2.3 Mixed motion analysis

Overall, to make aircraft more stable requires that aircraft could generate constant, smooth and steady positive lift force, positive average thrust force. So an optimal mixture of twist and flapping motion is necessary.

Firstly, from the given thrust result, it needs to set flapping amplitude with less twist effect. From previous result, in 15 m/s cruise speed, 0.4 m flapping amplitude is good for aircraft since it could generate 115 N average thrust. Besides, this wingtip amplitude motion is feasible to achieve and the velocity and acceleration is not very high. In other words, the wing structure can be made lighter with adequate strength and the required power can be minimized.

Fig.4.21 shows that a wing section of 1 m at wingtip could generate 901 N lift force at 0.44s, and -901 N minimum lift force at 0.94s.

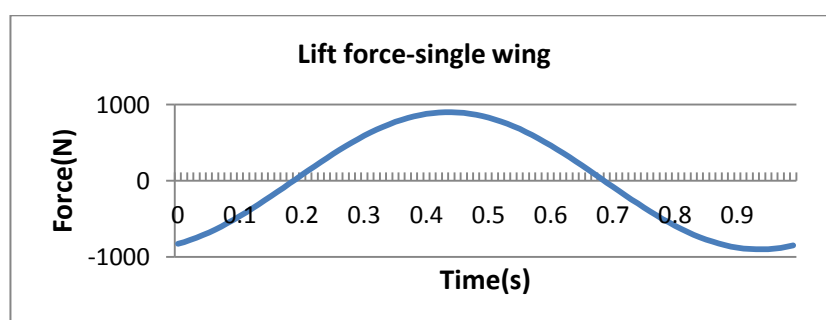


Figure 4.21 Total Lift force with single wing

From the previous result, the maximum and minimum lift force from 8° twist is almost same as this one, only has ± 70 N difference for a single wing as shown in Fig.4.22.

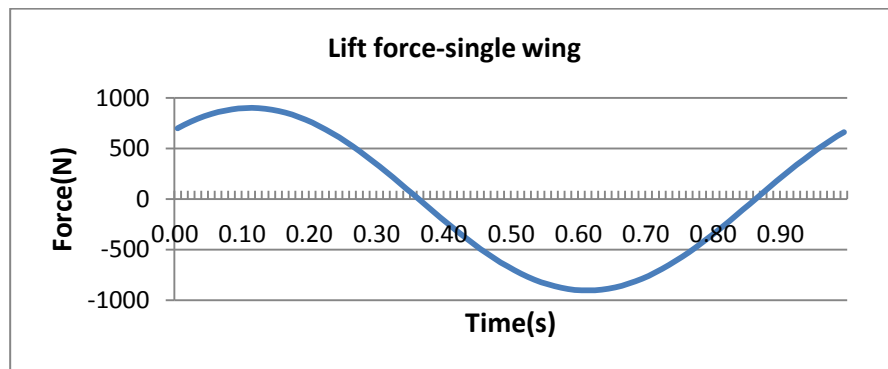


Figure 4.22 Total Lift force with single wing

To improve the result, one solution is to shift the phase of the forces due to twist. For example, the twist was advanced in time for 0.19s with the motion function changed to $tw = \sin(2\pi(t + 0.17))$. After the combination, the peak value difference is reduced. As shown in Fig.4.23, the peak only reaches 14.03 N and the negative -14.02 N. Since there are only less than 28N differences between them, the aircraft becomes more stable.

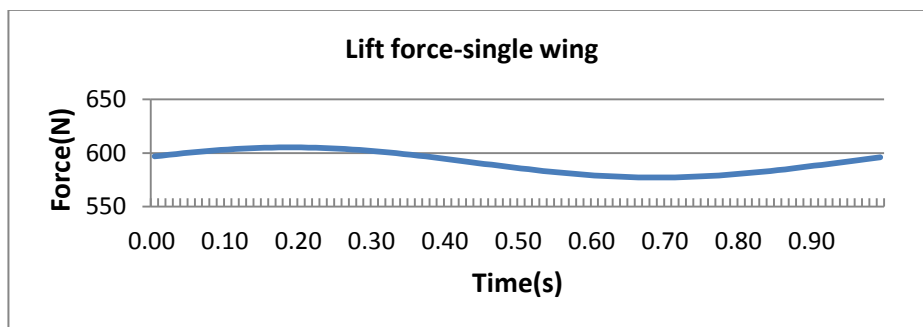


Figure 4.23 Total Lift force with single wing

Case 11 (AOA=5°, Tw=3.37°, Amp=0.4m, Freq=1Hz, U=15m/s): With 5 degree initial AoA in this case, the minimum lift force became 971.4 N, and the maximum 999.5 N as shown in Fig.4.24. In other words, it could lift a 190 kg aircraft with two wings. For man-powered aircraft, if the pilot weight is less than 80 kg, the airframe could have about 110 Kg weight, which is possible.

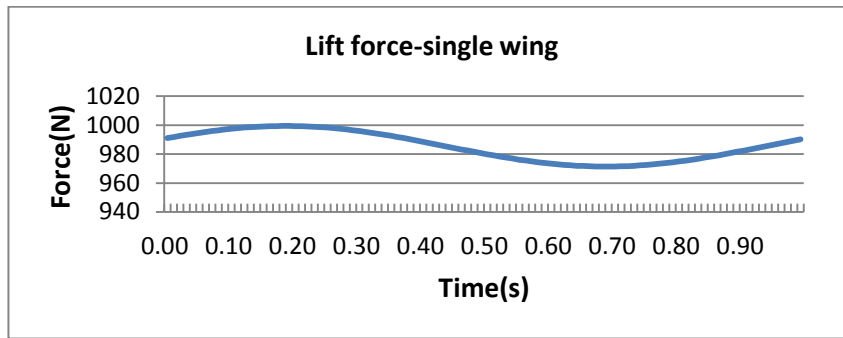


Figure 4.24 Total Lift force with single wing

In this case, the thrust was shown in Fig.4.25. The thrust peak lift reached 351 N at 0.52s, and the negative -94 N appeared at 0.19s. From this curve, the thrust force is not steady as previous. Although the time last for positive and negative force is equal, the average thrust is positive 76.8 N. This value is not as large as the previous with flapping only, but is adequate enough to maintain cruise.

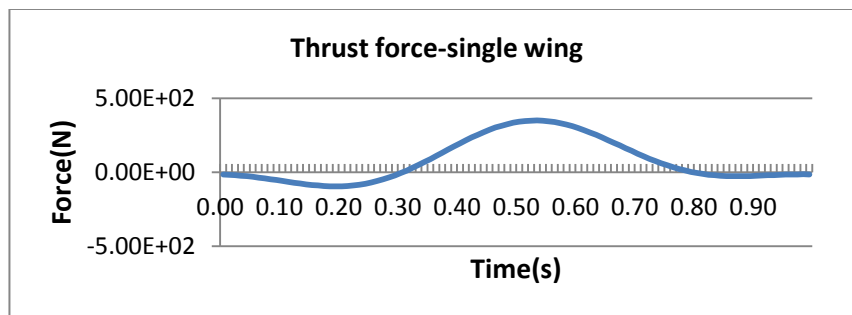


Figure 4.25 Total Thrust force with single wing

Case 12 (AOA=8°, Tw=3.37°, Amp=0.4m, Freq=1Hz, U=15m/s): To gain larger average lift force for powered flapping aircraft, larger initial set AoA is required. In this case with 8 degree initial AoA, the minimum lift was increased to 1562.68N and the maximum 1590.72N as shown in Fig.4.26. Same as the previous one, the difference from maximum and minimum lift force is less than 28 N, which means it is as stable as the previous one. The only difference in this case is that the total aircraft weight could be about 220 Kg.

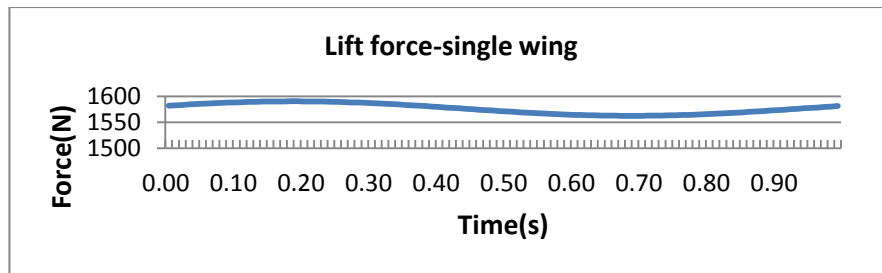


Figure 4.26 Total Thrust force with single wing

With this high lift motion, the peck appeared at 0.52s reached 452 N, and the bottom appeared at 0.14s dropped to -184 N. Time of positive and negative force is 50:50 as well. Unlike the last one, the average thrust force of this motion is only 68.1 N. Even this motion could only generating a smaller average thrust force, it could be appropriate for most of aircraft and polit. What’s more, this motion would be good for cruising.

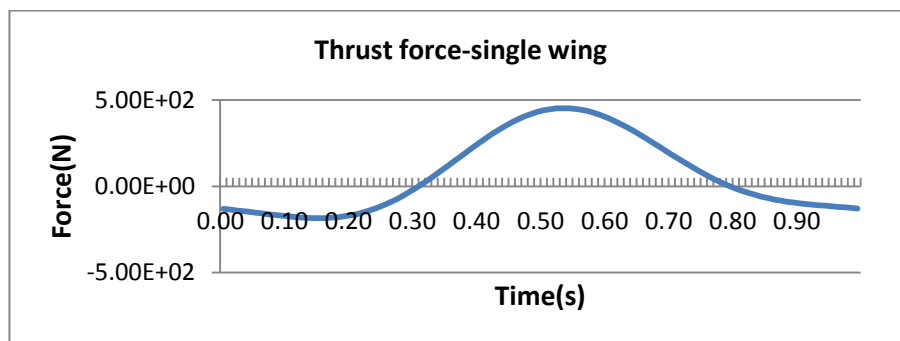


Figure 4.27 Total Thrust force with single wing

Case 13 (AOA=3°, Tw=3.37°, Amp=0.4m, Freq=1Hz, U=15m/s): For the case of setting the initial AoA=3 degree, the lift force dropped significantly with the lowest force 577.24N and the highest 605.29 N as shown in Fig.4.28. Although the average lift force was only 591.26 N, it seems enough for ultra-light aircraft of weight around 40Kg.

The average thrust force as shown in Fig.4.29 is 80.4 N, which is about 4.7% higher than the case with 5° AOA. The thrust force is larger and steadier than any previous case. There is negative thrust force appears for only 0.23s in this motion. For take-off, this motion could be used for increasing speed as well.

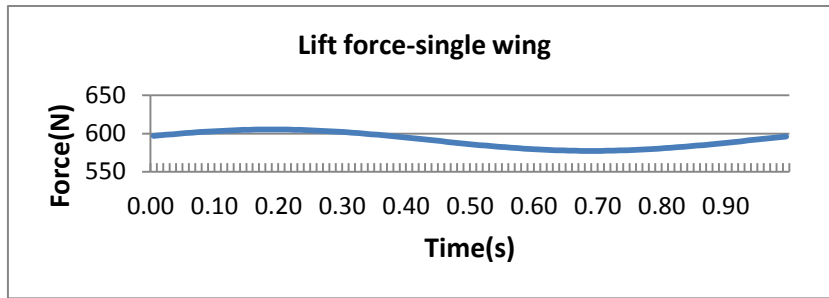


Figure 4.28 Total Lift force with single wing

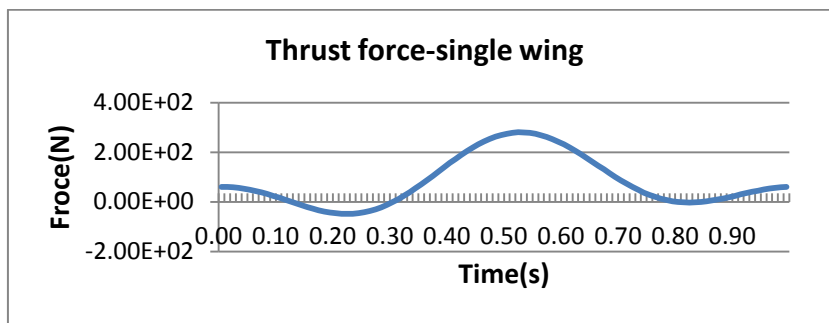


Figure 4.29 Total Thrust force with single wing

Summary

From previous results, it is known that flapping wing could generate thrust and enable aircraft at low speed. With different angle of attack, aircraft performance could be controlled to achieve speed increase or keep cruise. To make aircraft much stable, it requires flapping and twisting at the same time but in optimal phase or time difference. The study shows that the flapping amplitude 0.4 m and AOA=3.37° is an ideal case, where cruise aircraft of a 200Kg ULFWA is feasible.

4.3 Power estimating

To investigate into the flying feasibility by human power, the study on power estimation and requirement is carried out in this section. The principle of conservation of energy was used as the theory. Basically, total energy consists of kinetic energy and potential energy.

$$W = E_k + E_p = \frac{1}{2}mv^2 + mgh \quad (4.1)$$

where

W is energy

E_k is kinetic energy

E_p is potential energy

m is mass

v is velocity

If without any force from outside such as drag, aircraft could be maintained at constant height and initial speed. In reality however, to generate the lift and thrust to maintain flying, enough power input is required due to loss of energy. So drag force is to be evaluated for power estimation.

Figure 4.30 shows the drag results of the wing at $U=15$ m/s, $AOA=5^\circ$ by the Xflr5 program. The resulting drag coefficient is 0.0443. The single wing is 17.5 m². Thus based on the following equation, the single wing total drag force is 18.30 N.

$$F_D = \frac{1}{2}\rho v^2 C_D A \quad (4.2)$$

F_D is drag force

C_D is drag coefficient

A is area

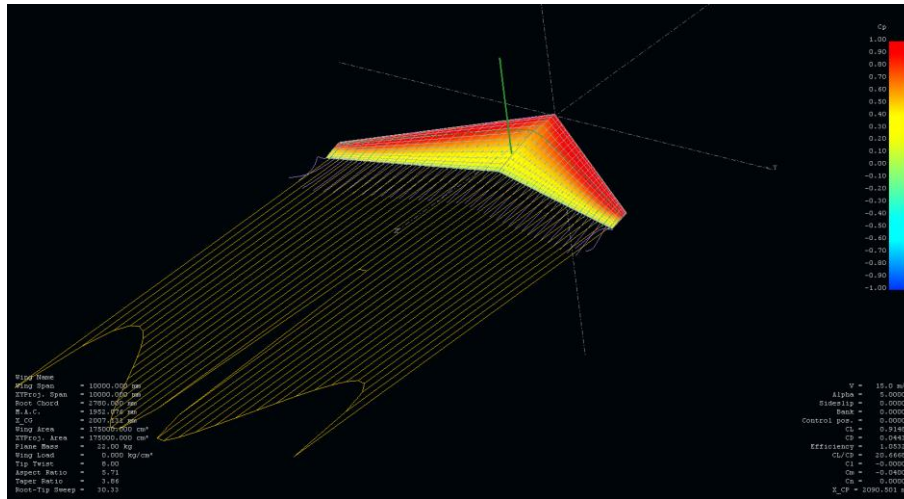


Figure 4.30 The drag result from xflr5

For the aircraft body drag, consider a car having drag coefficient between 0.3 and 0.5. To predict the worst case, a drag coefficient 0.4 has been used for this model. Taking the projected front area of the aircraft body about 0.5 m², the estimated drag force is 27.11N. As a result, the total drag force of the whole aircraft is 63.71N. With one flapping cycle at U=15 m/s, the energy is 955.65J. So the power input to wing would be 955.65W minimum. It is equivalent to 1.28Bhp (British Horse Power), which is much higher than human power.

Inertia force

For flapping and twisting motion, inertia force would cost extra energy.

$$W = FL \tag{4.3}$$

m is mass

a is acceleration

W is energy

F is inertia force

L is length

As the chosen flapping amplitude is 0.4 m and twist 3.37°, the energy required to overcome inertia force is 203.80J per wing per second. It means that 407.60W power for a pair of wings would be needed to overcome inertia force.

Power to against lift

Because lift force impact on wings, human need to overcome it to make wings move. So extra power need to be given. But this theory based on the situation with no resonance at all. If the mechanism with resonance, the power cost would be much lower.

$$F_{need} - L = ma \quad (4.4)$$

$$a = r\dot{\omega} \quad (4.5)$$

$$P_{max} = F_{needmax}v = F_{needmax}r\omega \quad (4.6)$$

F_{need} is force against inertia force

L is lift force

a is acceleration

m is mass

r is radius

ω angular velocity

P is power

In this case that the flapping motion is the same as designed without resonance, it needs 1049w power equivalent to 1.41Bhp.

As the conclusion, the total power requirement would be 2452.25 Watt, which is equivalent to 3.29BHP. An excellent athletics can produce 1.50BHP for a few seconds. Thus it is unlikely to fly by human power unless a power storage system is installed. Even through the human power cannot maintain cruising, it may help to achieve shorter and safer landing by practically reduced flapping amplitude and frequency just like a bird and applied to hang glider.

5. Detailed Design

5.1 Landing gear design

For lightweight flapping aircraft, it required having lightweight and practical landing gear. Type, install position, function and further equipment on it needs to be considered for landing gear.

First of all, type of landing need to be considered for it would decide the weight and stabilize on road.

5.1.1 Tricycle-Type Landing Gear

This type of landing gear was widely used for civil aircraft.

This type of landing gear is structured like a tricycle, with one nose wheel in the front and two wheels located in the back. [28] This type of landing gear is advantageous in many ways: it allows the pilot to apply the brakes more forcefully without making the plane nose over, offers better stability because the rear wheels are close to the centre of gravity and permits better visibility for the pilot during take-off, landing and taxiing. The majority of modern aircraft are fitted with tricycle landing gear.

Advantages:

- 1) Landing would be easy and reliable. Lift force decreasing constantly with decreased angle of attack during landing.
- 2) Direction is easy to control during taking off and landing.
- 3) Good view for pilot.

Disadvantages

- 1) Front landing gear is big and complicated because it would bear very large force. Thus, it is quite heavy. [29]
- 2) Cannot speed down by using air resistance while landing due to low AOA.

5.1.2 Tail Wheel-Type Landing Gear

This type of landing gear was invented in the early years, and widely used for light aircraft such as sport aircraft and agriculture aircraft nowadays. Two main landing gears are installed slightly in front of gravity centre and tailing wheel is installed at the tail of aircraft, far from GC. With this type of landing gear, aircraft would not be agile.

Advantages:

- 1) Structure of landing gear is very simple, so the weight of this type is quite low.
- 2) Large angle of attack while taking off.
- 3) Structure of tailing wheel is simple and it is easy to be installed, so the size and weight of tailing is low.
- 4) Three wheels would touch ground at the same time when landing. Large AOA could help aircraft decreasing speed and landing distance.

Disadvantages:

- 1) Direction is not easy to control while taking off and landing. Force from cross wind could affect a lot on direction.
- 2) Bad view for pilot while taking off and landing.
- 3) Crash or jumping could happen during landing for breaking or high speed.

5.1.3 Bicycle type

This type of landing gear is not widely used by aircraft for it is difficult for pitching. Bicycle type was widely used on manned aircraft for lighter weight. Moreover, a large part of manned aircraft was retrofitted from bicycle to use it for man powered engine and landing gear at the same time. With this kind of transmission or landing gear, it can achieve moving forward and starting engine at the same time, easy control of direction and easy to be retrofitted. But at the same time, balance would not be easy to control and the efficiency is low because of too many transmission gears would be used.

For flapping aircraft, this would not be a good solution for balance problem. Even a small error could cause a crash while taking off with bicycle landing gear.

5.1.4 Car type

With car type of landing gear, flapping aircraft would be stable during taking off and landing with flapping. Control are designed the same as the car, so the direction is easy

to maintain, and it is easy to learn for most people. Unfortunately, this type would be much heavier than any other type of landing gear, and air resistant would be much larger than others. Thus, this would not be a good choice for landing gear.

Summary

For a practical ULFWA, every piece of component needs to be designed as multifunction to minimize the airframe weight. In the landing gear design, the triangle frame is used as part of the landing gear truss and also support the pulling cables for wing flapping as illustrated in Fig.5.1.

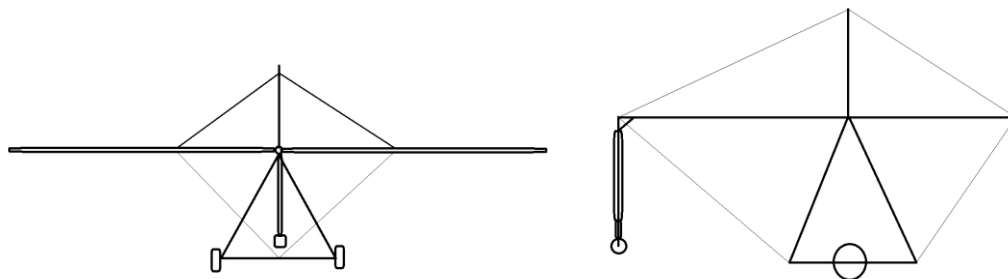


Figure 5.1 Landing gear arrangement

5.2 Mechanism design

5.2.1 Man powered mechanism design

As previously mentioned, boating motion allows human to use over 90% extensor muscles and give maximum power output. So the man-powered flapping mechanism can be designed based on rowing machine as shown in Fig.5.2. With this machine, people could imitate boating motion and change resistant force to gain maximum power.



Figure 5.2 Air Rowing machine

Different from real boating, with this machine, people only need to pull the handle bar that linked a cable to resistant part and power calculator. For the flapping mechanism, the cable could be used to connect human motion to the wing spars. As a result, the entire human power can be transferred to the wing down stroke through the cable.

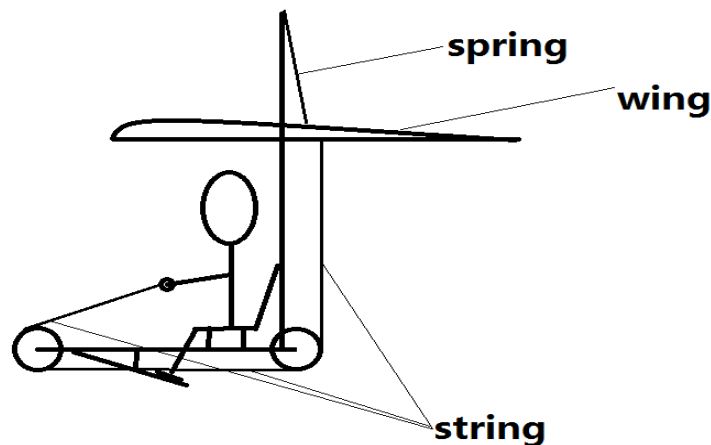


Figure 5.3 Human powered mechanism design

For the wing upstroke, an elastic band or spring is installed on the top of the wing as shown in Fig.5.3. Only two gears or bearings are needed for changing the cable direction to pull the wings downward. This mechanism should be light and efficient.

With this kind of mechanism, human could develop entire power. After a test by author who is 171cm high 68Kg weight, with medium resistant, 380-watt power output for 2 second had been measured. In the second test, the output power range is between 350watts and 368watts last less than 20 seconds. At the third trial, around 285 to 320 watts power had been measured. In this power range, this activity could last long

enough. In this test, the frequency of motion is around 0.75Hz, which is not high enough to meet the flapping wing requirement.

5.2.2 Engine powered mechanism detailed design

For engine-powered mechanism, there are lots of choices for engine, such as piston engine, servo motor and electromagnet, each of which has different characteristics.

5.2.2.1 Piston engine

Piston engine is a high-powered engine widely used in normal life. It means that this is a mature technology with low price. The fuel density is quite low and could last for a long time. This would make piston much lighter than electronic engines.



Figure 5.4 Single piston engine

For a single piston engine as shown in Fig.5.4, the power is almost enough for a flapping aircraft. But the minimum frequency is about 4 Hz, which is too high for a manned aircraft. The cylinder stroke is not long enough is another problem needs to be solved. But if the piston can be installed at wing root as illustrated in Fig.5.5, the cylinder stroke will be enough. It also means it need two single piston engines, and wing structure should be strong enough to bear force. However, at this position, engine would be steady.

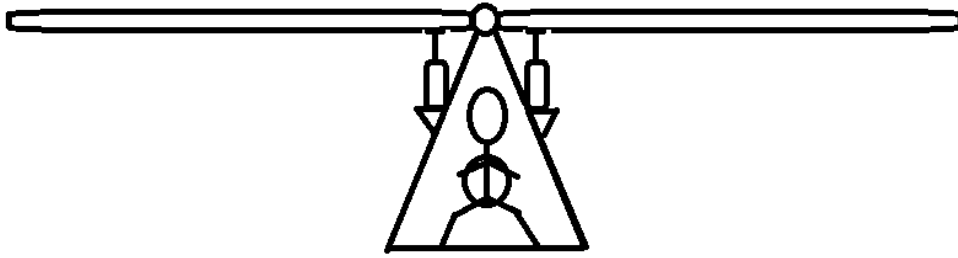


Figure 5.5 Mechanism design – two piston engine

With multi piston engine, high frequency, it is necessary to speed down the frequency and increasing pulling distance. Wheel gear and connecting rod have to be used to speed down and change circle motion to rectilinear motion.

This mechanism would be heavy because of speeding down gear. However, it would be very powerful so that it could drive huge wings.

There is a motor called out-swing door cylinder as shown in Fig.5.6, which could achieve pulling or pushing 50 cm distance in 1 second, and its pushing force is 4.71×10^5 N, pulling force is 4.29×10^3 N. This engine could be used as a severo motor for flapping aircraft. The only problem with this engine is its weight. The engine with battery would be more than 40 Kg.



Figure 5.6 Out-swing door cylinder

5.2.2.2 Electromagnet

Electromagnet is a magnetic device by energization to pass the electric current to generate the electromagnetic.

Electric motor is a typical magnetic device. Around the outside of the core of the power to match the conductive winding, the electric current through a magnetic coil like a magnet is also called solenoid (electromagnet). It is usually put into the shape of strip or plate to make the core more easily magnetized. In order to enable the electromagnet demagnetization immediately, it is actually used a fast demagnetization of soft iron or silicon steel to make material. Such a magnetic solenoid has magnetic power when energized.

Electromagnet has many advantages: it can be controlled by through electric current; the degree of magnetic relies on the electric current strength or the number of turns of the coil; also the magnetic poles are dependent on the directions of its pole and so on. Namely: controlling the presence or absence of magnetism can change the strength of the magnetic; the magnetic pole direction can be changed, the disappearance of the magnetic because the current is vanished away.

Electromagnet could generate huge magnetic force, and frequency can be controlled. This can be used for engine powered flapping wing aircraft.

In this project, there are two kind of electromagnet engine conceptual design. The first one as illustrated in Fig.5.7, two electromagnets face to face are installed on the top of each wing. One of electromagnet is used as permanent magnet; the electric current of the other one would be controlled by pilot to change magnetic pole. If two magnetic poles are same, wings would flap downwards, otherwise, they would flap upwards. Between the two electromagnets a damper is used as shock absorption and energy saver.

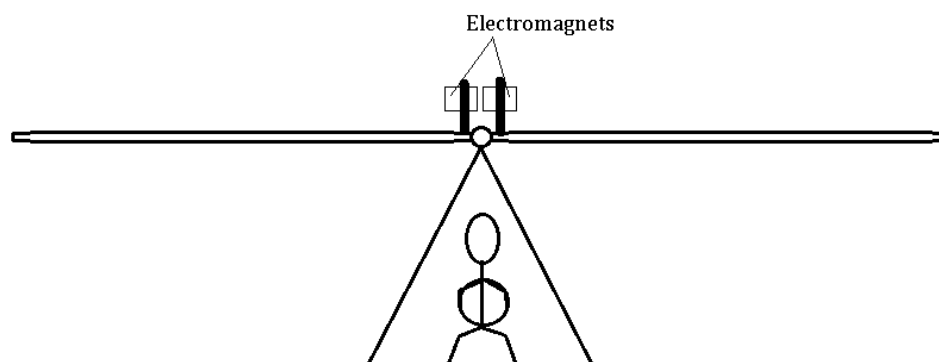


Figure 5.7 Mechanism design – electromagnet engine

The second design concept is to install two electromagnets under each wing as illustrated in Fig.5.8. There is a permanent magnet faced to each electromagnet. The two electromagnets could be changed magnet pole by changing current at the same times by pilot. Otherwise, pilot could set up two wings with different motion as well. Between electromagnet and permanent magnet, damping equipment is set as previous one. The advantage of this design is to make aircraft flying like bird, every motion could be controlled.

With this kind of engine, aircraft could be heavier especially due to the battery weight. To increase magnet force needs to have a large number of coil and high electric current. However with this type of engine, the frequency and flapping amplitude would be controllable.

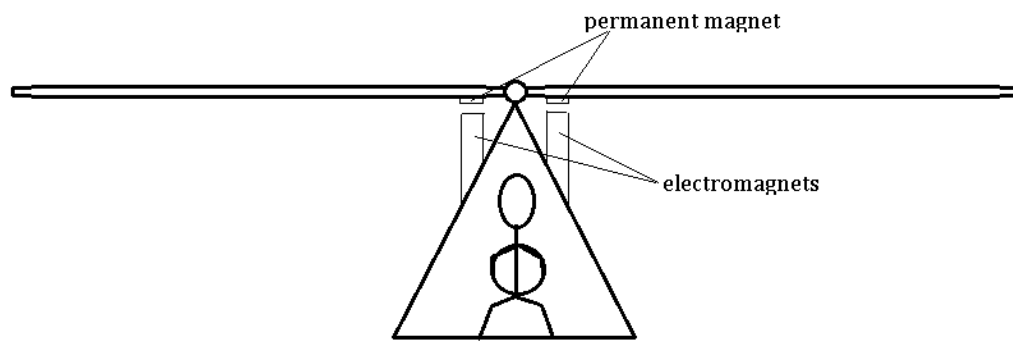


Figure 5.8 Mechanism design – two electromagnet engines

5.3 Structure design

Unlike fixed wing aircraft, the structure of flapping wing aircraft undertakes larger and dynamic forces at low flying speed. The triangle frame of a hang glider is a simple, light and strong configuration, hence adapted for the flapping wing aircraft as illustrated in Fig.5.9.

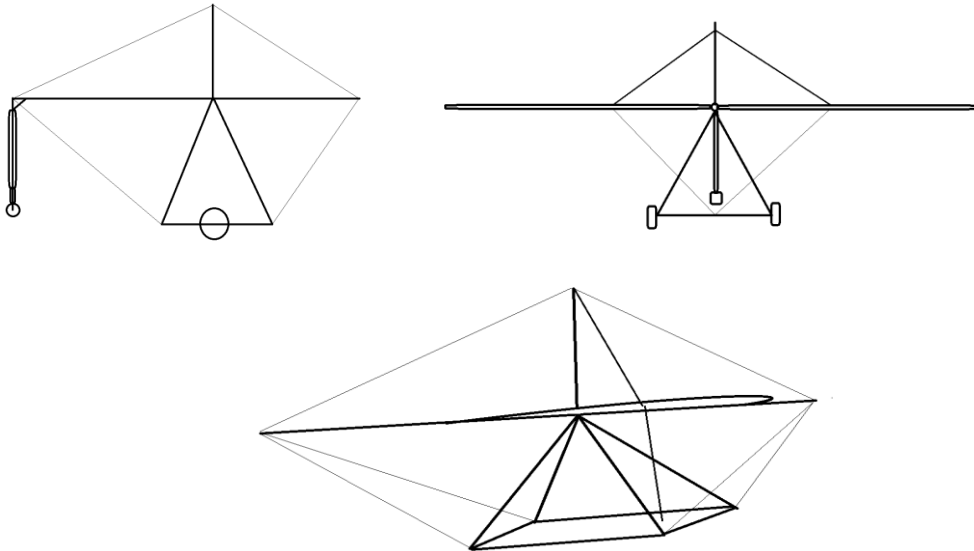


Figure 5.9 Structure design

Similar to a hang glider, the main beam was designed as the backbone of the aircraft. This beam would be very stiff to work as the flapping wing axial and transfer the wing load to the body. The pair of flapping wings is connected to this beam directly as the rotating axle. Above the wings, there is a vertical beam used to install the spring and vertical fin. Below the main beam, there are two triangle frames to support the body. The power plant, transmission and control mechanism are mounted onto the body. Mechanism and transmission could be mounted under the main beam to save weight. At the lower beam ends, two wheels are installed at each side as landing gear. The tailing wheel is located at the tail of the aircraft with an electronic controlled stretch beam.

5.4 Wing structure

The flapping wing is the most important component of the ULFWA. In nature, birds have very strong wing and the feathers are extremely light. Flexibility is another characteristic of birds' wings. The rachis is like a tube with material like polyfoam. It makes birds easy to fly and the rachis are hard to rive even it is flexible. Birds' wing provides a good example of flapping wings in this project.

Different from a fixed wing aircraft, the flapping wing spars need to be stiff but the ribs are designed to be flexible. This particular flapping wing of NACA 0009 airfoil has 30

degrees sweptback. The reason to choose NACA 0009 airfoil is its better performance in high AOA than other options. The stall angle (critical angle) of this airfoil is larger.

Regarding the structure layout, a D-shape beam made of carbon/epoxy with foam core inside is used as the leading edge (LE) spar as shown in Fig.5.10. Another carbon/epoxy beam as the secondary spar is mounted at one third of the spar length from wing root to reinforce the wing. Eight flexible ribs are set from leading edge (LE) spar to trailing edge (TE) to maintain the airfoil shape.

The ribs are elastically bent to the ideal curved shape by using a string connecting and pulling the LE to the TE of each rib. The string connection allows the ribs to bend downwards to increase the wing camber in upstroke, but prevents the ribs bending upward in down stroke to improve the flapping wing aerodynamic performance.

Film or canvas would be used as lighter weight wing skins. The skins could be designed with adaptive slots so that flow can go through when they opened in upstroke, and block the flow when closed in down stroke.

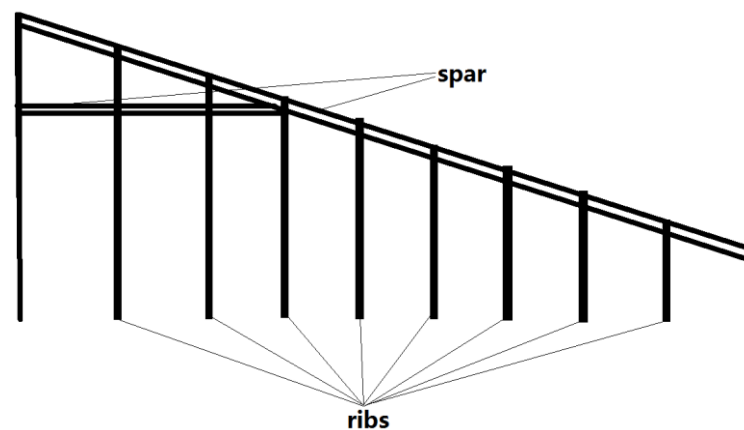


Figure 5.10 Wing structure design

6. Manufacture, Experiment and Measurement of a Scaled Model

6.1 Manufacture of a scaled model

In order to demonstrate the ULFWA feasibility and validate the mechanism and structure design, a 1:10 scaled flapping wing aircraft model of 1m span was made as shown in Fig.6.1 and tested.

To simulate the man-powered flapping mechanism, linear actuation motion was implemented by using a servo motor to power the flapping wing. All the frames were made of carbon/epoxy beams and the power plant was mounted on the base frame.

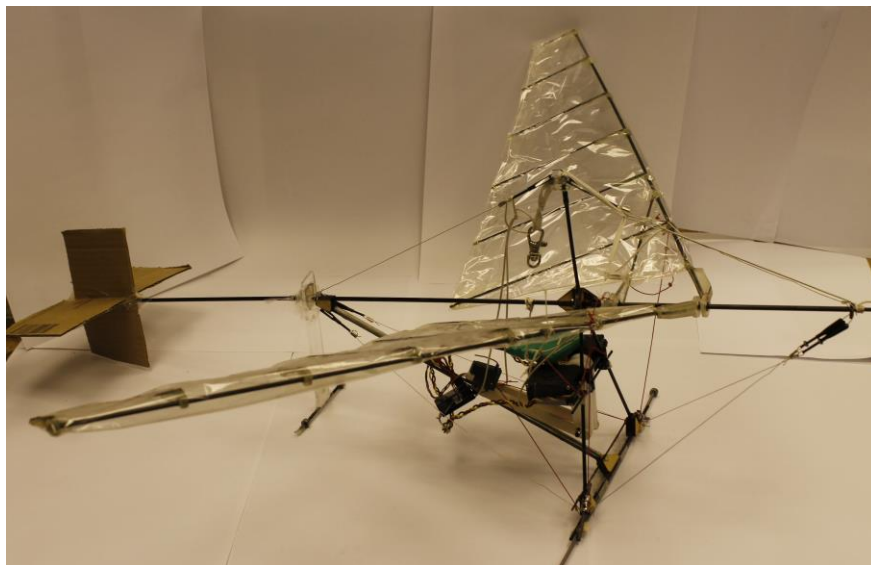


Figure 6.1 Scaled model

6.1.1 Wing model manufacture

The weight and strength of the wing structure was the major concern in the design due to the flapping motion and dynamic load. Carbon fibre reinforced plastic (CFRP) seems to be the best material option to produce the spars. Carbon/epoxy tubes of 3mm and 1.5mm diameters were chosen for the LE and secondary spars as shown in Fig.6.2.

For the same reason, CFRP was initially chosen for the ribs too. Square cross section tube of 2 mm outside and 1mm inside was used for the rib as shown in Fig.6.2. The CFRP rib is light but too stiff to be deformed by inertia and aerodynamic force.

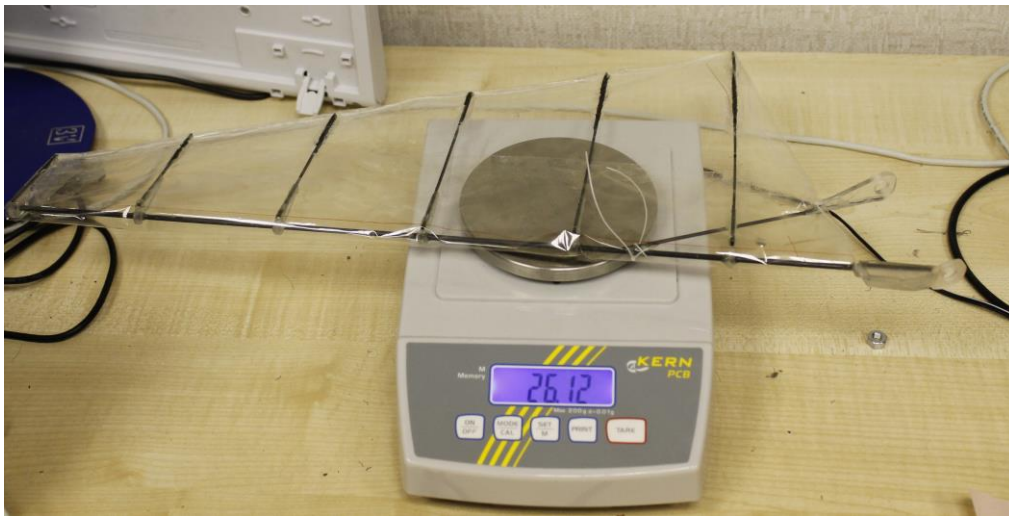


Figure 6.2 A flapping wing made of CFRP beams

Glass fibre reinforced plastic (GFRP) is another material option to make the ribs for its higher impact energy absorbance and flexibility. In another word, GFRP ribs could achieve the required unsymmetrical elastic deformation in upstroke and down stroke motion. The downside of GFRP is its larger density similar to Aluminium Alloy. The GFRP ribs as shown in Fig.6.3 leads to about 1/3 heavier ribs than CFRP ribs.



Figure 6.3 Single glass fibre reinforce plastic wing

Manufacture of the Components and Parts

Engineering plastics has adequate strength and convenience of manufacture process although it is much heavier than glass fibre. Thus, engineering plastics was selected only to make the joint parts of the ribs to the wing LE spar as shown in Fig.6.4.



Figure 6.4 Joints of rib to wing spar

Steps of producing carbon fibre wing

- 1.1 Firstly, using engineering plastics to make parts of the wing which including the junction between the aircraft and the wing spar and the leading edge of ribs.
- 1.2 Measure the engineering plastic and CFRP to make sure every part one the wing could be work well. This including the stiffness, measurement and intensity.
- 1.3 Choice the most appropriate material by considering weight, stiffness, process ability and shape. Then make the best design for these materials.
- 1.4 Processing the general shape of parts by gridding head with drill as previous design and carving the accurate processing position.
- 1.5 To hold span spar tight, and due to the thickness of engineering plastics, it needs 3 layers to make the whole part of junction and put the spar inside. Before process, sweep angle need to be considered and designed carefully because this part is the only junction which connects to the model body and could decide the sweep angle. So this part was a key point of the wing. After processing, gluing and drying 3 layers and wing spar, the junction needs to be drilled and sanded another time for decreasing weight.
- 1.6 Then, using sanding paper sanded the other parts with accurate size and measured them to make sure they are good to use. Especially the connection of the spar and ribs. This connection needs to be processed very accurately, for it not only connects the spar and ribs, but it created leading edge itself. Because these parts need to be drilled, even a bit error could cause the leading edge forward or backward, the sanding after drilling required to be much careful. To solve this, put these parts together and use a spar size stick crossing through these holes to make then like one piece, then gridding and sand them carefully.
- 1.7 This is the last step of the CFRP wings structure assembling. Before assembling, glue needs to be tested to ensure adequate strength of these parts. Then, set everything on the right position and adjust the ribs' position to change the angle

of attack of the wing. At last, glued them and made sure every part kept steady. After a period of time, when glue was dried, the structure of wings is complete.

- 1.8 Fasten cables at the trailing edge and wing root to create edge for setting skin. Fixing the leading edge firstly, and make sure the skin was set tight with the leading edge. Then, gluing the lower skin and trailing edge.

Making GFRP ribs

To generate more thrust force, the flapping wing was made flexible chordwise by using GFRP ribs.

The work was focused on making GFRP ribs. To allow the ribs bend down during flapping motion, the rib was made an open section without the lower half of the airfoil. To produce ribs in required shape, a mould was made and used to layup the GFRP laminate in the airfoil shape as shown in Fig.6.5. Firstly, fasten layers at the mould's leading edge and apply force to tight the layers. Then, lay down woven fabric plies and brush the mixed resin and hardener on the surface of each layer. Stretch the edges of each layer to apply pressure while process. Finally, brush the surface to squeeze extra resin away and smooth the surface.

Different number of layers from 1 to 5 layers laminates was made and cut into strips as shown in Fig.6.6 to measure the stiffness. It was fund that 1-3 layers were too flexible and 5 layers were too stiff. Finally 4 layers of GFRP laminates were used to make the ribs. To make the ribs have desirable flexibility for variable camber during the flapping motion, number of rib cutting trial and bending test was carried out.

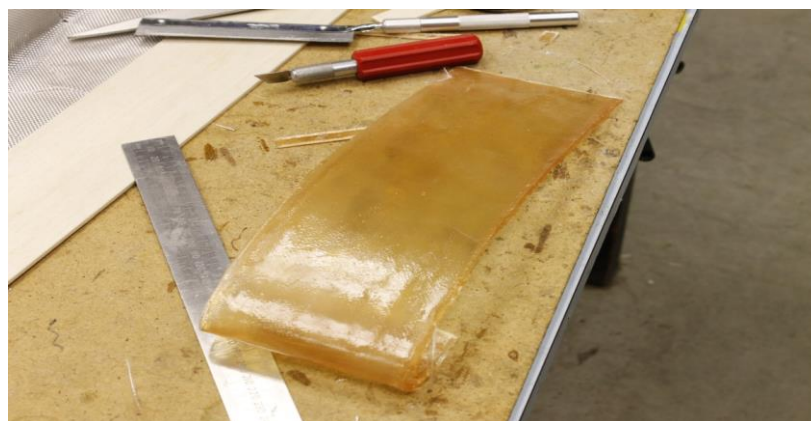


Figure 6.5 Glass fibre reinforced plastic ribs



Figure 6.6 Glass fibre reinforce plastic rib

According to the test, the glue was not strong enough to carry the load from the ribs to the spar. As a solution, resin was used to mount the rib leading edge to the spar as shown in Fig.6.6. This option has weight penalty. The mounting angle was carefully measured to keep the initial angle of attack.

To assemble the skin onto the wing, wires were used at the trailing edge and connected to the wing root. First hold the skin tight and glue the skin surface on the leading edge. Then glue the upper skin but keep the skin flabby for downward bending. Finally, fix the lower skin tight to prevent wing upward bending.

6.1.2 Actuation and flapping mechanism

To achieve the flapping wing motion, a servo motor was used to simulate the man-powered linear movement.

As shown in Fig.6.7, the actuation mechanism was designed similar to a rowing machine. The actuated linear motion of the wood bars along the base beam working as a rail pulls the wing spars downwards through wires. By tuning the mounting position of the motor, the motion distance and hence the flapping amplitude could be changed in the test.

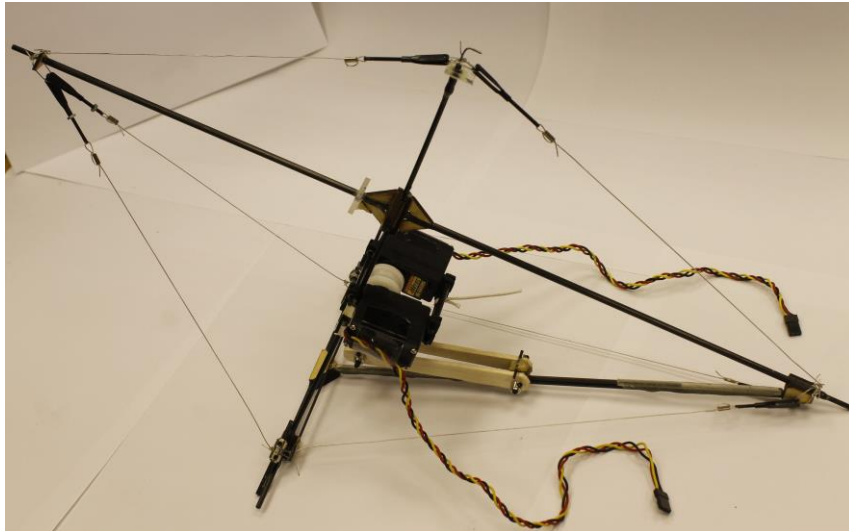


Figure 6.7 Actuation mechanism and supporting frame

To drive the wings upwards, spring or elastic band was connected from the spars to the upper beam as designed for a light weight and practical solution. When the flapping wings are actuated at the resonance frequency of the wing system, the inertia would be balanced by the elastic force so that minimum power is required.

6.2 Test and measurement

To verify calculation and result, experiment of the aircraft model was conducted.

Usually wind tunnel test should be carried out for measurement of lift force and thrust [30]. Due to the limit of time and facility of measuring the dynamic forces however, wind tunnel test cannot be operated. So four experiments were conducted in the laboratory to measure the lift and thrust forces.

6.2.1 The first experiment

The model was hanged up in the air using a wire at the model central of gravity as shown in Fig.6.8. Another wire was used to connect the model and a weight, which is a little heavier than the model and seat on an electronic scale to measure the thrust as shown in Fig.6.9. A frame and a roller have been set to guide the wire and transfer the force. When the model generates thrust force, the weight on the scale would be reduced and the scale will display the change immediately.



Figure 6.8 Model set up for experiment 1

In order to stop the aircraft model shaking due to thrust and inertia and unsteady aerodynamic force, two holes in boards were used to restrict the horizontal movement. However the model is not steady enough during flapping. Overall, the measurement result was not accurate enough.



Figure 6.9 Model Test Setup for Measurement

To solve this problem, the model was put on a metal plate on a table to reduce the friction and stabilize the model as shown in Fig.6.10. A weight of 3 gm seating on the electronic scale was connected to the model tail by a wire to measure the thrust. A wheel was mounted on a shaft to tune the wire direction at the back of the model.

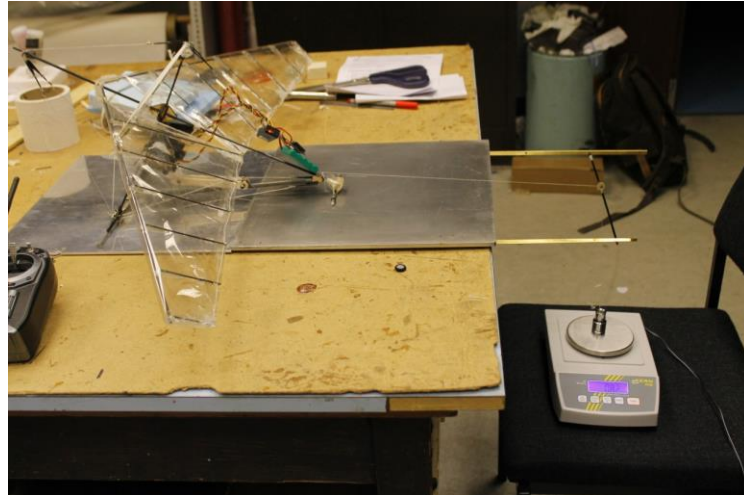


Figure 6.10 Model Test Set on Table with large AoA

This test results are not optimistic. Because of inertia force of the model at high AOA, the weight was shaking during the experiment. A stick was set on the tail of the model to decrease the AOA as shown in Figure 6.11. As a result, the model could hardly move forward, which means that the thrust force is less than 0.03N to pull up the 3 gram weight.



Figure 6.11 Model Test Set on Table with reduced AoA

6.2.2 The Second experiment

This experiment was set in a suspended free model manner as shown in Fig.6.12. The first test was to measure the model position during flap; the second test was to measure the thrust during the model motion due to flapping.

In the first test, a long wire was used to hang the model near the centre of gravity to have the required angle of attack. Before flapping, keep the model still and put a ruler in model direction as shown in Fig.6.13. As the model flapping, measure the forward movement distance and the change of AOA.

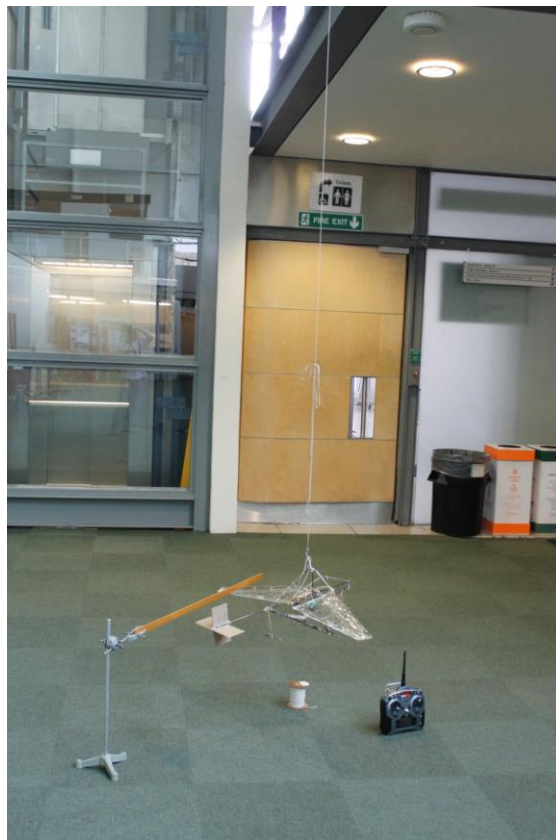


Figure 6.12 Model suspended in Experiment 2

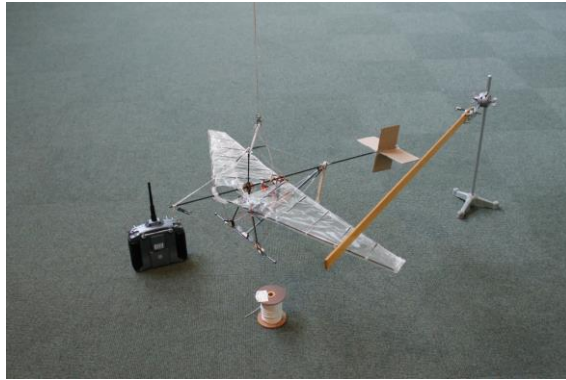


Figure 6.13 Model Test Setup in Experiment 2

In the second test, set the model on the table similar to the first experiment and set the AOA same as the first test. Connect a wire from the tail of the model to a weight seating on an electronic scale as shown in Fig.6.14 and Fig.6.15. A frame and a roller were mounted on the table at the back of the model to change the wire direction. As the flapping wing producing thrust, the wire pulls the weight on the scale. The scale displays the weight change, which is directly related to the thrust. Since the model is in still condition, the thrust measured only represent a small part of the thrust in flight with air flow velocity.

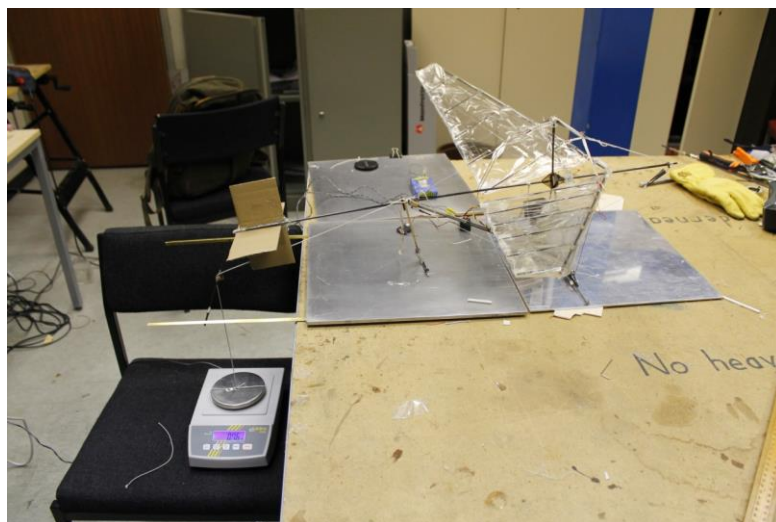


Figure 6.14 Model Test Setup on Table for Thrust Measurement

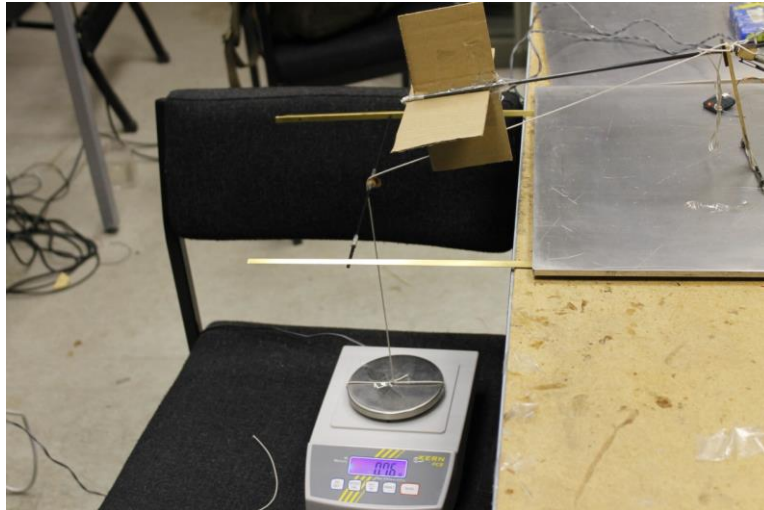


Figure 6.15 Model Test for Thrust Measurement

In this experiment, with the measurement of the AOA and the thrust force, the lift force would be calculated and presented below following the equations and the triangle shown in Fig.6.16.

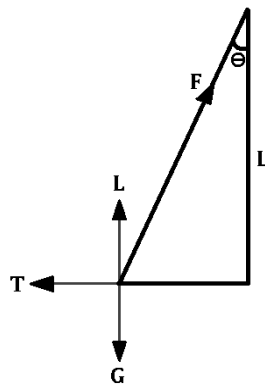


Figure 6.16 Force diagram for experiment 2

$$T = F * \sin \theta \tag{6.1}$$

$$L + F * \cos \theta = G \tag{6.2}$$

$$L = G - T * \cot \theta \tag{6.3}$$

In this experiment,

The hanging rope is 260 cm

The forward movement is 4 cm

So the Angle $\theta = 0.88^\circ$

The weight of model $G=358\text{g}$

The thrust force $T= 4\text{g}$

The AOA is 8 degrees

The flapping amplitude is 10 cm

After calculation the lift force $L=0.9\text{N}$

6.2.3 The third experiment

To measure the thrust and lift of the model in the condition of having forward air flow, the third experiment was carried out. In this experiment, the model was hanged up from a high position by using a 8.9 m long wire so that it could fly in large circle as shown in Fig.6.17.



Figure 6.17 Model Test setup in the 3rd Test

The initial angle of attack was 8 degrees and the flapping amplitude at wing tip was measured as 100 mm. By measuring the flight path radius and velocity with the power

input, the thrust and lift can be calculated based on the equations in the previous section and Fig.6.18. The data shows the radius of flight path circle for a period of time $t=6.2$ seconds. The measurement results are showed in Table 6.1.

Time to pass 0 axis	0	1	2	3
Without flapping	153 cm	116 cm	92 cm	72 cm
Without flapping	157 cm	118 cm	93 cm	73 cm
Without flapping	164 cm	116 cm	85 cm	
With flapping	159 cm	115 cm	85 cm	
With flapping	157 cm	118 cm	90 cm	
With flapping	157 cm	117 cm	98 cm	85 cm
With flapping	153 cm	113 cm	88 cm	
With flapping	151 cm	110 cm	88 cm	

Table 6.1 The original measurement results from experiment 3

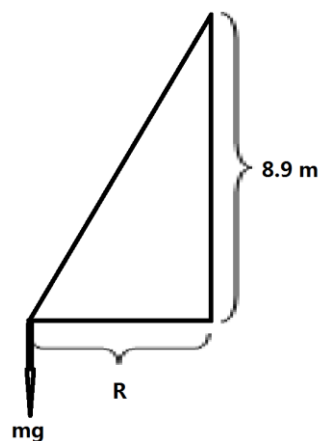


Figure 6.18 Force diagram for experiment 3

Since the flight path was not exactly a circle during the time, the directly measured data were processed to take the difference into account. The improved test data were obtained and presented in Table 6.2.

Time to pass 0 axis	0	1	2	3
Without flapping	153 cm	116 cm	92 cm	72 cm
Without flapping	157 cm	118 cm	93 cm	73 cm
With flapping	159 cm	115 cm	85 cm	
With flapping	157 cm	118 cm	90 cm	
With flapping	153 cm	113 cm	88 cm	
With flapping	151 cm	110 cm	88 cm	

Table 6.2 The processed experiment results

From the test data, the thrust force was calculated based on the principle of energy conservation. Because the fling height change can be ignored, potential energy was assumed to be constant in the calculation. Therefore, the energy loss was only due to drag.

Energy loss without flapping

$$W_{\text{lose}} = E_{k1} - E_{k2} = \frac{1}{2}mv_1^2 - \frac{1}{2}mv_2^2 = F_D L \quad (6.4)$$

In this formula L stands for flying distance.

After calculating the drag, the thrust can be obtained.

$$W_{\text{lose}} = E_{k3} - E_{k4} = \frac{1}{2}mv_3^2 - \frac{1}{2}mv_4^2 = F_D L - TL \quad (6.5)$$

$$v = \frac{2\pi r}{t}$$

where W is energy, E_k is kinetic energy, m is mass, F_D is drag force, v is velocity, T is thrust force, t is time (6.2s)

As the results, the thrust force was about $8 \times 10^{-2}\text{N}$, which is smaller than initially calculated result $13.8 \times 10^{-2}\text{N}$. This is because of measurement accuracy and some influence factors may be ignored.

6.2.4 The forth experiment

The forth experiment setup is similar to the second to measure the thrust force. In this experiment however, high-speed camera was used to record the detailed motion, such as flapping frequency, amplitude and wing twist in the same time. Three case studies at slow, medium and high flapping frequency levels were tested in this experiment.

Case-1. Low frequency

In this case as shown in Fig.6.19, the flapping frequency setting was 0.4Hz, which is achievable by man powered motion. In this frequency, the measured wing twist angle was 2 degrees and the flapping amplitude at wing tip was 40 mm. The thrust force measured was in the range of $2.3 \times 10^{-2}\text{ N}$ to $3 \times 10^{-2}\text{ N}$ (equivalent to 2.3 - 3.0 grams).

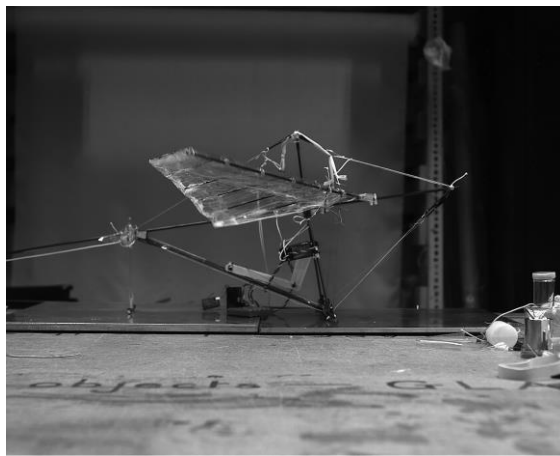


Figure 6.19 Measurement by high-speed camera (case-1)

Case-2. Medium frequency

In this case as shown in Fig.6.20, the flapping frequency setting was 0.75Hz, which is also within the capability of man powered motion. In this frequency, the measured wing twist angle was also about 2 degrees and the flapping amplitude at wing tip was 40 mm. The

measured thrust force has increased to the range of 3.8×10^{-2} N to 4.7×10^{-2} N (equivalent to 3.8 - 4.7 grams).

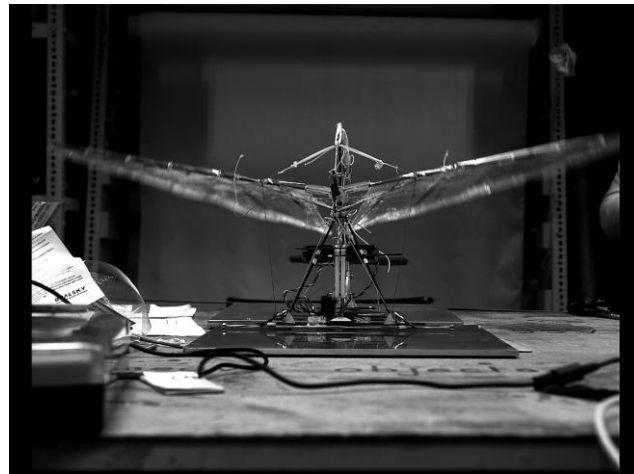


Figure 6.20 Measurement by high-speed camera (case-2)

Case-3. High frequency

In this case as shown in Fig.6.21, the flapping frequency setting was 1.25Hz, which is slightly beyond the capability of man powered motion. In this frequency, the measured wing twist angle was increased to 3 degrees due to the rib bending. However the flapping amplitude at wing tip was reduced to 20 mm because the motor produced the same power but could not deliver the same force at higher frequency. The measured thrust force was in a slightly higher level of 4.1×10^{-2} N to 4.8×10^{-2} N and could maintain a stable 4.5×10^{-2} N for much longer time.

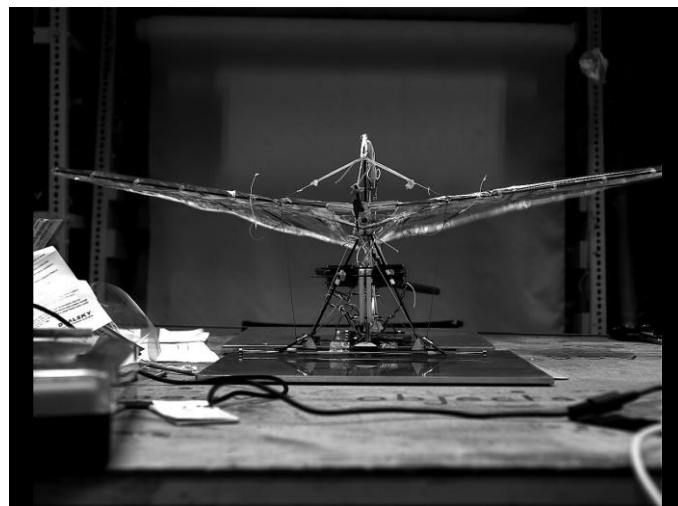


Figure 6.21 Measurement by high-speed camera (case-3)

Summary

From this experiment, it was noted that high frequency could generate more thrust force in general. However, this was limited by the motor power similar to the man power in higher frequency actuation. In addition, the ribs were still not flexible enough to achieve larger camber variation as expected.

6.3 Structure model and analysis of the wing

In order to improve the design of the flapping wing, effort was made to model the wing structure especially the dynamic behaviour by using Nastran software in the FE analysis.

The FE model and analysis of the test model, where the material and structural parameters were obtained by measurement. The modelling and analysis procedure is listed below.

1) Geometric model

From the wing geometry and physical parameters and wing layout, create a geometric model by using PATRAN.

2) Mass distribution

The mass of each component was weighted by digital scale and allocated on the local CG as concentrated mass. For example, the joints mass is listed in Table 6.3.

Item	Mass (g)
Wing front joint	5.4
Wing rear joint	2.3
Rib joint on front spar	2.3
Rib joint on trailing edge	1.0

Table 6.3 The wing spar-rib joint mass

The mass of spars, ribs and skins were also measured as shown in Table 6.4 and applied to the FE model. The total mass of the wing FE model is 43.7g which is close to the actual test model mass of 44g.

	CFRP spar		GFRP rib	
	Mass (g)	Displacement (mm)	Mass (g)	Displacement (mm)
	0	0	0	0
	20	17	3	2.8

	40	30	5.1	4.2
	60	45	8.5	6.8

Table 6.4 The wing spar and rib mass

3) Measurement of equivalent modulus of the spars and ribs

To obtain accurate component properties, experiment was performed to measure the equivalent modulus of the CFRP spars and GFRP ribs.

In the experiment, the spars and ribs were clamped at root like a cantilever beam on a test platform.

From the following equation, the equivalent E value of the beams can be solved with the results shown in Table 6.5.

$$f_0 = \frac{Fl^3}{3EI} \quad (6.6)$$

Where, f_0 is the vertical displacement, F is the applied force, l is the length of the cantilever beam.





	CFRP			GFRP
	Front spar	Rear spar	Root rib	Other ribs
Beam length (mm)	465	210	115	230/190/ 150/110/65
Section size (mm)	 D=3.0 d=1.5	 D=2.0 d=1.0	 L=1.4 d=0.8	 w=6.5 t=1.1
I (mm ⁴)	3.35	0.74	0.29	0.78
E (GPa)	140			55.7

Table 6.5 The wing spar and rib dimensions and equivalent E values

4) FE model constraints

The wing model was fixed exactly at the root of front and rear joints. Only the rotational degree of freedom around the global X axis (Rx) was released to simulate the flapping motion as shown in Fig.6.22. A linear spring element was used to simulate the elastic cable connecting the upper supporting beam and the front spar hitch point.

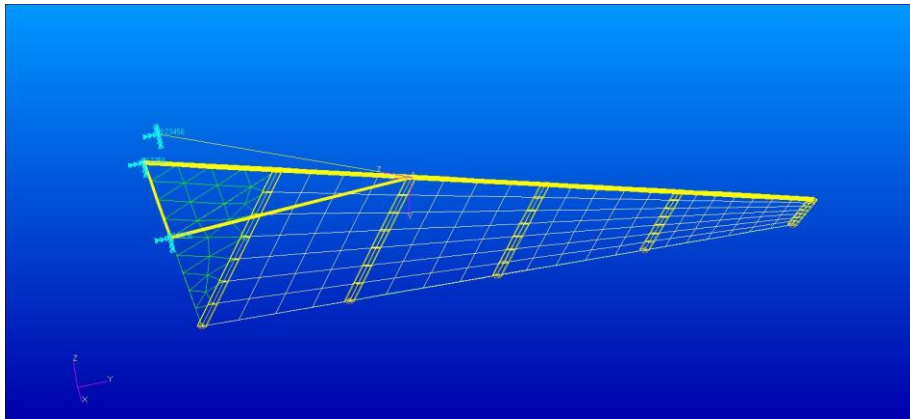


Figure 6.22 FE model of the flapping wing

5) FE Analysis and Results

The spring elastic constant was selected from 10N/m to 1000N/m in the study. The result shows that the wing vibration frequency in the rigid mode varied from 0.6Hz to 5.3Hz. Taking the elastic constant of 30N/m, the frequency is just 1.0Hz as shown in Fig.6.23, which agrees with the initial design of the ULFWA. This flapping frequency can be achieved by man powered actuation to overcome the wing inertia during flapping motion. The wing structure elastic modes were predicted as 17.4Hz, 25.0Hz and 28.8Hz respectively as shown in Fig.6.24-6.26.

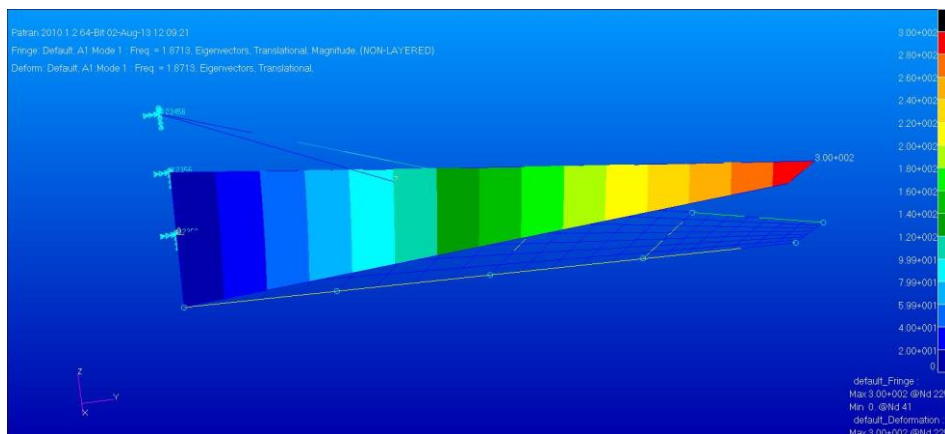


Figure 6.23 Rigid mode of the flapping wing

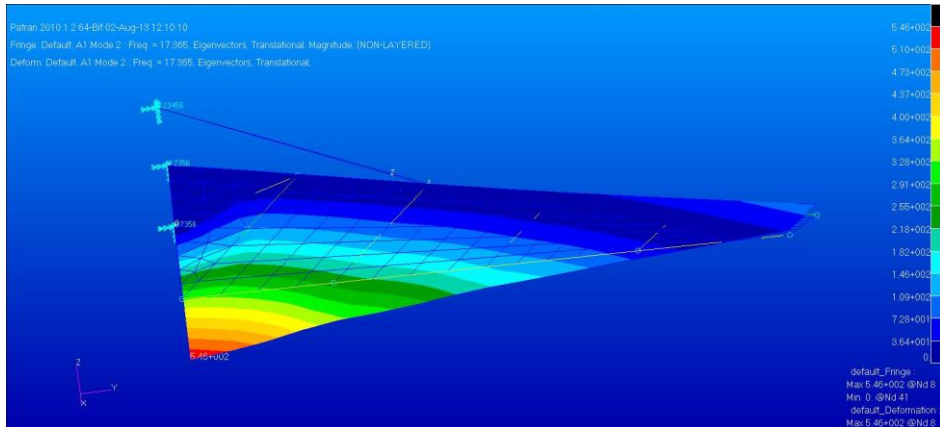


Figure 6.24 First elastic mode of the flapping wing

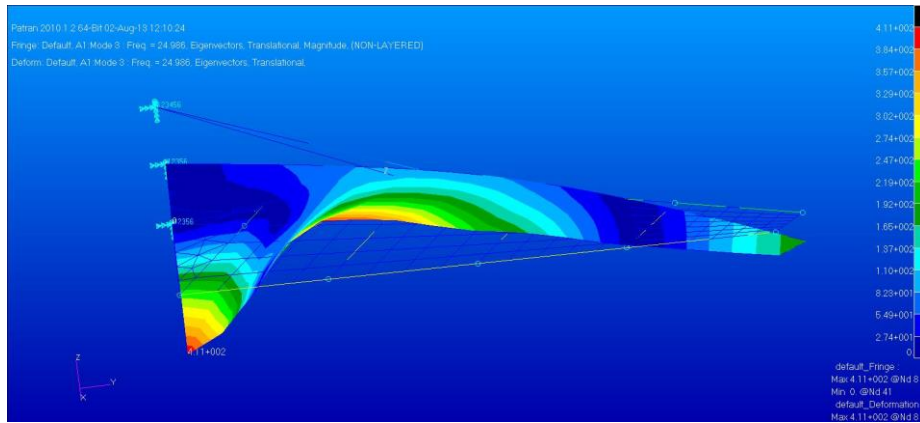


Figure 6.25 Second elastic mode of the flapping wing

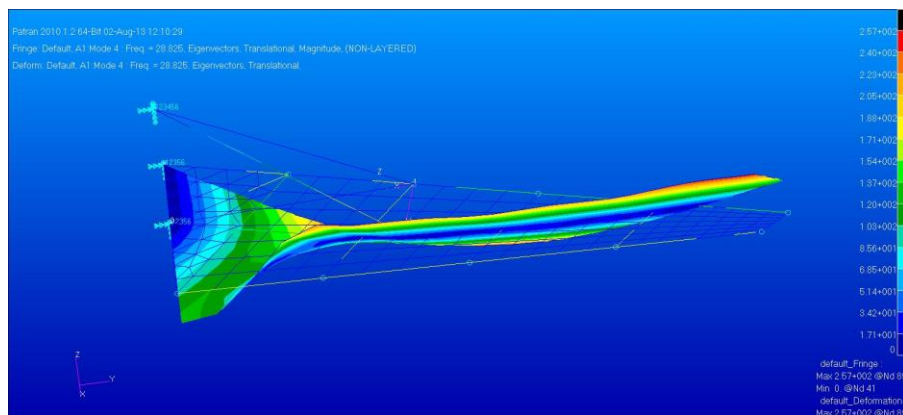


Figure 6.26 Third elastic mode of the flapping wing (torsional)

7. Conclusions

Although flapping wing aircraft has been demonstrated by flying animals in nature for millions of years, manned especially human powered flapping wing aircraft remains as a challenging dream in aviation. This thesis presents the study and research carried out towards developing a manned ultra-light flapping wing aircraft. By achieving the objectives, the approach and results obtained in the project have led to the following conclusions.

Throughout the initial literature review in terms of bionics, lightweight aircraft could be extended to flapping wing aircraft. Actually, the research on flapping wing animal and micro flapping wing aircraft is massive; on the contrary, the manned flapping wing aircraft has attracted much less attention. However the manned flapping wing aircraft has great potential for an alternative way of aircraft in the future. Specifically based on deeper and better understanding of biological flyer mechanism, human now has more confidence and attempted to develop manned flapping wing aircraft. It is clear that the biological flyer kinematics is too complicated for manmade ultra-light flapping wing aircraft to mimic. However the basic wing motion and characters can be adapted to develop the flapping wing aircraft. In addition to practical design issues, previous research on flapping wing aircraft showed that it is possible to achieve engine powered flapping aircraft. However the development needs to consider the minimum unsteady motion due to flapping aircraft. The wing structures design and manufacture is another challenge to achieve efficient aircraft and performance.

This thesis proposed a human powered flapping wing aircraft concept with maximum steady aircraft by combining the actuated flapping and passive twisting the wing at the same time. This required the use of rectilinear motion engine and flexible wing. The ULFWA design especially the actuation and flapping mechanism presented in this project is simple and practical. It also has the flexibility to adapt different flapping movement and velocity.

The calculation and analysis results show that both twisting and flapping motions could generate positive and negative lift force resulting in zero average lift. Whilst the twist motion could generate positive thrust for a short time, but the average is negative. With the same value of peak and bottom lift force, flapping motion could generate a large sum of positive thrust. In addition, the value of average positive thrust is much higher than that produced by twist motion. Within the design constraint especially the limited

very low flapping frequency, the flapping kinematics to achieve the optimum Strouhal number seems impossible.

From the process of evaluation of power requirement, approximately 5113W power at the minimum level is needed to maintain the designed cruising. However, it would require more power beyond human power to overcome resistant force. It seems impossible for man powered. However, if the aircraft is equipped with power storage system it is possible to achieve a short distance powered aircraft and enhance short distance landing. To save the flapping power in cruise, a resonance flapping system to overcome the inertia is part of the design. Spring or elastic cable is one option for such a system. Only when a different flapping motion such as extra acceleration at higher frequency is required in take-off and landing, extra power is required to overcome the inertia.

A 1:10 simplified scaled model was built to test the airframe and flapping mechanism and measure the motion and forces. The scaled model is made of elastic cable to achieve upstroke motion and for down stroke, a string, which connects to engine, pulling wings to achieve this. The upper elastic cable would simplify the mechanism system to make wings upstroke, but it would require a larger force for engine to pull the string. In addition, it would decrease the speed of down stroke, even frequency. This mechanism is aim to simulate boating motion by human. The scaled model has shown a large part of the concept of design in this project. Limited by processing, auto kinetic twisting system could not be produced, so the twisting motion could only be achieved by aerodynamic. Therefore, the ribs of wings were made of composite materials.

During the processes of testing and measurement, the results would be affected by the setting conditions. Though the testing and measurement were done very carefully, it seemed that some indistinguishable deviation had happened. Wind tunnel test could not be operated for time reason. This would be the biggest regret in this project. No matter under which kind of situation, this scaled model is reliable to do any kind of test in the future.

About the limitation of this project is lack of real experiment on full-scale model. Even scaled model had been established and measured; full-scaled model would have some improvements. For structures, real aircraft would be much heavier than model, for instance, in this project scaled-model had been made with ratio 1:10, while with the same structure in full scale, the weight would be one thousand time as scaled-mode. It means excluding the weight of engine itself, structure would be about 100Kg. However, with better process, weight of structure would be decreased, and main structure would be stronger. For the real aircraft, there are more forces affecting aerodynamic results, for example, the vortex. For mechanism system and engine, the number of choices for

equipping with the either the mechanism system or the engine would be more than scaled model, and they are so powerful. During the process of controlling in full-scale aircraft, it would be more advanced than that in scale model. Thus, besides aerodynamic affection, full-scaled aircraft would be much better than scaled model.

As experiment presented in this project, in the future, wind tunnel test could be used for more accurate measurement. The further test could include force in different air flow speed with different angle of attack and motions. About controlling system, it could be improved with motion control system to set up flapping or twisting frequency and amplitude. With better process, ribs and spar are able to use thinner carbon fibre and make ribs more flexible to achieve larger twisting. Additionally, in the future, not only flapping and twisting, but also more motions such as swing could be designed and analysed for flapping aircraft.

In summary, a practical design of the human powered ULFWA and a satisfactory scaled model had been completed in the project. The work completed in this thesis showed that it is difficult to achieve sustainable flapping wing aircraft by human power but practical by engine powered flight. A full-scale ULFWA with sufficient power should be produced to demonstrate the design in the future. Even with human power, it could still be useful to slow down the descending rate in flying and reduce landing speed.

Reference

- [1] HEDENSTRÖM, A., 2002. Aerodynamics, evolution and ecology of avian flight. *Trends in Ecology & Evolution*, 17(9), pp. 415-422.
- [2] Thomas J. Mueller and James D. DeLaurier, "AERODYNAMICS OF SMALL VEHICLES", *Annu. Rev. Fluid Mech.* 2003.35:89-111.
- [3] Harijono Djodihardjoa, Alif Syamim Syazwan Ramli and Surjatin Wiriadidjaja, "Kinematic and Aerodynamic Modelling of Flapping Wing Ornithopter", *International Conference on Advances Science and Contemporary Engineering 2012 (ICASCE 2012)*
- [4] GUO, S., LI, D. and WU, J., 2012. Theoretical and experimental study of a piezoelectric flapping wing rotor for micro aerial vehicle. *Aerospace Science and Technology*, 23(1), pp. 429-438.
- [5] William Paul Walker, "Unsteady Aerodynamics of Deformable Thin Airfoils", Thesis submitted to the Faculty of the Virginia Polytechnic Institute and State University
- [6] E Liani, S Guo and G Allegri. Potential-flow-based aerodynamic analysis of a flapping wing. 37th AIAA Fluid Dynamics Conference. AIAA 2007-4068. Miami, Florida, 25-28 June 2007.
- [7] J.H. Wu, D. Wang, S. Guo, Unsteady aerodynamic simulation of a flapping wing at low Reynolds number, IFASD-2011, Paris, 26-30 June 2011, IFASD-2011-187
- [8] ROZHDESTVENSKY, K.V. and RYZHOV, V.A., 2003. Aerohydrodynamics of flapping-wing propulsors. *Progress in Aerospace Sciences*, 39(8), pp. 585-633.
- [9] W. Shyy, H. Aono, S.K. Chinmakurthi, P. Trizila, C-K. Kang, C.E.S. Cesnik, H. Liu, "Recent progress in flapping wing aerodynamics and aeroelasticity", *Aerospace Sciences* 46 (2010) 284-327
- [10] Zhang, Y. , Wu, J. and Sun, M. (2012), "Lateral dynamic flight stability of hovering insects: Theory vs. numerical simulation", *Acta Mechanica Sinica/Lixue Xuebao*, vol. 28, no. 1, pp. 221-231.

-
- [11]C Zhou, J Wu, S Guo, Experimental study of a mechanical flapping rotor wing model, Applied Mechanics and Materials, Mechanical and Aerospace Engineering IV, Vol. 390 (2013), pp.23-27. doi:10.4028/www.scientific.net/AMM.390.23
- [12]S Guo, D Li, J Wu, Theoretical and experimental study of a piezoelectric flapping wing rotor micro aerial vehicle, Aerospace Science and Technology, Vol.23, Issue.1 Dec. 2012, pp.429-438 (published on-line in Oct 2011)
- [13]Marco La Mantia, Peter Dabnichki, "Effect of the wing shape on the thrust of flapping wing", Applied Mathematical Modelling 35 (2011) 4979-4990
- [14] Edward C. Polbamus, "A CONCEPT OF THE VORTEX LIFT OF SHARP-EDGE DELTA WINGS BASED ON A LEADING-EDGE-SUCTION ANALOGY", NASA TECHNICAL NOTE, NASA TN D-3767
- [15] K. Mazaheri, A. Ebrahimi, "Experimental investigation on aerodynamic performance of a flapping wing vehicle in forward flight", Fluids and Structures 27 (2011) 586–595
- [16]Taro Fujikawa, Kazuaki Hirakawa, Shinnosuke Okuma, Takamasa Udagawa, Satoru Nakano, Koki Kikuchi, "Development of a small flapping robot Motion analysis during takeoff by numerical simulation and experiment", Mechanical Systems and Signal Processing 22 (2008) 1304 – 1315
- [17] K.D. von Ellenrieder, K. Parker, J. Soria" Fluid mechanics of flapping wings", Experimental Thermal and Fluid Science 32 (2008) 1578–1589
- [18]Rambod F. Larijani and James D. DeLaurier, "A Nonlinear Aeroelastic Model for the Study of Flapping Wing Flight", FIXED AND FLAPPING WING AERODYNAMICS FOR MICRO AIR VEHICLE APPLICATIONS, chapter 18
- [19] J.D. DeLaurier, (1999), The Development and Testing of a Full-Scale Piloted Ornithopter, Canadian Aeronautics and Space Journal, Vol. 45, No. 2, June 1999.
- [20]Markku Ikonen, "About the Possibilities to Power Vehicles with Human Muscles", LLP Erasmus Intensive Programme: POWERING THE FUTURE WITH ZERO EMISSION AND HUMAN POWERED VEHICLES – Terrassa, Spain, 20.3. - 2.4.2011
- [21] MIKALSEN, R. and ROSKILLY, A.P., 2007. A review of free-piston engine history and applications. Applied Thermal Engineering, 27(14–15), pp. 2339-2352.
- [22] Chol-Bum M. Kweon Vehicle Technology Directorate, ARL, A Review of Heavy-Fueled Rotary Engine Combustion Technologies.

-
- [23] Parlikar, T. A. (1.), Chang, W.S. (1,2), Qiu, Y. H. (1.), Seeman, M.D. (1,3), Perreault, D. J. (1.), Kassakian, J. G. (1.) and Keim, T. A. (1.). (2005), "Design and experimental implementation of an electromagnetic engine valve drive", IEEE/ASME Transactions on Mechatronics, vol. 10, no. 5, pp. 482-494.
- [24] The effect of processing on the structure and properties of carbon fibres, D.D.Edie. Carbon, Volume 36, Issue 4, 1998, Pages 345–362
- [25] THOMASON, J.L. and SCHOOLENBERG, G.E., 1994. An investigation of glass fibre/polypropylene interface strength and its effect on composite properties. Composites, 25(3), pp. 197-203.,
- [26] Wills Wing inc., Falcon 3 145, 170, 195 and Tandem Owner / Service Manual, 2009
- [27] Marco La Mantia, Peter Dabnichki, " Unsteady panel method for flapping foil", Boundary Elements 33 (2009) 572–580
- [28] LANDING GEAR SYSTEM, Information content from the NSTS Shuttle Reference Manual (1988)
- [29] Aircraft Landing Gear Systems, FAA, Handbooks Manual
- [30] Yeo, D., Atkins, M.E., Bernal, P.L and Shyy, W (2012) "Experimental Investigation of the Pressure, Force, and Torque Characteristics of a Rigid Flapping Wing", University of Michigan, Hong Kong University of Science and Technology.
- [31] Aditya, K., Malolan, V., 2007. Investigation of strouhal number effect on flapping wing micro air vehicle. AIAA Paper 2007-486

APPENDICES

Appendix A: Relevant Theodorsen Theory

$$R = F_y \cos(\theta) - N \sin(\theta)$$

$$L = N \cos(\theta) + F_y \sin(\theta)$$

$$N = N_{aero} + N_{inertia}$$

$$N_{aero} = N_c + N_a$$

$$N_c = \frac{1}{2} \rho U V C_n c \Delta x$$

$$C_n = 2\pi(\alpha' + \alpha_0 + \bar{\theta}_a + \bar{\theta}_{wash})$$

$$\alpha' = \frac{AR}{2 + AR} \left[F'(k) \alpha + \frac{c}{2U} \frac{G'(k)}{k} \dot{a} \right] - \frac{2[\alpha_0 + \bar{\theta}_a + \bar{\theta}_{wash}]}{2 + AR}$$

$$k = \frac{c\omega}{2U}$$

$$\alpha = [h \cos(\bar{\theta}_a + \bar{\theta}_{wash}) + (0.75c - y_{ea}) \dot{\theta}] / U + \bar{\theta}$$

$$\dot{\alpha} = [(\dot{h}_0 + \ddot{h}) \cos(\bar{\theta} + \bar{\theta}_{wash}) - \dot{h} \dot{\theta} \sin(\bar{\theta} + \bar{\theta}_{wash}) + (0.75c - y_{ea}) \ddot{\theta}] / U + \dot{\bar{\theta}}$$

$$\theta = \bar{\theta} + \bar{\theta}_a + \bar{\theta}_{wash}$$

$$h = h_0 + \tilde{h}$$

$$h_0 = \Gamma_0 x \cos(\omega t)$$

$$V = \sqrt{[U \cos \theta - \dot{h} \sin(\bar{\theta} + \bar{\theta}_{\text{wash}})]^2 + [U(\alpha' + \bar{\theta}_a + \bar{\theta}_{\text{wash}}) - (0.5c - y_{\text{ea}})\dot{\theta}]^2}$$

$$N_a = \frac{1}{4} \rho \pi c^2 \left(U \alpha - \frac{1}{4} c \ddot{\theta} \right) \Delta x$$

$$D_c = -2\pi \alpha_0 (\alpha' + \bar{\theta}_a + \bar{\theta}_{\text{wash}}) \frac{\rho U V}{2} c \Delta x$$

$$T_s = \eta_s 2\pi \left(\alpha' + \bar{\theta}_a + \bar{\theta}_{\text{wash}} - \frac{c \dot{\theta}}{4U} \right)^2 \frac{\rho U V}{2} c \Delta x$$

$$D_f = C_{df} \frac{\rho V_y^2}{2} c \Delta x$$

$$Y_y = U \cos \theta - \dot{h} \sin(\bar{\theta} + \bar{\theta}_{\text{wash}})$$

$$F_y = T_s - D_c - D_f$$

$$N_{\text{inertia}} = (m_{\text{spar}} + m_{\text{fr}})(g_r - \dot{h}_0)$$

$$\begin{aligned}
& \overset{R}{=} F_y \cos(\theta) \\
& - \left(\frac{1}{2} \rho U \left(\sqrt{[U \cos \theta - \dot{h} \sin(\bar{\theta} + \bar{\theta}_{wash})]^2 + [U(\alpha' + \bar{\theta}_a + \bar{\theta}_{wash}) - (0.5c - y_{ea})\dot{\theta}]^2} \right) 2\pi \left(\frac{AR}{2 + AR} \left[F'(k) ([\dot{h} \cos(\bar{\theta}_a + \bar{\theta}_{wash}) + (0.75c - y_{ea})\dot{\theta}] / U + \bar{\theta}) \right. \right. \right. \\
& \left. \left. \left. + \frac{c}{2U} \frac{G'(k)}{c\omega} ([(\ddot{h}_0 + \ddot{h}) \cos(\bar{\theta} + \bar{\theta}_{wash}) - \dot{h}\dot{\theta} \sin(\bar{\theta} + \bar{\theta}_{wash}) + (0.75c - y_{ea})\ddot{\theta}] / U + \dot{\theta}) \right] - \frac{2[\alpha_0 + \bar{\theta}_a + \bar{\theta}_{wash}]}{2 + AR} + \alpha_0 + \bar{\theta}_a + \bar{\theta}_{wash} \right) c\Delta x + N_a \right. \\
& \left. + N_{inertia} \right) \sin(\theta) \\
& L = \left(\frac{1}{2} \rho U \left(\sqrt{[U \cos \theta - \dot{h} \sin(\bar{\theta} + \bar{\theta}_{wash})]^2 + [U(\alpha' + \bar{\theta}_a + \bar{\theta}_{wash}) - (0.5c - y_{ea})\dot{\theta}]^2} \right) 2\pi \left(\frac{AR}{2 + AR} \left[F'(k) ([\dot{h} \cos(\bar{\theta}_a + \bar{\theta}_{wash}) + (0.75c - y_{ea})\dot{\theta}] / U + \bar{\theta}) \right. \right. \right. \\
& \left. \left. \left. + \frac{c}{2U} \frac{G'(k)}{c\omega} ([(\ddot{h}_0 + \ddot{h}) \cos(\bar{\theta} + \bar{\theta}_{wash}) - \dot{h}\dot{\theta} \sin(\bar{\theta} + \bar{\theta}_{wash}) + (0.75c - y_{ea})\ddot{\theta}] / U + \dot{\theta}) \right] - \frac{2[\alpha_0 + \bar{\theta}_a + \bar{\theta}_{wash}]}{2 + AR} + \alpha_0 + \bar{\theta}_a + \bar{\theta}_{wash} \right) c\Delta x \right. \\
& \left. + N_a + N_{inertia} \right) \cos(\theta) + F_y \sin(\theta)
\end{aligned}$$

-
- AR aspect ratio
 - b stiffness-proportional damping constant
 - Cd drag coefficient
 - Cdf skin-friction drag coefficient
 - Cn normal force coefficient
 - c wing segment chord length
 - D, drag due to camber
 - Df friction drag
 - F, total chordwise force
 - $F'(k), G'(k)$ terms for modified Theodorsen function
 - h total plunging displacement
 - h elastic component of plunging displacement
 - h_0 imposed displacement
 - I moment of inertia
 - L total lift

-
- R total thrust
 - T, leading edge suction force
 - U freestream velocity
 - x distance from flapping axis to middle of segment
 - y distance from the leading edge
 - α relative angle of attack at 1-chord point due to wing segment
 - α' the flow's relative angle of attack at 1-chord point
 - Γ_0 magnitude of flapping dihedral angle
 - Δx length of an element
 - $\tilde{\theta}_{\text{bar}}$ leading-edge suction efficiency
 - θ elastic twist angle
 - $\bar{\theta}_a$ angle of flapping axis with respect to U
 - $\tilde{\theta}_{\text{wash}}$ built-in pretwist

Appendix B: Fortran code

Relevant Theodorsen Theory

```
program main
```

```
integer t
```

```
real(8)::sumR,sumL,average
```

```
real(8)::pi,AR,rho,omega,Gamma
```

```
real(8)::h,h0,hbar,h2dot,hdot,h02dot,hbar2dot
```

```
real(8)::R,L,Fy,N
```

```
real(8)::U,V,Nc,Na,Vy
```

```
real(8)::Naero,Ninertia,Cn
```

```
real(8)::theta,thetabar,thetaa,thetawash,thetabardot,thetabar2dot
```

```
real(8)::Fcommak,Gcommak,k,C1,C2
```

```
real(8)::alpha,alphacomma,alpha0,alphadot
```

```
real(8)::c,yea,x,deltax,etas
```

```
real(8)::Ts,Dc,Df,Cdf
```

```
real(8)::mspar,mfr,gr
```

```
real(8)::q,angle,amp
```

```
pi=3.1415927
```

```
AR=4.44444444444444
```

```
rho=1.205000000/1000000000
```

$\omega=360*\pi/180$

U=15

Cdf=0.0045

gr=9.80000/1000

open(1,file="data.txt",mode='read')

read(1,*)c

read(1,*)x

read(1,*)q

close(1)

Do amp=-5,40,1

$\Gamma_0=\text{amp}*\pi/180$

sumR=0

sumL=0

DO t=1,1000,1

!deltax(deltax)

!deltax length of an element

deltax=500

!yea(yea)

!yea distance of elastic axis from the leading edge

!q

yea=q*c

!Hight(h,h0,hbar,hdot,h02dot,hbar2dot)

!h total plunging displacement

!h0 imposed displacement

!hbar elastic component of plunging displacement

!Gamma0 magnitude of flapping dihedral angle

h0=Gamma0*x*cos(omega*t/1000)

hbar=0

hbar2dot=0

h=h0+hbar

hdot=-Gamma0*x*omega/1000*sin(omega*t/1000)

h02dot=-Gamma0*x*(omega**2)/1000000.00000*cos(omega*t/1000)

h2dot=-Gamma0*x*(omega**2)/1000000.00000*cos(omega*t/1000)

!Theta

!theta total segment twist angle with respect to U

!thetabar elastic twist angle

!thetaa angle of flapping axis with respect to U

!thetawash built-in pretwist

thetabar=0*pi/180*cos(omega*t/1000)

thetabardot=0*pi*omega/180000*sin(omega*t/1000)

$$\text{thetabar2dot}=0*\pi*\omega**2/180000000*\cos(\omega*t/1000)$$

$$\text{thetaa}=3*\pi/180$$

$$\text{thetawash}=0*\pi/180$$

$$\text{theta}=\text{thetabar}+\text{thetaa}+\text{thetawash}$$

$$\text{angle}=\text{theta}*180/\pi$$

$$!Vy(Vy)$$

!Vy relative velocity tangential to a wing segment

$$Vy=U*\cos(\text{theta})-\text{h02dot}*\sin(\text{thetabar}+\text{thetawash})$$

$$!Ninertial(\text{mspar},\text{mfr},\text{gr},\text{Ninertia},\text{h02dot})$$

!mspar distributed moment per unit length-spar

!mfr distributed moment per unit length-fabric & rib

!gr acceleration due to gravity

$$\text{mspar}=2.700000/1000000*7*c*\text{deltax}$$

$$\text{mfr}=0.500000*2.700000/1000000*7*c*\text{deltax}$$

$$\text{Ninertia}=(\text{mspar}+\text{mfr})*(\text{gr}-\text{h02dot})$$

$$!Theodorsen(\text{Fcommak},\text{Gcommak},\text{k},\text{C1},\text{C2},\pi,\omega)$$

$$\text{k}=\text{c}*\omega/(2*U)$$

$$\text{C1}=0.5*AR/(2.32+AR)$$

$$\text{C2}=0.181+0.772/AR$$

$$\text{Fcommak}=1-\text{C1}*k*k/(k**2+\text{C2**2})$$

$$\text{Gcommak}=-\text{C1}*\text{C2}*k/(k**2+\text{C2**2})$$

!Alpha(alpha,alphacomma,alphadot)

!alpha relative angle of attack at 3/4-chord point due to wing segment moment

!alphacomma the flowcommas relative angle of attack at 3/4-chord point

!alpha0 wing segment's angle of zero-lift line

$$\alpha_0 = -4 \cdot \pi / 180$$

$$\alpha = (\dot{h} \cos(\bar{\theta} + \theta_{wash}) + (0.75 \cdot c - y_{ea}) \cdot \dot{\bar{\theta}}) / U + \bar{\theta}$$

$$\dot{\alpha} = ((\dot{h}^2 + \dot{\bar{h}}^2) \cos(\bar{\theta} + \theta_{wash}) - \dot{h} \cdot \dot{\bar{\theta}} \sin(\bar{\theta} + \theta_{wash}) + (0.75 \cdot c - y_{ea}) \cdot \dot{\bar{\theta}}^2) / U + \dot{\bar{\theta}}$$

$$\alpha_{comma} = AR / (2 + AR) \cdot (F_{commak} \cdot \alpha + c \cdot G_{commak} \cdot \dot{\alpha} / (2 \cdot U \cdot k)) - 2 \cdot (\alpha_0 + \theta_{ta} + \theta_{wash}) / (2 + AR)$$

!Cn(Cn)

!Cn normal force coefficient

$$C_n = 2 \cdot \pi \cdot (\alpha_{comma} + \alpha_0 + \theta_{ta} + \theta_{wash})$$

!Na(Na)

!Na apparent-mass normal force

$$N_a = 0.25 \cdot \rho \cdot \pi \cdot (c^2) \cdot (U \cdot \dot{\alpha} - 0.25 \cdot c \cdot \dot{\bar{\theta}}^2) \cdot \Delta x$$

!V(V)

!V relative velocity at 1/4-chord location

$$V = \sqrt{((U \cos(\theta) - \dot{h} \sin(\bar{\theta} + \theta_{wash}))^2 + (U \cdot (\alpha_{comma} + \theta_{ta} + \theta_{wash}) - (0.5 \cdot c - y_{ea}) \cdot \dot{\bar{\theta}})^2)}$$

!Nc(Nc)

!Nc the circulatory normal force one the wing segment

$$N_c = 0.5 \cdot \rho \cdot U \cdot V \cdot C_n \cdot c \cdot \Delta x$$

!Total chordwise force(Fy,Ts.Dc,Df)

!Fy total chordwise force

!Ts leading edge section force

!Dc drag due to camber

!Df friction drag

$$\eta_{ts} = (2.35 - 2.35 \cdot 2^2 / (\pi \cdot AR)) \cdot \sin(\theta)^2 / \cos(30 \cdot \pi / 180)$$

$$T_s = \eta_{ts} \cdot 2 \cdot \pi \cdot (\alpha_{\text{comma}} + \theta_{\text{ta}} + \theta_{\text{wash}} - c \cdot \dot{\theta}_{\text{bar}} / (4 \cdot U))^2 \cdot \rho \cdot U \cdot V / 2 \cdot c \cdot \Delta x$$

$$D_c = -2 \cdot \pi \cdot \alpha_0 \cdot (\alpha_{\text{comma}} + \theta_{\text{ta}} + \theta_{\text{wash}}) \cdot \rho \cdot U \cdot V / 2 \cdot c \cdot \Delta x$$

$$D_f = C_{df} \cdot \rho \cdot (V_y^2) \cdot c \cdot \Delta x / 2$$

$$F_y = T_s - D_c - D_f$$

!N(N,Naero)

!N total normal force acting on a wing segment

$$N_{\text{aero}} = N_c + N_a$$

$$N = N_{\text{aero}} + N_{\text{inertia}}$$

!final

!R total thrust

!L total lift

$$R = F_y \cdot \cos(\theta) - N \cdot \sin(\theta)$$

$$L = N \cdot \cos(\theta) + F_y \cdot \sin(\theta)$$

```
sumR=sumR+R
```

```
sumL=sumL+L
```

```
end DO
```

```
averageR=sumR/1000
```

```
averageL=sumL/1000
```

```
open(255,file="haha3.xls",status='unknown',access='append',mode='write')
```

```
write(255,*)'amp=',amp
```

```
write(255,*)'averageR=',averageR
```

```
write(255,*)'averageL=',averageL
```

```
close(255)
```

```
end Do
```

```
end
```